EFFECTS OF
PARTICLE ACCUMULATION
IN
AEROSOL FILTRATION

Thesis by

Charles Edgar Billings

In Partial Fulfillment of the Requirements

For the Degree of

Doctor of Philosophy

California Institute of Technology

Pasadena, California

1966

(Submitted May 20, 1966)

ACKNOWLEDGMENTS

This research was supported primarily by a Public Health Service Fellowship (2 F3 AP 16,258) from the Division of Air Pollution. The investigation was also funded in part by the Division of Biology and Medicine of the United States Atomic Energy Commission, and the Ford Foundation. The generous help of these sponsors is gratefully acknowledged.

This study was performed under the direction of Professor Sheldon K. Friedlander. His continuing assistance and encouragement are appreciated.

Light scattering photometers were provided for this study through the courtesy of Mr. A. J. Breslin, Health Protection Engineering Division, Health and Safety Laboratory, United States Atomic Energy Commission, New York, New York; and Mr. A. H. Wilson, Voyager Technical Facilities, Jet Propulsion Laboratory, California Institute of Technology, Pasadena, California, and National Aeronautics and Space Administration.

The manuscript of this thesis was ably typed by Mrs. Marjorie E. Connely, Mrs. Barbara Pincince, and Mrs. Sally Schwartz. Their kind help is appreciated.

ABSTRACT

The filtration of solid aerosol particles produces a decrease in filter penetration and an increase in filter resistance because of the accumulation of deposited material. Functions are derived for the effects of particle accumulation on filter penetration and resistance. A new aerosol tunnel is described which provides a uniform field of particle and fluid flow for extended periods. Data are presented on the effects of accumulation of 1.3-micron polystyrene particles on the performance of filter mats tested in the aerosol tunnel. A quantitative microscopic study of accumulation of 1.3-micron particles on single isolated 10-micron glass fibers is described. Photographs of deposit structure and measurements of aggregate size are included.

TABLE OF CONTENTS

LIST OF TABLES

LIST OF FIGURES

I.

INTRODUCTION

A. Background

A common type of aerosol filter consists of a porous mat of fibrous material through which the aerosol is passed to separate the suspended particles from the gas. At the start of filtration, particles much smaller than the pore openings collect on the fibers of the filter. Physical screening is not an important phenomenon in fiber filtration. Particles contact the fibers by diffusion, interception, inertial impaction, and by electrical or gravitational forces. Particles that collect on the fibers produce a change in the flow of the fluid nearby. If the particles are solid, they extend outward from the fiber and serve as additional obstacles for further capture of other particles. Filter efficiency will increase at the cost of greater resistance to air-flow resulting from the accumulating solid particle deposit.

Fiber filters are used for recovery of low concentrations of airborne solid and liquid particles (micrograms to milligrams per cubic meter). Examples of modern applications of large filters for control of hazardous or nuisance dusts have been given in recent books (1,2). An interesting history of the development of fiber filters for dust masks prior to 1948 has been prepared by Davies (3). Filters of graded fiber size are used to separate polydisperse aerosols into size fractions in the investigation of atmospheric dust burdens (4, 5, 6, 7, 8).

Filter performance for a particular application may be characterized by three factors: (a) the collection efficiency at the start of filtration, (b) the initial air-flow resistance caused by the clean filter, and (c) the changes in efficiency and resistance caused by accumulation of material during operation.

Several theoretical and experimental studies of initial collection efficiency of fibrous filters have been published. The components of a complete theory seem to be fairly well identified. It is possible to predict the initial collection efficiency of a clean fiber mat with limited success.

The air-flow resistance of clean fiber filters can be determined most simply by direct measurement. For flows at low Reynolds numbers, the resistance can be predicted by analysis in many cases. Extensions to higher Reynolds numbers and to the slip flow regime have been obtained.

The rational study of filter performance during operation has been largely neglected. This investigation provides the basis for a quantitative explanation of fiber filter performance during accumulation of solid particles.

B. Mechanisms of Aerosol Particle Capture in Fiber Filters

1. Fundamental Mechanisms and Assumptions

For purposes of analysis, the filter can be considered as a uniform array of individual fibers placed transverse to gas flow, as shown in Figure 1-1. As a first approximation, fibers can be assumed

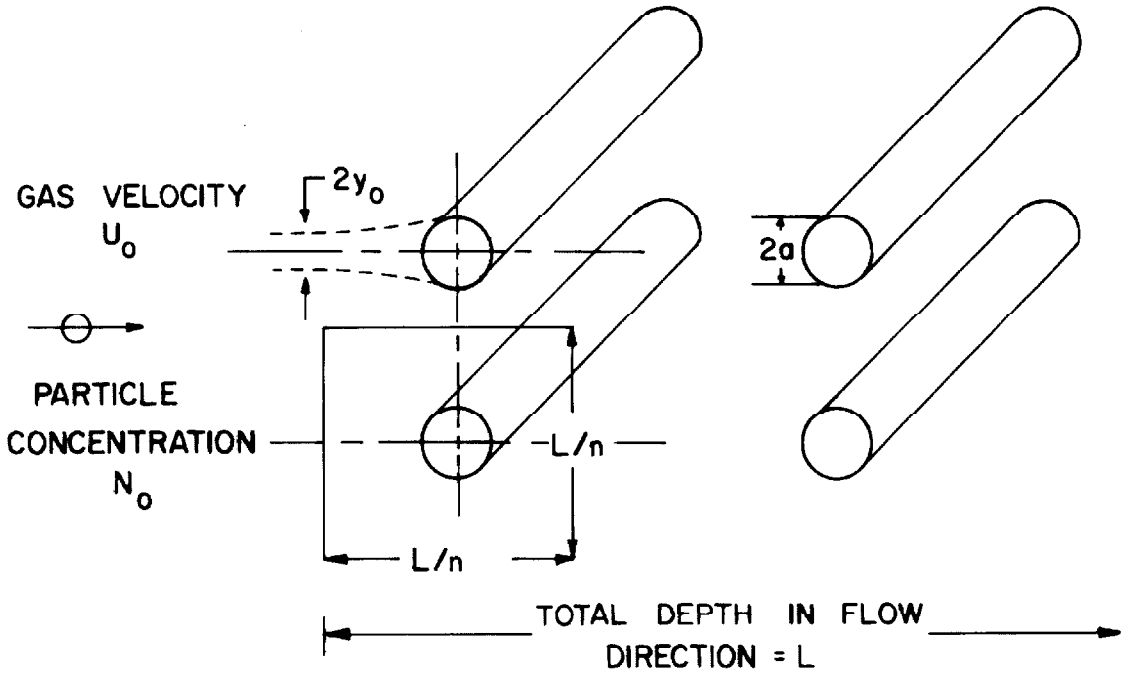

n = NUMBER OF THEORETICAL LAYERS OF PARALLEL FIBERS IN UNIFORM ARRAY

y_o = STREAM TUBE HEIGHT FROM WHICH ALL PARTICLES ARE REMOVED

a = FIBER RADIUS

Figure 1-1. Isolated Fiber Model of Aerosol Filter

to act independently. Particle capture can then be treated analytically by solving the equations of motion for particles in fluid flowing over a single cylinder.

The principal mechanisms for removal of small particles in fibrous filters are:

a) diffusion to surfaces of obstacles as a result of particle Brownian motion;

b) direct interception or streamline contact with surface; this can be treated as a modified boundary condition arising from finite particle size;

c) inertial deposition as a consequence of relative velocity between particle and fluid as fluid streamlines separate to pass the obstacle;

d) gravitational sedimentation;

e) electrical separation attributable to particle or fiber charge, and polarization and space charge effects.

Theories of particle capture by these primary mechanisms have been derived on the basis of the single fiber model by assuming that:

a) the fibers are sufficiently far apart, so that the fluid flow in the vicinity of a given fiber can be adequately represented by the flow near an isolated fiber, i.e., inter-fiber interference or fiber crossing effects are neglected;

b) the particles approaching a surface do not interact with or distort the flow to produce additional hydrodynamic lift or drag; and

c) the particles always adhere on contact, i.e., effective contacts, surface migration, and reentrainment are neglected.

Assumption (a) implies that the fluid streamlines near a fiber are not displaced significantly by the presence of other fibers. The effect of fiber interference on collection was included in the theory of Langmuir (9) by using an aerodynamically equivalent fiber size obtained from measured resistance. Davies (10) made a numerical approximation for the lateral displacement of fluid streamlines. Fuchs and Stechkina (11) have suggested that the influence of neighboring fibers may be included by using the streamlines of fluid motion for a bounded cylinder (12, 13).

Assumption (b) is always accepted, but recent studies on particles in laminar shear flow (14) indicate that a lift force may exist.

Assumption (c) has been investigated with single obstacles and test grids of parallel wires exposed to aerosol flow. Not all particles adhere on contact (15, 16, 17). Particles deposited at a given velocity may be removed by a higher velocity (18, 19, 20). There seems to be a surface accommodation coefficient, β, related to the ratio of an adhesion force to a hydrodynamic force. Presumably $0 \leq \beta \leq 1$, where $\beta = 1$ is equivalent to assumption (c) and $\beta = 0$ implies elastic collisions. Although $\beta \neq 1$ in all cases for isolated obstacles, it appears to be close to one for the total filter mat.

Current theories of filtration apply to bare fibers at the start of the process. Effects of deposited material on subsequent performance are the subject of this investigation.

2. Filter Penetration

Consider a filter of packing density ρ_b (gm/cm^3) composed of fibrous material of density ρ_m (gm/cm^3). The fraction of solids in the filter is defined as:

$$\alpha = \rho_b / \rho_m \tag{1-1}$$

The length of fiber per unit volume of filter is:

$$\ell = \alpha / \pi a^2 \tag{1-2}$$

where a is the fiber radius. Assume that all fibers are perpendicular to the flow as shown in Figure 1-1. Assume that the particle concentration is uniform at every distance from the filter entrance. Let $2y_o$ be the width of the fluid approaching the fiber from which all particles are removed. The change of concentration (particles/cm^3) in the direction of flow is:

$$-\frac{dN}{dx} = 2 y_o N \ell \tag{1-3}$$

where N is the particle concentration and x is the distance through the filter in the direction of flow. The fraction of aerosol particles penetrating the filter (penetration) can be obtained by integrating equation (1-3) from $N = N_o$ at $x = 0$ to $N = N_L$ at $x = L$. This yields:

$$\ln(N_o/N_L) = (y_o/a)\, 2L\alpha/\pi a , \tag{1-4}$$

after introducing the fiber length per unit volume of filter from equation (1-2). Let:

$$\eta = y_o/a \tag{1-5}$$

Then the filter fiber efficiency may be defined for practical purposes as

$$\eta = (\pi a / 2 L \alpha) \ln (N_o / N_L). \qquad (1\text{-}6)$$

The ratio of the outlet to the inlet aerosol particle concentration (N_L/N_o) is known as the filter penetration. The filter fiber efficiency can be determined experimentally by measuring the penetration of the filter with monodispersed aerosol particles and estimating the fraction of solids (α), filter depth (L), and fiber radius (a). The determination of η from particle and fluid flow characteristics is the objective of particle capture theories.

3. Particle Capture Theories and Comparison with Experiments

(a) Introduction

A general theory of aerosol filtration must provide for the effects of the five particle capture mechanisms given above. The effects of electrostatic charge on fiber efficiency have been considered by Zebel (21) and by Lundgren and Whitby (22). Analytical and experimental work has been limited to a few studies. Measurement of particle and fiber charge is difficult in practice, and is not usually done as part of the experimental determination of fiber filter efficiency. Capture by sedimentation is negligible for the small particles of concern in filtration. The three remaining mechanisms of diffusion, impaction, and direct interception form the basis of the mechanical theory of filtration. These mechanisms have received the majority of theoretical and experimental study.

In this thesis, two cylindrical fiber collection efficiencies are considered; (a) single fiber, and (b) filter fiber. There are some experimental indications that they are not identical. The filter fiber collection efficiency is defined by equation (1-6) in terms of experimental quantities. The single fiber collection efficiency is determined from consideration of an isolated fiber in the absence of any effects arising from the presence of adjacent fibers. Theoretical single fiber efficiency is considered below. Some experimental studies of single fiber efficiency are discussed in later chapters.

(b) Diffusion

The transport of suspended particles to a cylindrical fiber under the combined effects of diffusion and fluid motion can be determined from solutions to the equation of convective diffusion. From dimensional considerations, the solutions can be shown to be a function of the Péclet number, defined as:

$$Pe = 2 a U_o / D \qquad (1-7)$$

where a is the fiber radius, U_o is the undisturbed stream velocity, and D is the particle diffusion coefficient. The Péclet number is the characteristic parameter for the relative magnitude of the effects of convection and diffusion in particle transport.

Several theoretical solutions have been proposed for the fiber efficiency for particles of vanishing size (1,2,11,23,24,25,26,27,28, 29,30,31,32,33). They are of the form:

$$\eta \sim Pe^{-n} \qquad (1-8)$$

where $\frac{1}{2} \leq n \leq 1$. It is generally accepted by theoretical workers in mass transfer that $n = 2/3$ is the correct dependence for diffusion alone.

The solutions also depend upon the character of the fluid motion as measured by Reynolds number based upon fiber size:

$$Re = 2a U_o/\nu \tag{1-9}$$

where ν is the kinematic viscosity of the fluid. For most fiber filters in which diffusion is an important mechanism of removal, $Re \leq 10^{-1}$. The dependence upon Re is logarithmic, and its influence is slight over the usual range ($10^{-4} \leq Re \leq 10^{-1}$).

(c) Inertial Impaction

As fluid approaches an immersed obstacle, elements of the fluid accelerate and diverge to pass around the object. A particle suspended in the fluid may not be able immediately to accommodate to the local fluid acceleration and a difference in velocity between fluid and particle may develop. Inertia tends to maintain the forward motion of the particle while the diverging fluid tends to drag the particle aside. Subsequent motion of the particle is the resultant of the inertial projection and the fluid drag. From dimensional considerations, it can be shown that the solutions to the equation of particle motion depend upon the impaction group, defined as:

$$I = m U_o/a f \tag{1-10}$$

where m is the particle mass and f is the resistance of the fluid to the particle motion per unit of velocity. For small spherical particles

of radius a_p, the fluid resistance can be assumed to be given by Stokes approximation, so that:

$$f = 6\pi \mu a_p / C_s \qquad (1\text{-}11)$$

where μ is the fluid viscosity and C_s is the Cunningham-Millikan slip correction factor (2, 24, 34). The impaction parameter for small spherical particles becomes:

$$I = 2 C_s \rho_p a_p^2 U_o / 9 \mu a \qquad (1\text{-}12)$$

where ρ_p is the particle density. This parameter also represents the ratio of the distance a small particle will travel in a still fluid when projected with an initial velocity of U_o (stopping distance) to the characteristic dimension of the obstacle (cylinder radius).

Several numerical and empirical solutions have been presented for inertial collection of small spheres by cylindrical fibers. Most of these solutions have been discussed in recent reviews (1, 2, 24, 35). In general, the fiber collection efficiency is a function of the impaction parameter and the Reynolds number based on fiber size.

(d) Direct Interception

Particle capture arising from diffusion or inertial impaction can be determined by assuming the particle is a mathematical point having the property of random molecular motion or inertia. If a particle of finite size passes near a fiber as a result of (a) diffusion, or (b) inertia, or (c) because of fluid motion alone; contact can occur if the path of the center of the particle comes within a

distance of one particle radius (a_p) of the surface. The effect of finite particle size on capture is called direct interception. Fiber efficiency can be shown to be a function of the direct interception group:

$$R = a_p / a \tag{1-13}$$

It is possible to treat the effect of direct interception as a boundary condition in the solutions for fiber efficiency by diffusion and impaction. The solutions then contain the interception group as an additional parameter. If the particle passes near the fiber surface as a result of fluid motion alone, fiber efficiency because of direct interception is (25):

$$\eta \sim R^2 \tag{1-14}$$

for $R < 1$ and $Re < 1$.

(e) Combined Theories of Particle Capture

Theories of diffusion plus direct interception have been presented by several workers (9, 27, 28, 29, 31, 33). Many of these theories have been reviewed in recent texts (1, 2, 24, 36). Friedlander has obtained an analytical solution for the diffusional capture of particles of finite size (33). His solution is compared to the exerimental results of this study in Chapter V.

Approximations for the capture of particles as a result of the simultaneous effects of diffusion, impaction, and direct interception have been proposed by a few workers (10, 37, 38, 39). The complete problem has not been solved analytically as yet.

(f) Comparisons of Theory with Experiments

There have been several attempts to confirm theoretical solutions for particle capture through experiment. Most of these experimental investigations have been reviewed recently (12, 24, 35). It may be generally concluded that not all experimental data fit any given theory. For example, Friedlander and Pasceri (31) have presented a correlation of fiber efficiency for diffusion and direct interception in terms of a similarity variable:

$$\eta R Pe = C_1' R Pe^{1/3} + C_2' (R Pe^{1/3})^3. \qquad (1\text{-}15)$$

The coefficients C_1' and C_2' are of order one and were derived from experiments of Chen (23) and Wong (40). This correlation is shown as a solid line in Figure 1-2.

Upon extending the correlation to the data of other investigators, Friedlander and Pasceri found that these other data (lying within the range of the correlation for $Re < 1$, $I < 0.5$) did not agree in all cases. These data points are also shown in Figure 1-2. They note that "the data of Thomas and Lapple (41); Thomas and Yoder (42); and Ramskill and Anderson (43), are considered to be satisfactorily represented by the correlation." The data of Humphrey and Gaden (44), Stern et al. (45), and Sadoff and Almlof (46), are higher; those reported by Stern and by Sadoff being about an order of magnitude higher. The data of Sadoff and Almlof were taken at $RPe^{1/3} < 10^{-1}$ and are not shown in Figure 1-2.

Aiba, Humphrey, and Millis (36) have also presented a plot of the majority of experimental data taken with monodisperse aerosols in the

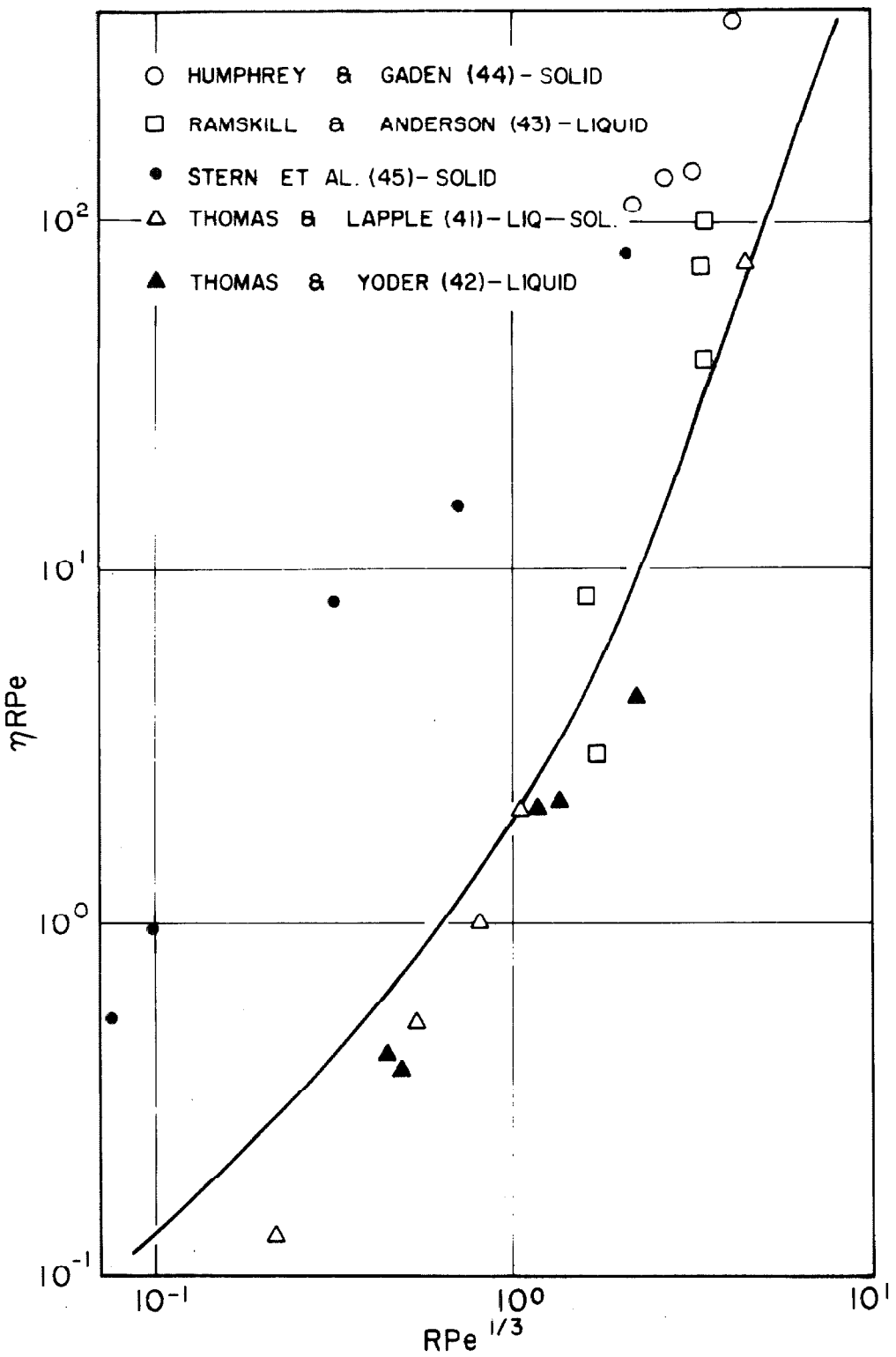

Figure 1-2. Comparison of Theory with Observation for Diffusion and Direct Interception, Equation of Line: $\eta RPe = 1.3RPe^{1/3} + 0.7(RPe^{1/3})^3$

diffusion plus direct interception range. These data were plotted on essentially the same coordinates shown in Figure 1-2. They also include data from studies of Aiba et al. (47), which are not shown in Figure 1-2.

Perhaps the most striking feature of these two presentations lies in consideration of the nature of the aerosol used in the experiments. All data which lie substantially above the proposed relationship of Friedlander and Pasceri (higher efficiency) represent collections of solid particles, while those which agree approximately with the correlation are primarily for liquid particles. Aiba et al. used bacteria, Humphrey and Gaden used spores, Sadoff and Almlof used bacteriophage, and Stern et al. used polystyrene latex. Data of Thomas and Lapple were taken with a condensation aerosol consisting of a supercooled liquid which crystallized at some later time ($\sim$ mins.).

There seems to be a consistent difference between the collection efficiency for solid and liquid particles, with the solid particles being collected at somewhat higher efficiency. The reason for this difference is not known, but it may be related to the methods of solid and liquid aerosol generation and electrostatic charge. The higher efficiency resulting from filtration of solid particles may also be related to particle accumulation effects in some of the studies cited above.

It is evident that a general relationship for fiber or filter efficiency is not available for all conditions of flow. In order to produce an expression suitable for both solid and liquid particles,

the particle and fiber charge will have to be characterized. Particle accumulation effects must also be considered.

C. Flow Through Fiber Filters

The flow of clean gas through a fibrous filter can be considered as a part of the general problem of flow through porous media. At the usual velocities and ambient pressures encountered in filtration, the gas can be considered incompressible. The volume occupied by fibers is usually small (< 10%) in contrast to granular porous media (> 30%). The average distance between fibers is several times larger than the fiber diameter, again in contrast to granular media where pore and particle size are approximately equal. The macroscopic flow is one-directional and fibers lie essentially perpendicular to the flow.

For steady flow through fiber filters under consideration here ($a < 10$ microns, $U_o < 100$ cm/sec), the Reynolds number based on fiber size is less than about one. Therefore, Darcy's Law (48) applies, namely:

$$\overline{U} = -\frac{k'}{\mu}\nabla p \qquad (1\text{-}16a)$$

where k' is the intrinsic permeability of the medium, and ∇p is the pressure gradient. For flow in fiber filters, it is usual to express Darcy's Law in the form (10):

$$\frac{\Delta p}{L}\cdot\frac{a^2}{\mu U_o} = K_o(\alpha) \qquad (1\text{-}16)$$

where Δp is the resistance to flow or pressure drop across the medium, and $K_o(\alpha)$ is the theoretical resistivity of the medium. The intrinsic permeability is related to the resistivity by $k' = a^2/K_o(\alpha)$.

Langmuir (9) solved the complete Navier-Stokes equation in cylindrical coordinates using a "free-surface cell" model for coaxial flow. He obtained:

$$K_o(\alpha) = \gamma 4\alpha/(-\ln\alpha - 3/2 + 2\alpha - \tfrac{1}{2}\alpha^2) \qquad (1\text{-}17)$$

where γ is an empirical coefficient, $1 \leq \gamma \leq 2$, to account for the random orientation of fibers.

Kuwabara (13) has presented a solution of an approximate form of the Navier-Stokes equation for the case of transverse flow over a cylinder using a "free-surface cell" model. Fuchs and Stechkina (11) and Pich (49) have extended this solution to the case of flow in fiber filters, obtaining:

$$K_o(\alpha) = 8\alpha/(-\ln\alpha - 3/2 + 2\alpha - \tfrac{1}{2}\alpha^2). \qquad (1\text{-}18)$$

This equation is identical to Langmuir's earlier solution, with $\gamma = 2$.

Happel and Brenner (12) present a solution of the approximate form of the Navier-Stokes equation for transverse flow over a cylinder with a slightly different assumption from that of Kuwabara. They obtained:

$$K_o(\alpha) = 8\alpha/(-\ln\alpha - \frac{1-\alpha^2}{1+\alpha^2}). \qquad (1\text{-}19)$$

According to Langmuir's analysis, both the Kuwabara and Happel solutions should over-predict the filter resistance slightly.

There have been a number of experimental determinations of fiber filter resistivity, defined as:

$$K_o' = \frac{\Delta p}{L} \cdot \frac{a^2}{\mu U_o} \qquad (1\text{-}20)$$

using measured values of the variables to calculate K_o'. Results of several of these studies are summarized in Table 1-1. Chen (23) compared many of these results with an empirical form derived from cylinder-in-tube drag measurements of White (57). Chen noted that the values given by the Langmuir equation (1-17) agreed fairly well with his assumed form shown in Table 1-1. The experimental form assumed by Chen is the only one with a logarithmic dependence on solids fraction. Values of $K_o(\alpha)$ from the Happel and Brenner solution, and K_o' determined from the experiments in this thesis are compared in Chapter III.

The last two studies shown in Table 1-1 were performed on submicron glass fibers which have recently become available. The molecular mean free path of the gas is of the order of the fiber radius in this case, and the fluid no longer acts as a continuous medium. The Knudsen number based on fiber size enters the solution for fluid flow as an additional parameter:

$$Kn = \lambda/a \qquad (1\text{-}21)$$

where λ is the molecular mean free path in the gas (2, 24) (λ is of order 0.1 micron for air at ambient temperature). Brooks and Reis (58) have obtained an expression for the drag coefficient of single cylinders as a function of Knudsen number. Pich (49) has presented

TABLE 1-1

Experimental Resistivity of Fiber Filters

Investigator	Experimental Resistivity (K_0')	Remarks
Sullivan (50)	$K'\alpha^2/K''(1-\alpha)^3$	K' = shape factor K'' = orientation factor
Blasewitz et al. (51)	$\alpha^{3/2}$	Glass fiber
Davies (10)	$16\alpha^{3/2}(1 + 56\alpha^3)$	Many materials
First et al. (52)	$(29/4)\alpha^{1.4}$	Glass fiber $10^{-3} \leqslant Re \leqslant 10^2$
Wong and Johnstone (40)	$(C_D Re/2)(1/\pi)\alpha$	Glass fiber C_D = fiber drag coef. $C_D Re \sim 10$
Chen (23)	$K_1\alpha/\pi(1-\alpha)(-\frac{1}{2}\ln K_2\alpha)$	Glass fiber $K_1 \sim 6.1$, $K_2 \sim 0.41$
Wright et al. (20)	$(C_D Re/2\pi)\alpha$	Glass and tungsten fibers $C_D Re \sim 4\pi$
Kimura and Iinoya (53)	$(2Re\alpha/\pi(1-\alpha)^2)(0.6 + 4.7Re^{-\frac{1}{2}} + 11Re^{-1})$	Glass and steel wool fibers $10^{-3} \leqslant Re \leqslant 10^2$
Aiba (54)	$C_D Re\,\alpha^{3/2}/2\pi(1-\alpha)^2$	Glass fibers $C_D Re \sim 50$

TABLE 1-1 (cont'd)

Investigator	Experimental Resistivity (K_o')	Remarks
Wheat (55)	$K_3\alpha/4(1-\alpha)^2$	Sub-micron glass fiber K_3 corrects for slip flow (~30 at STP).
Werner and Clarenburg (56)	$180C_c^{-5/2}\alpha^{3/2}$	Sub-micron glass fiber C_c is a function of the fiber Knudsen no.

an extension of equation (1-18) for flow in fibrous filters at small Knudsen numbers. Stern et al. (45) have studied the resistance of fibrous filters at low pressures.

D. Effects of Particle Accumulation in Fiber Filters

1. Mechanisms of Accumulation

The mechanisms which produce initial deposition of particles on fibers have been summarized above. Continued deposition of solid particles causes increased collection efficiency and resistance. The presence of a particle deposited on a fiber disturbs the local fluid flow and increases the drag force on the fiber. At the same time, the disturbance produces a local increase in the capture efficiency.

Mechanisms of capture of air-borne particles by deposited particles are assumed to be the same as given above for the bare fiber. The structure or geometry of the deposit controls the changing collection efficiency and resistance. Deposit structure will depend upon aerosol particle size and shape, and deposition velocity. Structure may also depend upon:

a) filter porosity and fiber size;

b) drag or lift on the deposit;

c) adhesion between particles.

A realistic model for the accumulation process depends upon a physical interpretation of the deposit structure. There may be characteristics of the aerosol material, as a result of its chemical nature or surface state, which influence the manner in which it builds up on a fiber or on a previous deposit. Great differences would be expected

between solid and liquid particle accumulation, for example. If such characteristics are of importance for solid particles, they could make a general theory of aerosol accumulation very difficult to construct. Investigation of some of these factors forms the subject of this thesis.

2. Observations of the Structure of Aerosol Particle Deposits on Fibers

The structure of aerosol particle deposits on fibers has been examined by several investigators, as shown in Table 1-2. Watson (59) described the general process of particle accumulation on a fiber in terms of a slow growth of chain-like aggregates. He noted that the 'new fibers' composed of the collected particles themselves acted as very efficient collectors.

Leers (60) studied the collection of spray-dried sodium chloride particles on cellulose and asbestos fibers in a low-power optical microscope. His time-sequence photographs showed the growth of chain-like dendritic structures.

Wright et al. (20) also photographed aerosol deposits on individual glass fibers. They indicated that the character of the deposit was influenced by the nature of the aerosol and the deposition velocity. They used liquid aerosol particles formed by condensation. Particles were supercooled while airborne, but crystallized on contact or shortly afterward (du Pont oil orange, Benzene Azo β -Napthol). They also used a solid aerosol of crystalline NH_4Br. These studies were made at relatively high velocities ($>$ 40 cm/sec). The authors concluded that high velocity changed the deposit structure through compaction.

TABLE 1-2

Observations of the Structure of Solid Aerosol Particle Deposits on Fibers

Investigator	Fiber Material (Diameter)	Particle Material (Diameter)	Particle Shape	Deposit Vel cm/sec	Structure	Magnific.
Watson (59)	Cellulose	Meth. blue	Sph.	-	Chains and clumps	4,700
	Rubber	NaCl	Cub.	-	Chains and clumps	2,300
	Glass	Carb. bl.	Sph.	-	Chains and clumps	10,000
Leers (60)	Cellulose-Asbestos	NaCl	Cub.	10	Chains	100 (est)
Wright et al. (20)	Glass (30 μm)	Oil Orange (0.3 μm)	Cryst.	200	Chains	100
	Glass (30 μm)	NH_4Br (1.2 μm)	Cub.	45	Short chains	100
	Glass (30 μm)	NH_4Br (1.2 μm)	Cub.	300	Short clumps	100
	Glass (30 μm)	NH_4Br (1.2 μm)	Cub.	700	Unif. deposit	100
Cheever (61)	Glass (0.5 μm)	MgO	Cub.	2.5	Chains and clumps	19,000
	Glass (0.5 μm)	ZnO	Stellar Cryst.	2.5	Needles and clumps	12,000
Dorman (62)	Glass	Meth. blue	Sph.	-	Chains	4,000
Radushkevich and Kolganov (63)	Asbestos (0.06 μm)	Polystyr. (0.25 μm)	Sph.	0.5-25	Chains of 2 or 3	-

Cheever (61) and Dorman (62) have provided other photographs of aerosol particle deposits in fiber filters. Radushkevich and Kolganov (63) observed chain aggregates of 2 or 3 particles, but no photographs were presented. LaMer (64) has referred to some observations by his group and by Langmuir but without including photographs.

The dendritic, chain-like, or feathery growth of aggregates seems to be a fairly common observation of deposit structure. The nature of the aerosol material does not seem to be of major significance, if the aerosol velocity is low. If the velocity is high, a more compact structure results. The structure of liquid particle deposition is substantially different and depends upon fiber surface treatments (65, 66).

The microscopic observations of Wright et al. (20) on deposit structure were made at right angles to the aerosol flow direction. All other observations cited in Table 1-2 were made by transmitted light or electron beam absorption looking into the deposit in the same direction as the aerosol flow. Wright et al. observed no deposition on the rear half of their glass fibers even at the highest velocities used ($\sim 10^3$ cm/sec).

Larsen (19) attempted to dislodge deposits from the forward half of single fibers ($>$ 10-microns diameter) with air jets. He observed migration of some particles to the rear of the fibers at velocities of 10^4 cm/sec. Still higher velocities were required to cause substantial migration or reentrainment. These two studies indicate that nearly all deposition of small particles at usual filtering velocities ($<$ 10^3 cm/sec) will occur on the forward face of fibers.

3. Previous Experimental Studies of Filter Performance as a Result of Particle Accumulation

The effect of solid particle accumulation on aerosol filter penetration has been studied experimentally by several investigators (1, 20, 51, 67, 68, 69, 70, 71, 72, 73, 74). Polydisperse particles were used in all studies except those of LaMer et al. (68) and Lindeken et al. (71). Data obtained by LaMer and by Lindeken are shown in Figure 1-3. The CC-5 filter paper, as nearly as can be established from the LaMer reports, was a rayon-cotton mixture with $a = 6.5$ microns, $\rho_m = 1.44$ gm/cm^3, $L = 0.043$ cm and $\alpha = 0.128$. These measurements are apparently based on a single determination supplied to them by Walter J. Smith of A. D. Little, Inc.* No specific information about filter characteristics was taken on the individual filters tested. The characteristics of the analytical filter paper (Whatman 41) used in the Lindeken study were not reported.

Useful experiments on the increase of filter air-flow resistance with time are limited to the work of LaMer and Drozin (74) and LaMer and coworkers (68), as shown in Figure 1-4. Data were obtained on CC-5 filter paper with wax spheres ($a_p = 0.2 - 0.5$ microns). The main results of their work indicate that penetration during filtration of solid aerosol particles decreases as a consequence of the plugging of the filter, and that resistance increases at the same time.

In the other studies of the change in penetration and resistance cited above, either the filters or the aerosols were not adequately defined. In the studies of Wright et al. (20), the supercooled liquid

* Cambridge, Mass.

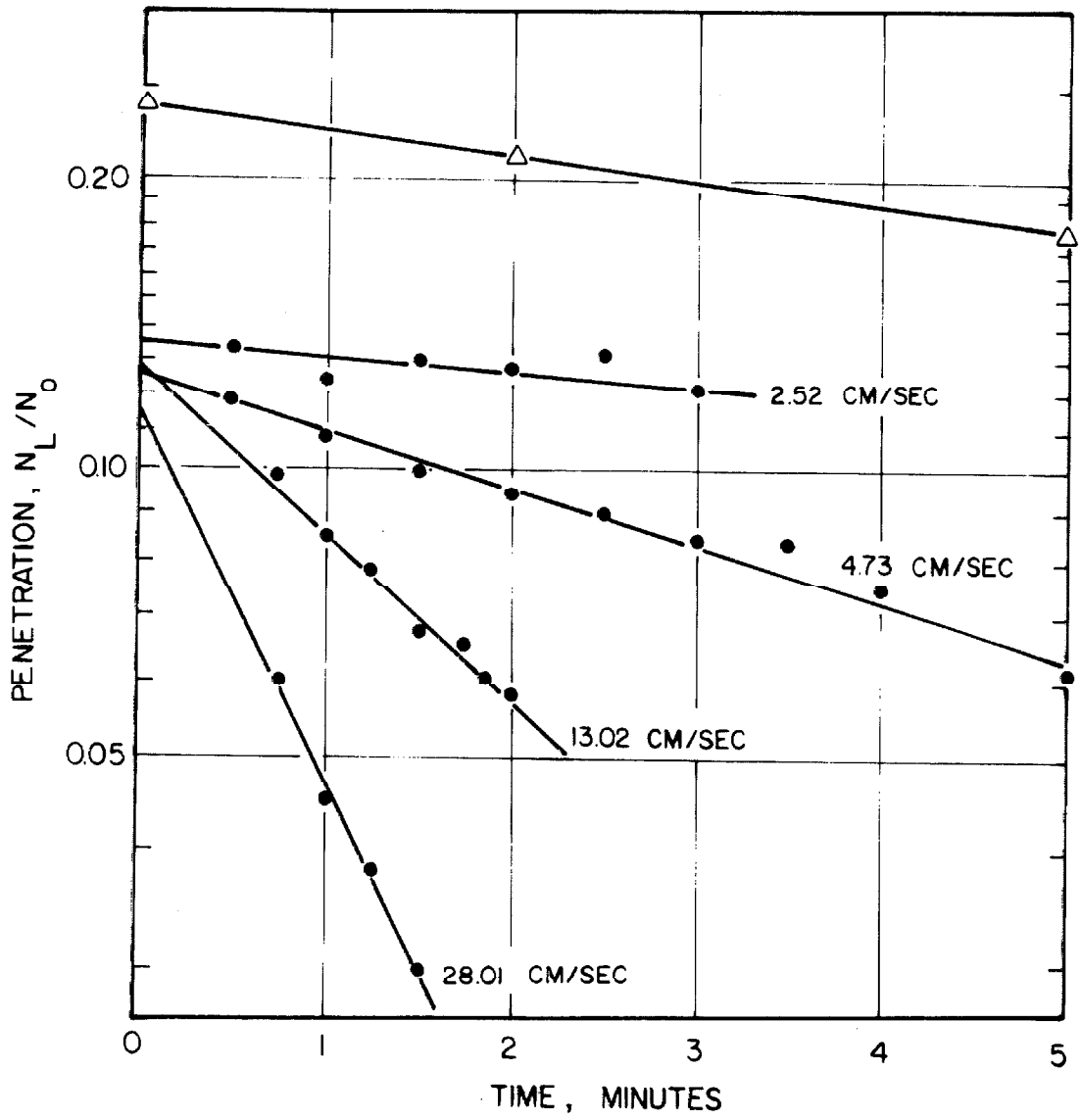

• LAMER ET AL., CC-5 FILTER, $a \cong 6.5\,\mu m$
$\alpha = 0.128$, $L = 0.043$CM, WAX AEROSOL
$0.2 \leq a_p \leq 0.5\,\mu m$, $N_o \sim 10^6$ p/CM^3

△ LINDEKEN ET AL., WHATMAN 41 FILTER
$a_p = 0.182\,\mu m$, $U_o \cong 15$CM/SEC, $N_o \cong 2 \times 10^4$ p/CM^3
POLYSTYRENE AEROSOL

Figure 1-3. Filter Penetration During Operation

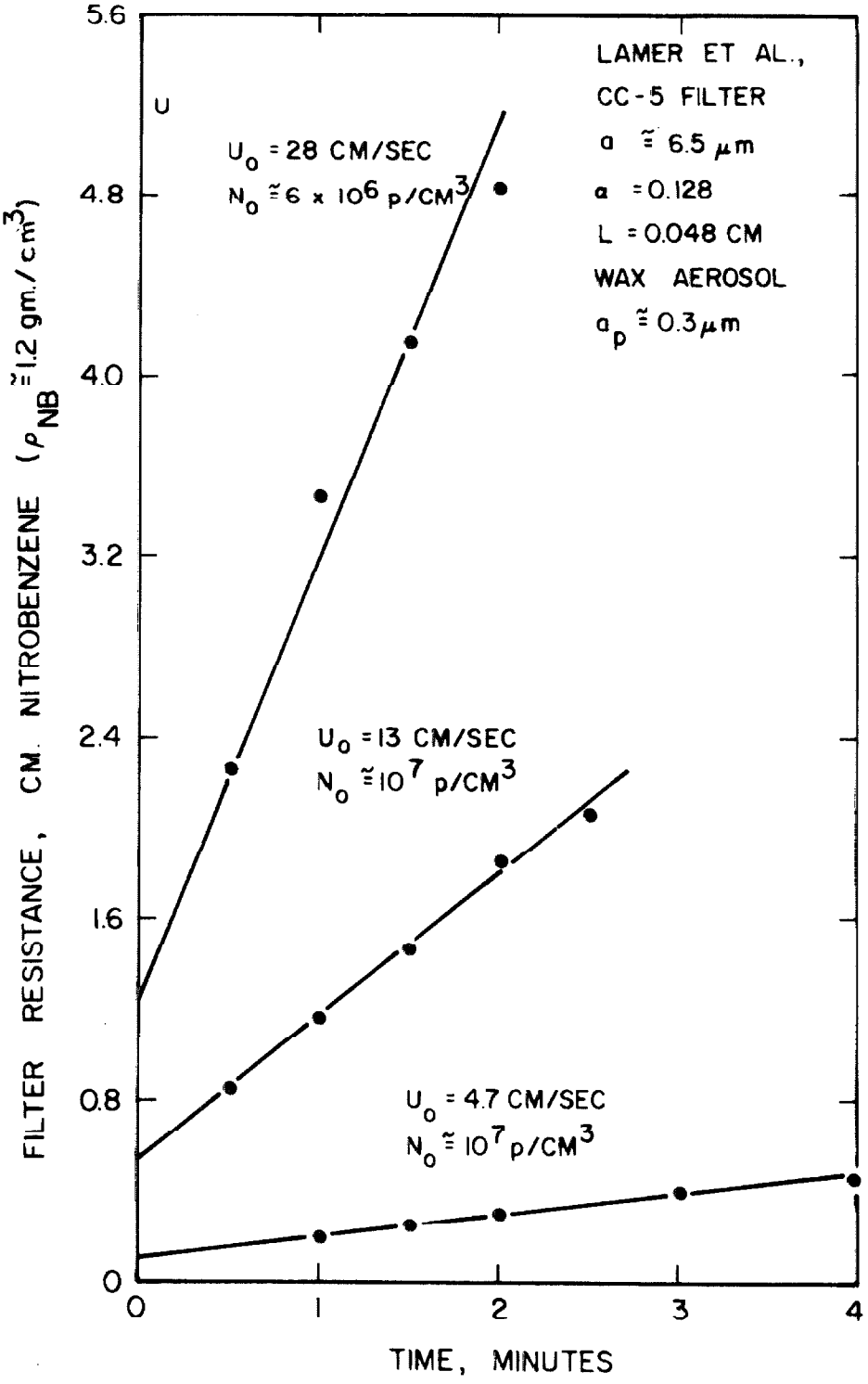

Figure 1-4. Filter Resistance During Operation

aerosol solidified (to crystals) on capture or shortly thereafter. In the study of Lindeken et al. (71), resistance and filter data were not included. The studies of Blasewitz (51), Pradel et al. (72), Smith and Suprenant (67) and others were performed with polydisperse clouds. Dorman (62) has recently presented considerable data on penetration and resistance changes with deposition for several filter media. The aerosols used were not monodisperse, and no data are available on particle concentration and size spectra for his test aerosols.

4. Effects of Particle Accumulation on Fiber Filter Performance

(a) Penetration and Accumulation

Let Z be the number of particles deposited per cm^2 of fiber cross-section normal to flow. The change in particle concentration when passing through a filter layer of thickness dx, with collection occurring on the fiber and on the deposit with efficiency $\eta(Z)$, is:

$$-\frac{dN}{N} = 2a\ell\,\eta(Z)\,dx \qquad (1\text{-}22)$$

where ℓ is the length of fiber (of radius a) per unit volume of filter mat as defined by equation (1-2):

$$\ell = \alpha/\pi a^2 \qquad (1\text{-}2)$$

If the change in deposition is small in the time required to pass through the filter (L/U_o), it is possible to integrate over the space from $x = 0$ to $x = L$, when concentration changes from N_o to N_L, to obtain:

$$\ln P = \ln(N_L / N_o) = -2\alpha \ell \int_0^L \eta(Z)\, dx \qquad (1\text{-}23)$$

The ratio of outlet to inlet aerosol concentration is defined as the filter penetration, P.

Define an average particle collection efficiency through the mat:

$$\eta_{AV} = \frac{1}{L} \int_0^L \eta(Z)\, dx \qquad (1\text{-}24)$$

Then:

$$\ln P = -2\alpha \ell L \eta_{AV} \,. \qquad (1\text{-}25)$$

At the start of filtration, with Z = 0:

$$\ln P(0) = -2\alpha \ell L \eta(0) \qquad (1\text{-}26)$$

where $\eta(0)$ is the fiber efficiency at the start of filtration, as given previously in equation (1-6). The difference in equations (1-25) and (1-26) becomes:

$$P = P(0) \exp\left(-2\alpha \ell L (\eta_{AV} - \eta(0))\right). \qquad (1\text{-}27)$$

Assume that the local collection efficiency of the fiber and the deposit can be represented in the form of an expansion as:

$$\eta(Z) = \eta(0) + S Z \qquad (1\text{-}28)$$

Second and higher order terms in the expansion of η (Z) with respect to Z have been omitted on the assumption that the $S_n Z^n$ ($n \geq 2$) terms are smaller than the leading terms. This assumption was tested experimentally as discussed in Chapter IV.

The coefficient S (cm^2/particle) is related to the area of the deposited particles and to the contribution of the deposit to the collection efficiency. The collection efficiency of the deposit will depend upon dimensionless capture groups similar to those given in Section B3 above. The geometry or area of the deposit will probably depend upon particle size and filtering velocity, and may depend upon fiber size as well. The coefficient S can be assumed to be independent of the filter structure (α, L) to a first approximation. No theory for particle capture by the deposit has been formulated as part of this investigation.

The distribution of deposited material within the filter is unknown, i.e., Z is an unknown function of x. The total accumulation of material throughout the depth per unit of filter face area can be determined from the inlet and outlet particle concentrations. Let this accumulation be A (deposited particles/cm^2 of filter face area). Then:

$$A = \int_0^L 2 \alpha \ell \, Z \, dx \qquad (1\text{-}29)$$

where $2a\ell\, dx$ is the projected area of fiber per unit filter face area (cm^2 fiber/cm^2 filter), and Z is the number of particles deposited per unit projected area of fiber (p/cm^2 fiber). Upon sub-

stituting equation (1-2) for the fiber length per unit volume of filter, the accumulation becomes:

$$A = \frac{2\alpha}{\pi a} \int_0^L Z \, dx \quad . \tag{1-30}$$

By integrating equation (1-28) over the length of the filter, and using the definition of equation (1-24), the average collection efficiency can be expressed as:

$$\eta_{AV} = \frac{1}{L} \int_0^L \eta(Z) \, dx = \eta(0) + \frac{S}{L} \int_0^L Z \, dx \tag{1-31}$$

and by using equation (1-30) for the integral of the local accumulation:

$$\eta_{AV} = \eta(0) + \left(\frac{\pi a S}{2\alpha L}\right) A \tag{1-32}$$

The filter penetration as a function of accumulation, equation (1-27), becomes:

$$P(A) = P(0) \exp(-SA) \quad . \tag{1-33}$$

An equation of continuity of matter for the whole filter mat requires that the rate of change of accumulation of particles in the mat be:

$$\frac{dA}{dt} = U_o N_o (1 - P(A)) \quad . \tag{1-34}$$

Integrating this equation, using the condition that $A = 0$ at $t = 0$, the accumulation for the mat becomes:

$$A = U_o N_o t + S^{-1} \ln\left[(1 - P(0))/(1 - P(A))\right]. \qquad (1\text{-}35)$$

The instantaneous penetration can be obtained by measurement of inlet and outlet concentrations at any time t. The accumulation in the filter mat is:

$$A = U_o N_o t\left[1 - \frac{1}{t}\int_o^t P(\tau)\, d\tau\right] \qquad (1\text{-}36)$$

where τ is a variable of integration. The cumulative accumulation over time interval Δt is:

$$A = U_o N_o \Delta t\,(\bar{E}) \qquad (1\text{-}37)$$

where $(\bar{E})$ is an average efficiency for the filter mat during time interval Δt. This definition of accumulation (A) has been used to determine S from filter mat tests in conjunction with equation (1-33), as discussed in Chapter III. The value of S has been determined from equation (1-28) by means of single fiber experiments discussed in Chapter IV.

(b) Resistance and Accumulation

Let F_D be the total drag force per unit length of a cylindrical fiber of radius a exposed to an aerosol stream at velocity U_o containing particles of radius a_p. As particles accumulate on the fiber and on previously deposited particles, the drag force will increase. Assume that the total drag force at any instant can be

represented by two independent terms, such as:

$$F_D = F_D(0) + (S_p \mu U_o a_p) 2a Z \qquad (1\text{-}38)$$

where $F_D(0)$ represents the initial drag force on the fiber at the start of deposition, $(S_p \mu U_o a_p)$ represents the drag per particle, and $2aZ$ is the local deposition of particles per unit length of fiber.

The drag force per unit volume of mat can be set equal to the pressure gradient (12):

$$\ell F_D = \frac{dp}{dx} \qquad (1\text{-}39)$$

where ℓ is the length of fiber per unit volume of mat (equation (1-2)) and p is the local pressure. By substituting equation (1-38) and integrating from $p = p_o$ at $x = 0$ to $p = p_L$ at $x = L$, the pressure drop across a filter mat becomes:

$$\frac{1}{L}\int_{p_o}^{p_L} dp = \frac{\Delta p}{L} = \ell F_D(0) + \frac{2a\ell}{L}(S_p \mu U_o a_p)\int_0^L Z\, dx . \qquad (1\text{-}40)$$

The increment in filter resistance arising from the deposition of particles will be:

$$\frac{\Delta p}{L} - \ell F_D(0) = \frac{\delta \Delta p}{L} = \frac{2a\ell}{L} \cdot \frac{\pi a}{2\alpha} \cdot A(S_p \mu U_o a_p) \qquad (1\text{-}41)$$

upon using equation (1-30) for the value of the integral of the deposition. The filter resistance as a function of accumulation becomes:

$$\delta \Delta p = (S_p \mu U_o a_p) A \qquad (1\text{-}42)$$

Equation (1-42) indicates that the resistance rise per unit of filter depth produced by the deposit ($\delta \Delta p/L$) should be proportional to the drag per particle ($S_p \mu U_o a_p$) and the particle concentration in the bed (A/L). Resistance rise has been studied experimentally as a function of accumulation and filtering velocity, as discussed in Chapter III.

As a first approximation, it has been assumed in equation (1-38) that the resulting drag of the deposited particles is independent of the characteristics of the filter material. It has been observed by others that, "Rapid clogging is more likely with materials of high packing density and fine fibers, ..." (1, p. 103) and "Thick fluffy...materials ...possess considerably greater dust holding capacity" (24, p. 213). These and other observations (2, p. 332) indicate that there may be some effect on deposited particle resistance proportional to L, α, or a. Variation of the coefficient S_p with the filter depth (L) and fiber fraction (α) is discussed in Chapter III. Effects of particle size and fiber size were not included in the present study.

II.

EXPERIMENTAL APPARATUS AND PROCEDURES

A. Apparatus

1. Description of Operation

Twelve fiber filters and seven single fibers were exposed to aerosol flow for varying periods to determine the effects of particle deposit on fiber collection efficiency and on filter resistance. A schematic diagram of the experimental apparatus used in these studies is presented in Figure 2-1. A photograph of the laboratory installation is included in Figure 2-2. Construction details are provided in Appendix 2-1.

In operation, a suspension of Dow polystyrene latex spheres ($\rho_p = 1.05$ gm/cm^3) was sprayed to a fine mist by atomizer A in Figure 2-1. The mist was then mixed with air from dryer B. The liquid evaporated, leaving an airborne suspension of monodispersed polystyrene spheres of 1.305-microns diameter.

The mist was electrically charged by the spraying process, and the aerosol particles contained a residual charge of unknown magnitude. To reduce this charge, the aerosol was mixed in a tee with an air stream containing bi-polar air ions from a sonic jet ionizer at C. The aerosol then passed through an annular precipitator D, with a 1-cm gap spacing, about 5 feet long. A low voltage d.c. power supply provided a radial field to precipitate any highly charged particles remaining. The charged aerosol particles deposited on the outer wall of the annulus which was

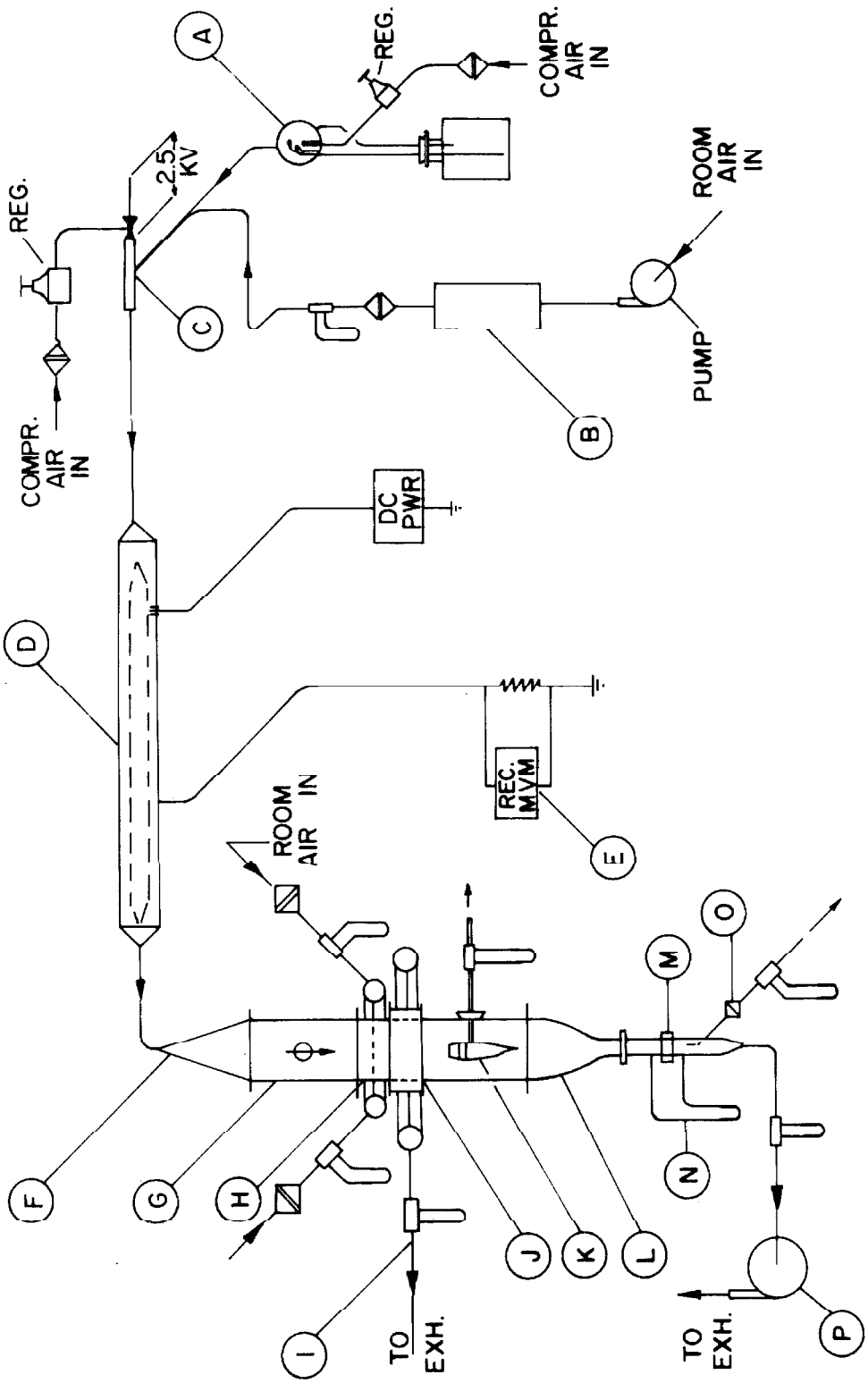

Figure 2-1. Schematic Diagram of Experimental Apparatus

LEGEND FOR FIGURE 2-1

A. Liquid Sprayer for Particle Suspension

B. Silica Gel Drying Column

C. Aerosol-Ion Mixing Tee

D. Electrostatic Precipitator

E. Recording Millivoltmeter

F. Aerosol Tunnel Entrance

G. Aerosol Dilution and Mixing Section

H. Dilution Tube Bank

I. Extract Exhaust Line

J. Extraction Section

K. Upstream Sampling Probe

L. 16:1 Tunnel Contraction

M. Test Section

N. Test Section Static Pressure Taps

O. Downstream Sampling Probe

P. Main Exhauster

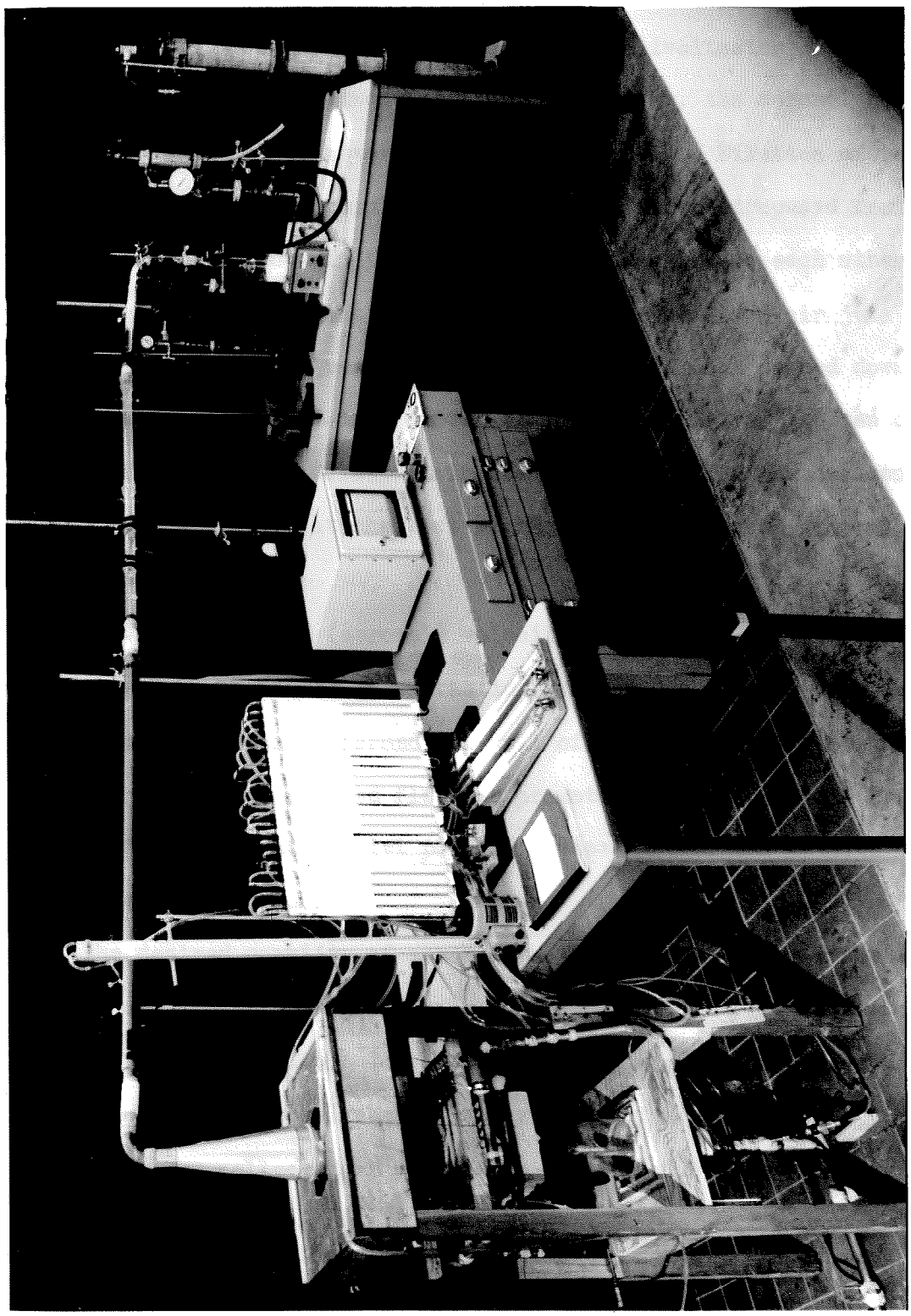

Figure 2-2. Photograph of Experimental Apparatus

grounded through a large resistor. The voltage drop across the resistor registered on the high impedance recording millivoltmeter E.

After leaving the electrostatic precipitator, the aerosol entered the top of a 6-inch diameter aerosol tunnel* at F. Dilution of the entering aerosol was accomplished by air jets directed upward from holes in a grid of ten tubes in two layers at right angles to each other at H. Mixing was promoted by the intermingling of the dilution air jets and the oncoming aerosol stream at G. The diluted aerosol passed down through the grid (~ 1-inch center-to-center) formed by the ten diluter tubes. The amount of dilution air was determined from the desired aerosol concentration at the test section and the aerosol generator air requirements.

To vary the fluid (aerosol) velocity at the test section, excess aerosol was removed through extraction section J following dilution. A cylindrical wire screen formed the wall of the tunnel in the extraction section. Symmetric outward flow was promoted by a cylindrical baffle between the screen and outlet pipes. Excess aerosol was metered and discharged through tube I.

The desired quantity of aerosol containing the proper concentration of particles left the extraction section through a single 16-mesh screen to promote uniform flow. The aerosol then entered the upstream sampling section where an aerosol sample was extracted isokinetically by probe K. Particles were collected on a membrane filter held in the probe. The

---

* The aerosol tunnel and contraction were built with the assistance of Mr. Elton Daly, Shop Supervisor, Hydraulics and Water Resources Laboratory, W. M. Keck Engineering Laboratories, Calif. Inst. of Tech., Pasadena, Calif.

probe was removed and the filter analyzed microscopically for particle number concentration.

The remaining aerosol passed through a 16 to 1 contraction, L, to test section, M. Design of the contraction (Figure 2-3) was based on a paper by Tsien (75). Offsets (x', R') are given in Appendix 2-1. They were scaled down from a similar design used for the entrance section of a 4-inch round wind tunnel.* The contraction was formed on a smooth waxed wooden pattern by applying layers of epoxy resin and fiberglass.**

The test section consisted of two pieces of 1-1/2 inch diameter hard-drawn copper tubing, each three inches long. A modified brass union was used to hold test mat and fiber specimens, as shown in Figure 2-4A. Static pressure holes (0.040 in. diam.) and pressure taps were provided to measure pressure differential across the test section screens and filters.

Filter mats were held in the test position by the two halves of the union and the union nut. They were retained between two screens supported by rings and a stiffening cross as shown in detail in Figure 2-4B. Distances of 1, 2, and 3 mm between the two screens were set by spacers. Two gaskets were made from all-glass filter paper and placed on either face of the test mat to reduce edge leakage or aerosol by-passing. Aluminum foil gaskets of the same diameters as the glass paper gaskets were placed between them and the screen surface to promote compression.

---

* Design specifications were kindly furnished for this study by Prof. F. Raichlen, Hydraulics and Water Resources Laboratory, W. M. Keck Engineering Laboratories, Calif. Inst. of Tech., Pasadena, Calif.

** Fabricated by Mr. Frank Pine, AMCO Corp., 541 S. Fair Oaks Ave., Pasadena, Calif., approx. cost $100.

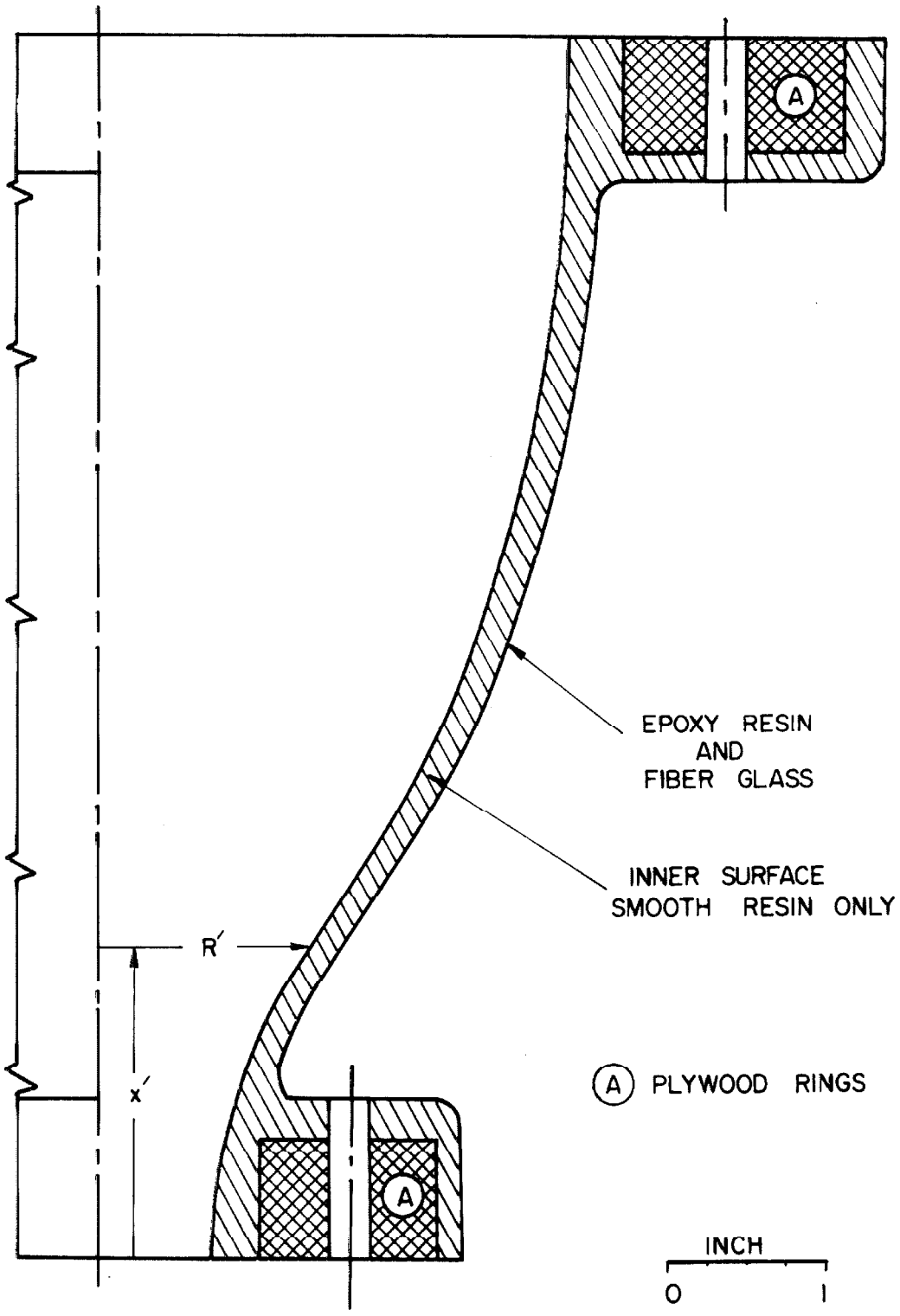

Figure 2-3. Aerosol Tunnel Contraction

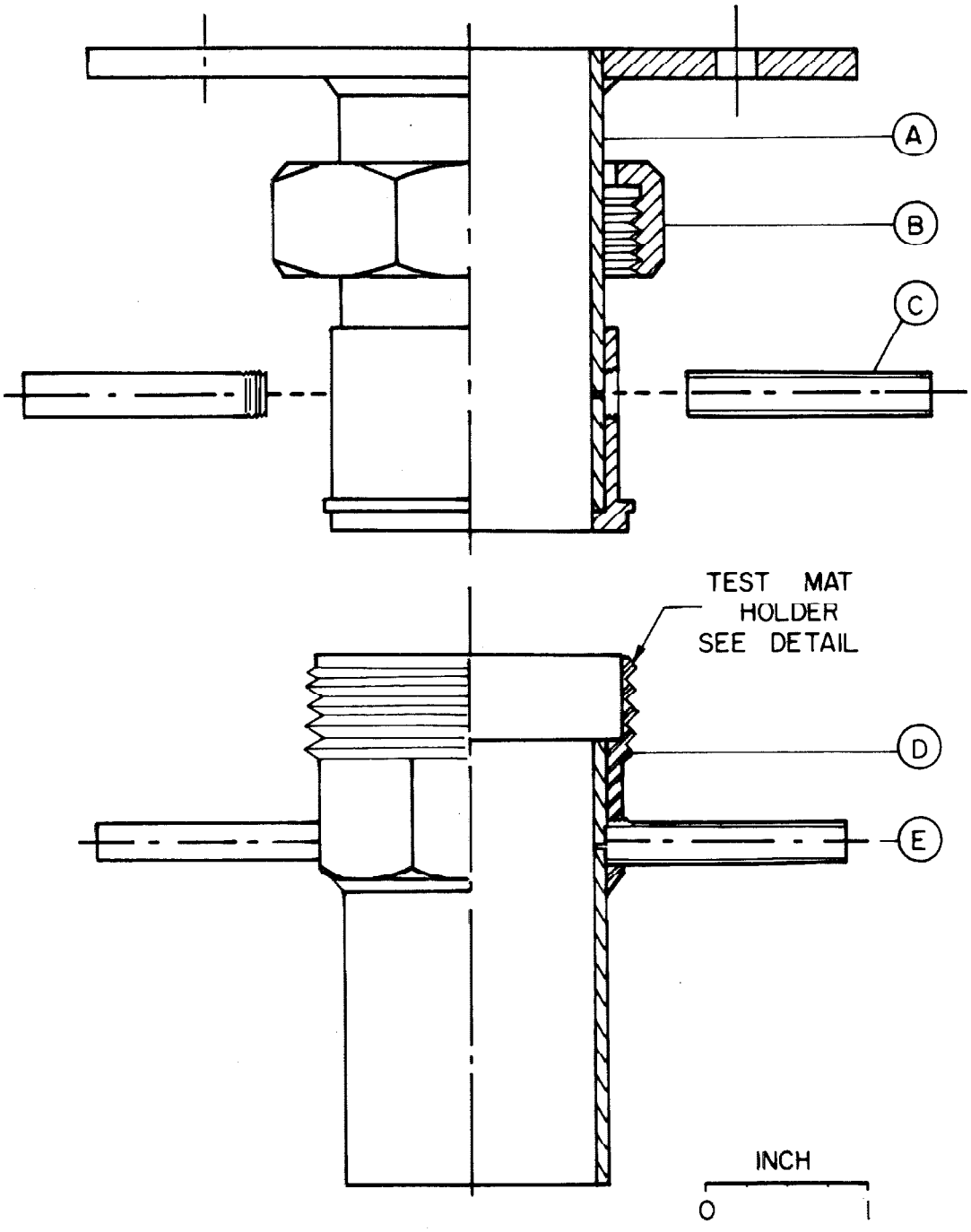

Figure 2-4A. Aerosol Tunnel Test Section

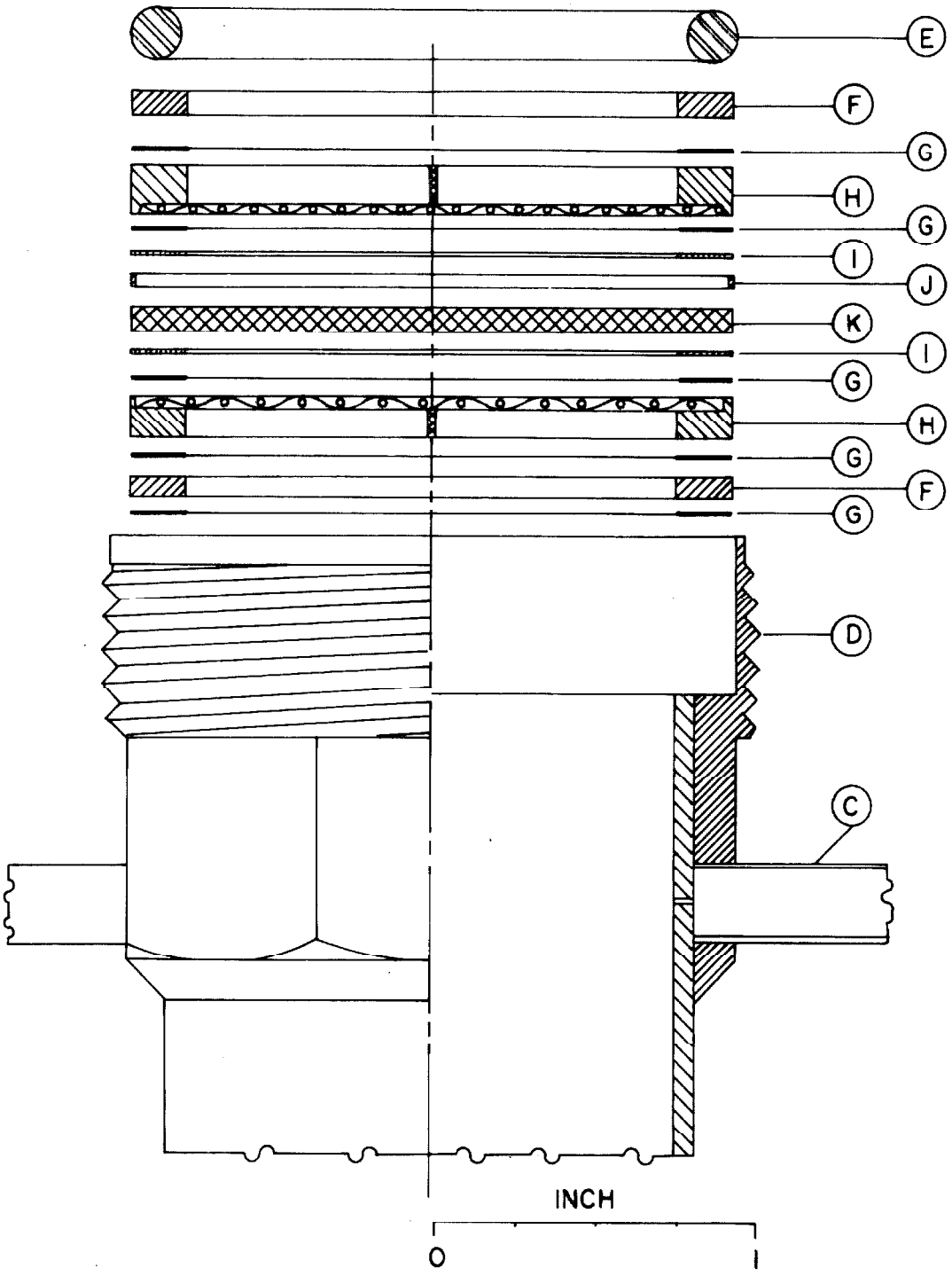

Figure 2-4B. Test Filter Holder Detail

LEGEND FOR FIGURE 2-4

A. Test Section Inlet from Contraction

B. Test Section Union Nut

C. Static Pressure Tap

D. Test Mat Holder and Test Section Outlet

E. Neoprene "O"-Ring

F. Aluminum Spacer Ring

48 mm O.D.x39 mm I.D.x2 mm Thick

G. Aluminum Foil Gasket (48x40)

H. Filter Mat Retaining Screen and Spacer

48 mm O.D.x39 mm I.D.x4 mm Thick with Soldered Screen (16 mesh x 0.010 in wire) and Reinforcing Cross

I. Glass Fiber Paper Gasket

48 mm O.D.x40 mm I.D.x1 mm Thick

J. Filter Thickness Spacer

48 mm O.D.x46 mm I.D.x1 mm or 2 mm Thick

K. Typical Test Filter Mat

Additional aluminum ring spacers and foil and rubber gaskets were used as required to fill the test section holder, and prevent leakage. A neoprene "O" ring was used between the top aluminum ring spacer and the companion flange of the upper half of the test section union as shown in Figure 2-4B. The whole assembly was placed up on the mating flange on the aerosol tunnel test section entrance and the union nut was screwed down to a firm tightness.

After passing the filter, the remaining particle concentration was sampled by a probe at 0 (Figure 2-1). The downstream sample filter holder was located outside of the tunnel because of size limitations. The remaining aerosol then passed through a flowmeter to variable speed exhauster P.

2. Criteria for Design of an Aerosol Tunnel

A wind tunnel for use in experimental fluid mechanics provides a controlled and reproducible velocity, pressure, and temperature field at its test section. An aerosol tunnel must also provide a defined particle field at the test section. Requirements of constant particle size and concentration for the particulate phase affect the design of an aerosol tunnel. Factors which must be considered include generation, sampling, and analysis of the particles, particle interactions with the tunnel walls, grids, etc.

The following criteria were developed during the design and construction of the aerosol tunnel used in this study. The tunnel should:

a) provide a uniform, reproducible aerosol flow field (particles and fluid) at the test section,

b) have low turbulence at the test section but turbulence reducing devices (wire mesh, grids, or honeycombs) should not remove substantial fractions of the particles (to reduce subsequent reentrainment of agglomerates).

c) supply aerosol particles to the test section at constant rate for extended periods (days).

d) have provision for the independent variation of particle concentration and fluid velocity.

e) have provision for continuous sampling or monitoring of particle size and concentrations with minimum disturbance to the aerosol stream,

f) provide means for measurement and control of particle electrostatic charge,

g) be oriented so that gravitational effect on particles is minimal,

h) be accessible for easy cleaning.

These criteria were developed with filter testing as the primary purpose of the tunnel. Additional criteria might be needed for other aerosol studies.

B. Test Procedure and Sample Analysis

1. Fiber Filter Test Procedure

Test mats were prepared by cutting circles (4.5-cm diameter) from a thin lap ($\sim$ 5 mm) of laboratory glass wool. No binder, lubricant, or adhesive was present on the fibers ($\sim$ 10-microns diameter, $>$ 10-cm long). Test filters were formed from 1/3, 2/3, 1, 2, or 3

layers of the lap, and were weighed after dessication. The desired thickness was placed in the aerosol tunnel test section holder. The resistance of the clean filter was measured at several air flow rates with an inclined manometer (10:1) containing petroleum gage oil (sp. gr. 0.826). Calibrated orifice meters were used to measure air flow through the test mat.

A dilute suspension of particles was placed in the reservoir of the spray generator and an aerosol was generated at the desired test flow rate. Aerosol samples were taken up- and downstream of the test mat in each 15-minute period for the first hour, and occasionally thereafter. Sampling time was usually 3 minutes. Up- and downstream sample volumes were 0.21 and 2.1 l/min, respectively, at 13.8 cm/sec test section velocity.

Aerosol particle concentrations were obtained by counting particles as described below. Continuous monitoring of aerosol particle concentration was conducted in some tests by means of light scattering photometers.

Test fiber filters were run for periods ranging from several hours to several days. A continuing record of filter resistance was kept. When the resistance had increased an appreciable amount, the aerosol flow was stopped and a final resistance-flow check was made. Final filter weight was recorded after dessication.

2. Analysis of Samples for Particle Concentration

Membrane filters used to collect particles from samples of the tunnel aerosol stream were removed and analyzed by counting individual particles in defined areas. Used filters were cut into two halves with

a scalpel and one half was stored for reference. The other half was placed face up on a clean glass microscope slide and three drops of immersion oil* were placed on the filter near its periphery. After the semicircular filter had become transparent, its radial bisector was examined with a compound microscope** using a 100X oil immersion objective. The 1.305-micron spherical particles were clearly visible and a distinctive green color. A field was defined by a Whipple reticule in one eyepiece (76). (Field area was measured initially with an AO stage micrometer.)

All particles in the defined field were counted across two grids in the radial direction. Area counted was usually 0.005 cm^2, or about one-thousandth of the filter surface exposed to the aerosol. Particle counts ranged from about 200 to 2000 per total counted area depending upon aerosol concentration, sampled volume, etc. A separate count was obtained for observed multiple particles. These ranged from 5 to 15 percent of the total count, depending upon hydrosol dilution, aerosol sample size, generator air pressure, etc.

Aerosol particle concentration (particles/cm^3 of air) was calculated from the total particle count (including multiplets as one particle) and the total air volume as obtained from calibrated flowmeters located in each probe.

---

* R. P. Cargilles, New York, N.Y., Type B viscosity, N_D = 1.5150.
** American Optical Co., Buffalo, N.Y., Binocular, Series 10, Micro-Star Microscope with 15X WF oculars.

3. Single Fiber Test Procedure

Single 10-micron diameter glass fibers were taken from the roll stock used for test mat preparations. Fibers were used as removed without further treatment. They were placed on an aluminum spacer ring (48 mm O.D.x39 mm I.D.x3 mm thick) and held in place by strips of "Scotch" brand cellophane tape as shown in Figure 2-5.

A one-thousandth inch (~ 25 micron) tungsten wire had been previously stretched across the ring and mounted as shown at right angles to the glass fiber. For stability, a drop of adhesive ("Scotch" cellophane tape adhesive thinned with benzene) was used to fasten the glass fiber to the tungsten wire where they crossed. These manipulations were performed with the help of a stereoscopic microscope and dissecting needles.

The single fiber test preparation was then examined in the binocular microscope*, using a 40X short mount metallurgical objective** (NA ~ 0.6, working distance ~ 1 mm) corrected for use without a cover glass. The fiber was inspected for cleanliness and reasonable strength, and then photographed in the region marked "OA" in Figure 2-5 (about 2 mm from the junction). The field of view there was judged to represent a part of the fiber that was fairly free from interference effects of the tunnel wall, the tungsten support, or the glue drop at the junction.

---

* See footnote, page 47 .

** AO-Spencer Lens, Catalog No. 1289, Serial No. C79109, kindly furnished for these studies by J. Perschelli, Instrument Division, American Optical Co., Los Angeles, Calif. (not parfocal).

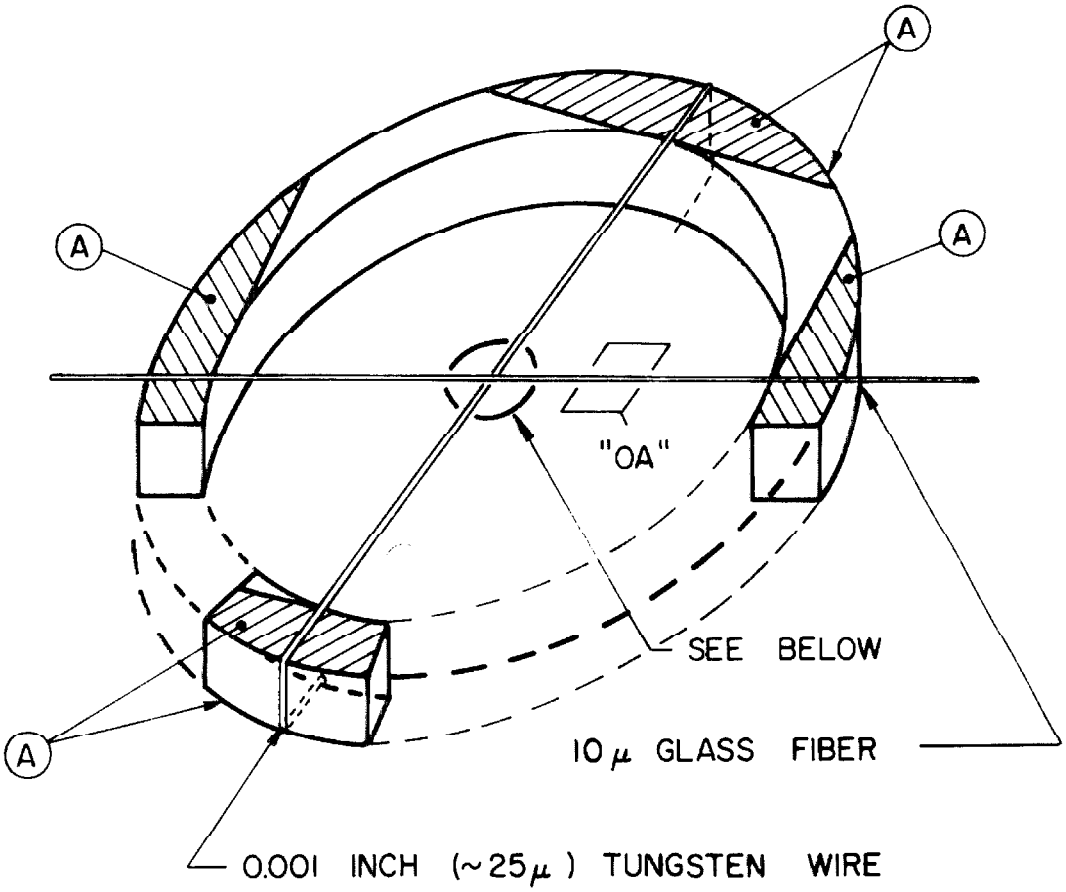

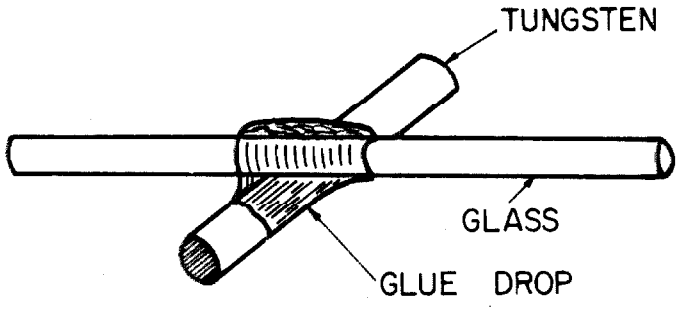

Figure 2-5. Single Fiber Test Preparation

The fiber preparation was installed in the tunnel test section and exposed to aerosol flow at a known rate for periods of one-half to two hours. It was removed and the deposit photographed and analyzed in the microscope. This procedure was repeated until the deposit became too heavy to analyze.

The aerosol particle concentration was established before inserting the fiber preparation, by operating the tunnel with an open throat or with a test mat in place. Up- and downstream aerosol samples were taken with the sampling probes in the manner described in a previous section. The concentration determined from these samples was used to estimate the value during the fiber exposure. Because of the tenuous nature of the deposit structure on the single fiber, the tunnel was not opened (thus changing the pressure suddenly) to insert or remove sampling probes during these accumulation tests.

4. Measurement of Particle Accumulation on Single Fibers

After exposure to aerosol, the single fiber test mounting was removed from the aerosol tunnel in the lower half of the test section. The whole assembly was covered and taken to the microscopy room. All manipulations were performed as gently as possible. The aluminum ring holding the glass fiber and wire cross was carefully placed on a slide on the microscope stage. Under low power (10X objective), the fiber-wire cross was aligned with the center of the graticule defining the field of view. The fiber was then moved over a fixed amount so that the region shown as "OA" in Figure 2-5 was viewed again. The low power objective was then carefully replaced by the 40X metallurgical objective and the fiber and structures brought into focus. A through-

focus series of photographs was obtained. The depth of the deposit on the fiber usually required that 5 to 10 photographs be taken, in order to record the total 3-dimensional structure. Successive photographs of the field were taken at 2-1/2 micron intervals in the vertical traverse. Each roll of film was also used to record the stage micrometer at the same magnification.

After photography, the deposit was evaluated by counting and recording the number of individual particles present in each structure. Usually, a few hundred particles were counted, in several adjacent fields. Only the first field viewed was photographed.

Only the top half of the fiber and structures was examined and analyzed. A preliminary investigation had indicated that a negligible number of particles was present on the rear half of the fiber, at the velocities employed in these studies. This confirms the findings of Wright et al. (20) whose photographs were taken looking into the side of the deposit (perpendicular to flow). Little or no deposition was observed on the rear half of their fibers.

III.

FIBER FILTER TEST RESULTS AND DISCUSSION

A. Time Dependence of Particle Accumulation

Twelve glass fiber mats of varying depth and density were used to filter 1.305-micron polystyrene spheres for periods of 477 to 2728 minutes. Test air velocities ranged from about 14 to 139 cm/sec. Velocity was maintained constant in each test. Up- and downstream aerosol samples were taken occasionally during tests, and analyzed for particle concentrations. Filter resistance was observed and recorded periodically. A summary of test data and results is presented in Table 3-1. Some changes were made in aerosol generation and sampling during these tests, as indicated.

At the end of each test, a cumulative record was prepared of (a) filter operating time, (b) filter resistance, (c) filter penetration, and (d) aerosol particle concentrations. These records are reproduced in Appendix 3-1. The data were used to construct time graphs of variations in filter resistance, filter penetration, and aerosol concentration for each test mat.

Cumulative particle deposition (accumulation) in the filter was calculated ($60U_o \Delta t \overline{\Delta N}$) for various intervals of time (Δt) during each test. The average difference in up- and downstream aerosol concentration ($\overline{\Delta N}$) was estimated from the concentration-time plot. Arbitrary time intervals were selected to coincide with major events during the test. Shorter time intervals (50 and 100 minutes) were used during preliminary data reduction on early tests. No major changes in total

TABLE 3-1

Summary of Fiber Filter Test Data and Results

Test No.	Test Time min.	Vel. cm/sec	Total Accum. 10^6p/cm^2	Filter Depth cm	Filter Weight gm	Resistance[a] Init.	Resistance[a] Final	Efficiency Init.	Efficiency Final	Sample Probe[b]	Aerosol Gen.[c]	Ions[d]	Pptr.[e]
1	2678	139	406	0.29	0.383	1.40	1.78	0.91	0.98	I	I	-	-
2	1876	13.8	47	0.21	0.254	0.070	C.0745	0.44	0.54	I,II	I	-	-
3	572	13.8	121	0.21	0.141	0.0355	0.0470	0.24	0.38	II,I	I	-	-
4	779	13.8	167	0.21	0.108	0.0275	C.0350	0.44	0.46	I	I	-	-
5	2728	13.8	1097	0.21	0.129	0.0310	C.0990	0.33	0.70	I	I	-	-
6	1636	13.8	391	0.21	0.129	0.0330	C.0500	0.42	0.64	I	II	on	-
7a	1773	13.8	402	0.11	0.039	0.0085	C.0190	0.21	0.38	I	II	on	170[f]
7b	942	13.8	434	0.11	0.069	0.0195	C.0450	0.32	0.63	I	II	on	170
7c	1440	13.8	597	0.11	0.120	0.0380	C.0790	0.50	0.72	I	II	on	170
8	1084	13.8	177	0.11	0.034	0.0070	C.0130	0.11	0.19	III	II	on	170

TABLE 3-1 (cont'd)

Test No.	Test Time min.	Vel. cm/sec	Total Accum. 10^6p/cm^2	Filter Depth cm	Filter Weight gm	Resistance[a] Init.	Resistance[a] Final	Efficiency Init.	Efficiency Final	Sample Probe[b]	Aerosol Gen.[c]	Ions[d]	Pptr.[e]
9	1170	29	1069	0.11	0.053	0.0280	0.1570	0.29	0.40	III	II	on	170
10	477	58	803	0.11	0.040	0.0460	0.1545	0.28	0.40	III	II	on	170

a. Resistance, inches of petroleum gage oil (sp. g. 0.826).
b. Sample probes I, II, and III illustrated in Appendix 2-1.
c. Aerosol generators I and II operated at 30 and 60 psig pressure, respectively; shown in Appendix 2-1.
d. Ionizer operated at 30 psig pressure and 2500 volts a.c.
e. Electrostatic precipitator operated at 170 volts d.c. on center tube; outer tube grounded.
f. Some parts of test conducted at different collecting voltages.

accumulation were observed as a result of taking longer intervals.

Calculated values of particle accumulation for each test are tabulated in Appendix 3-2. The instantaneous value of filter resistance and filter penetration at the end of each time interval (Δt) was estimated from the time plots of these variables. The instantaneous values are also given in the tables in Appendix 3-2.

The accumulation of particles as a function of time is shown in Figure 3-1 for test mat numbers 7a, 8 and 9 and 10. These four mats were composed of 1/3-layer of fiber lap in 0.11-cm depth (Table 3-1), and represented an attempt to obtain uniform particle deposition in a differential thickness. The shape of these curves is consistent with the form of the equation derived for the variation of accumulation with time (Chapter I, Section D4a, equation (1-35)).

B. Initial Filter Resistance

The initial resistance of the twelve fiber filters tested in this study was used to calculate the resistivity:

$$K_o' = \frac{\Delta p(o)}{L} \cdot \frac{a^2}{\mu U_o} \quad . \qquad (1\text{-}20)$$

The coefficient K_o' is a function of the solids fraction, α , for slow viscous flow ($Re < 1$). Count median fiber diameter ($d_f = 2a$) was determined to be 9.54 microns ($\sigma g = 1.07$) from microscopic measurement of 100 fibers, as shown in Appendix 3-3. Reynolds numbers based on this fiber diameter ranged from 0.087 (13.78 cm/sec) to 0.88 (139 cm/sec). Values of the experimental resistivity (K_o') and solids fraction (α)

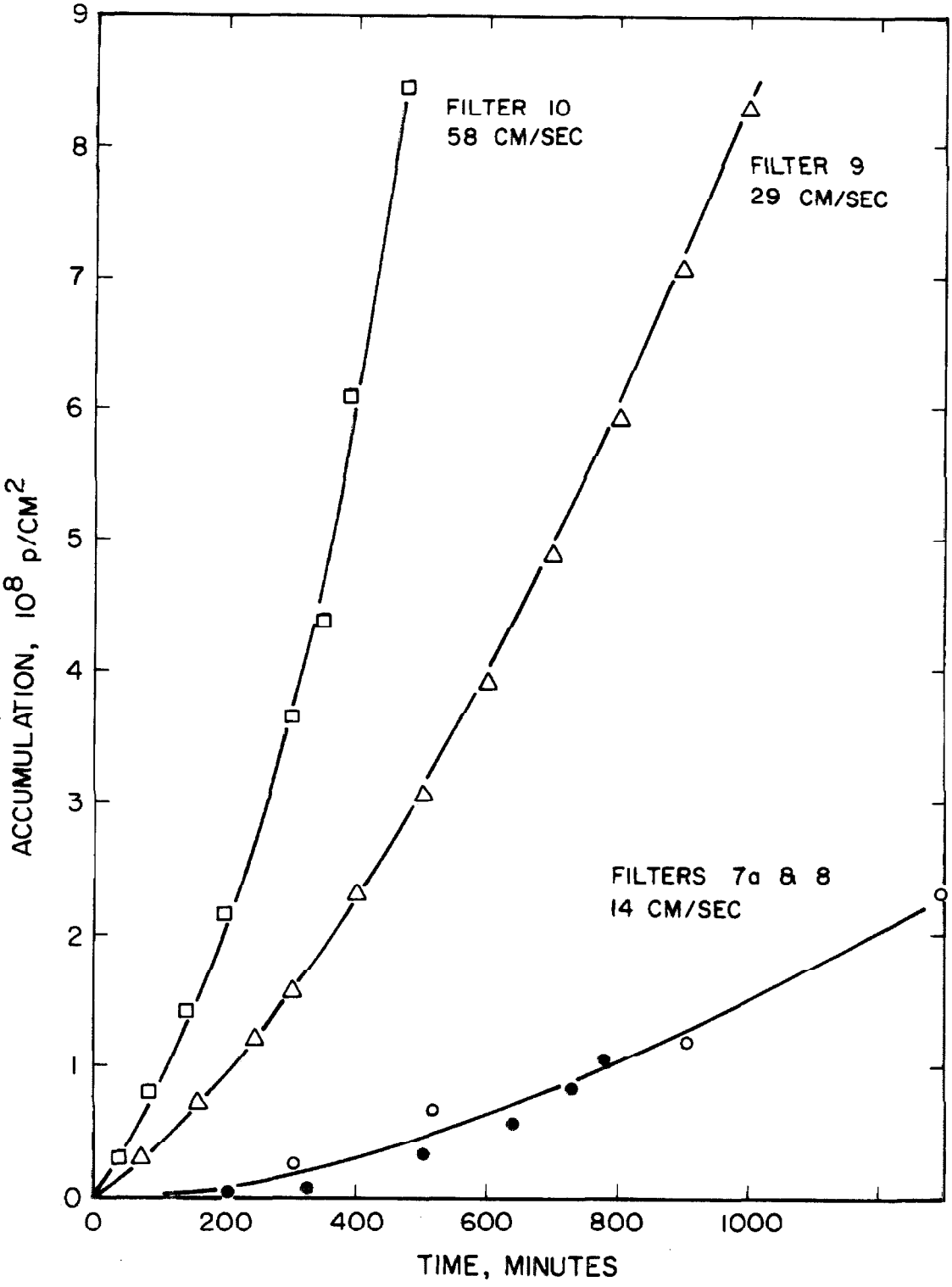

Figure 3-1. Time Dependence of Particle Accumulation

are given in Table 3-2. Initial resistance, velocity, and mat depth used to calculate K_o' are shown in Table 3-1.

Solutions of the Navier-Stokes equations for flow over a bounded cylinder have been discussed in Chapter I, Section C. The theoretical resistivity from these solutions is of the form:

$$K_o(\alpha) = 8\alpha/(-\ln\alpha - C_o + C_1\alpha - C_2\alpha^2) \qquad (3\text{-}1)$$

where the coefficients C_i are of order one. For $\alpha << 1$, as in these experiments ($0.007 < \alpha < 0.035$), the theoretical resistivity is approximately:

$$K_o(\alpha) = 8\alpha/(-\ln\alpha - C_o). \qquad (3\text{-}2)$$

The coefficient C_o has been found to be 1.0 by Happel and Brenner (12) and 1.5 by Kuwabara (13), and Pich (49).

Experimental resistivity (K_o') is plotted in figure 3-2 as a function of α for the 12 test mats. Experimental values of the resistivity lie slightly below the theoretical values in all but one case.

Experimental data were also used to calculate values of C_o, as indicated in Table 3-2. The arithmetic average value of C_o was found to be about one-half in these tests.

C. Effect of Particle Accumulation on Filter Penetration

Fiber filtration of an aerosol containing solid particles produces a decrease in particle penetration as a function of the accumulation of particles. Accumulation (p/cm^2 of filter face area) was determined for

TABLE 3-2

Resistivity of Test Filters

Test Filter No.	Fiber Fraction α[a]	Experimental **Resistivity** K_o'	Theoretical **Resistivity** $K_o(\alpha)$	Calculated C_o[b]
1	0.0324	0.0948	0.106	0.70
2	0.0296	0.0680	0.0941	0.04
3	0.0164	0.0336	0.0421	0.21
4	0.0126	0.0268	0.0299	0.61
5	0.0151	0.0306	0.0379	0.24
6	0.0151	0.0321	0.0379	0.42
7a	0.00871	0.0158	0.0186	0.34
7b	0.0155	0.0372	0.0390	0.84
7c	0.0271	0.0704	0.0832	0.53
8	0.00756	0.0130(est.)	0.0156	0.25
9	0.01186	0.0247	0.0276	0.59
10	0.00905	0.0203	0.0196	1.13

a. α = wt./Area·Depth·ρ_m; fiber glass density $\rho_m = 2.54$ gm/cm^3.
b. $C_o = \ln(1/\alpha) - 8\alpha/K'_o$.

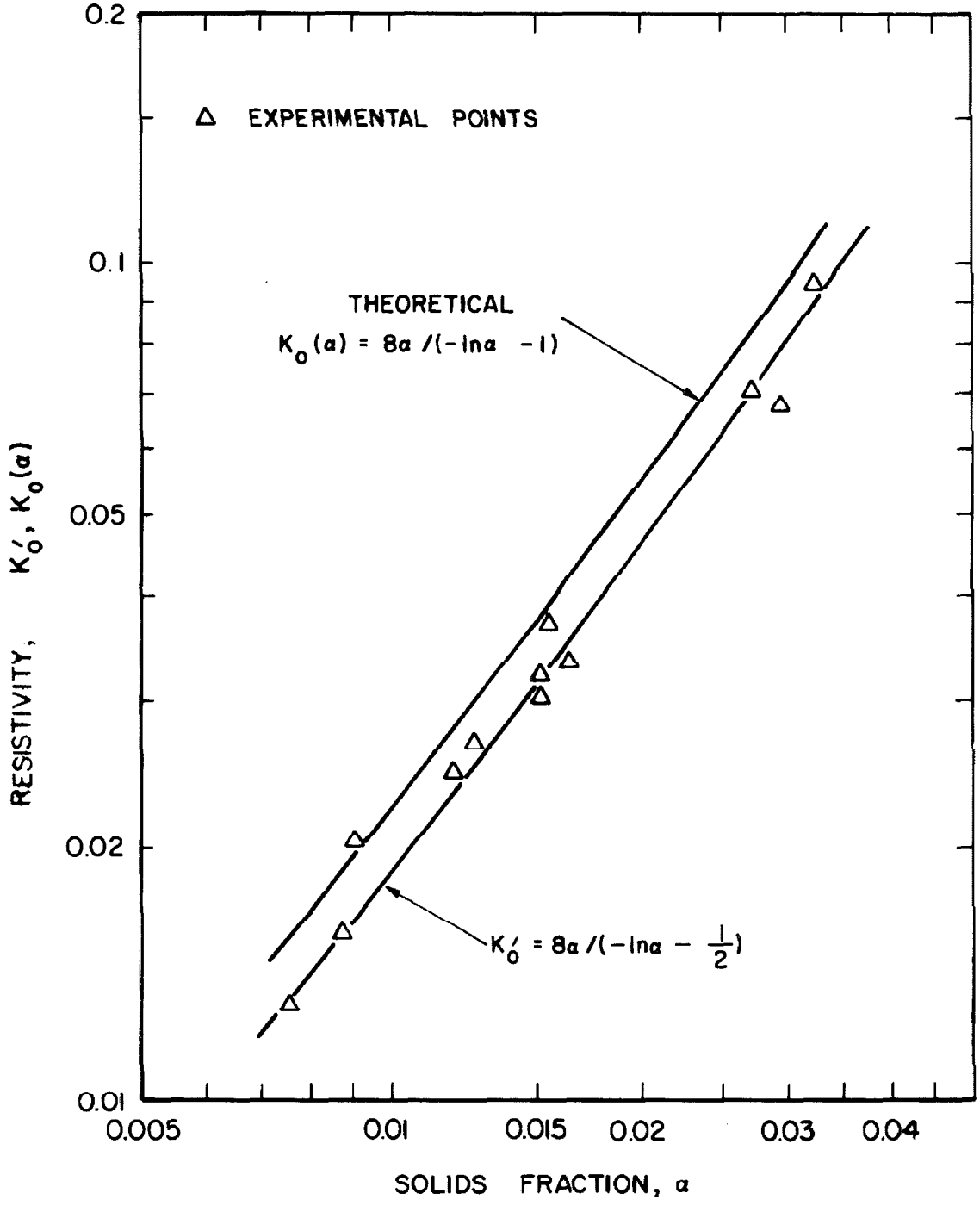

Figure 3-2. Theoretical and Experimental Fiber-Filter Resistivities

each filter as shown in tables in Appendix 3-2. Experimental penetrations were plotted at several values of accumulation, as shown in Figures 3-3 and 3-4. A line of best fit was drawn among the points by observation. No attempt was made to apply statistical curve-fitting techniques. Changes in slopes of the lines for data of test nos. 1 and 7a was due to experimental errors.

Filter penetration resulting from accumulated deposit was shown to be (Chapter I, Section D4a):

$$P(A) = P(0)\exp(-SA). \qquad (1\text{-}33)$$

Values of S were calculated as shown in Table 3-3. The coefficient S was assumed to be a constant in the analysis presented in Chapter I. It should be related to the geometry of the deposit structures and the capture efficiency of the structures for additional particles. The average value of S for the 12 test filters was 1.88×10^{-9} cm^2/p. Variations in the coefficient did not seem to be related to velocity, filter structure, length of test, or total accumulation. The reason for the substantially larger values of S found in test numbers 1 and 2 is not known. The average value of the coefficient for the tests numbered 3 through 10 (excluding tests 1 and 2) was 1.13×10^{-9} cm^2/p (range 0.6 to 2.5). In three out of four replicate tests (numbers 4, 5, and 6), the coefficient varied from 0.60 to 0.68×10^{-9} cm^2/p. The original assumption that the coefficient S should be a constant seems to be approximately correct.

Values of particle accumulation were estimated from the data of LaMer et al. (68), shown in Figure 1-3. Their average wax aerosol

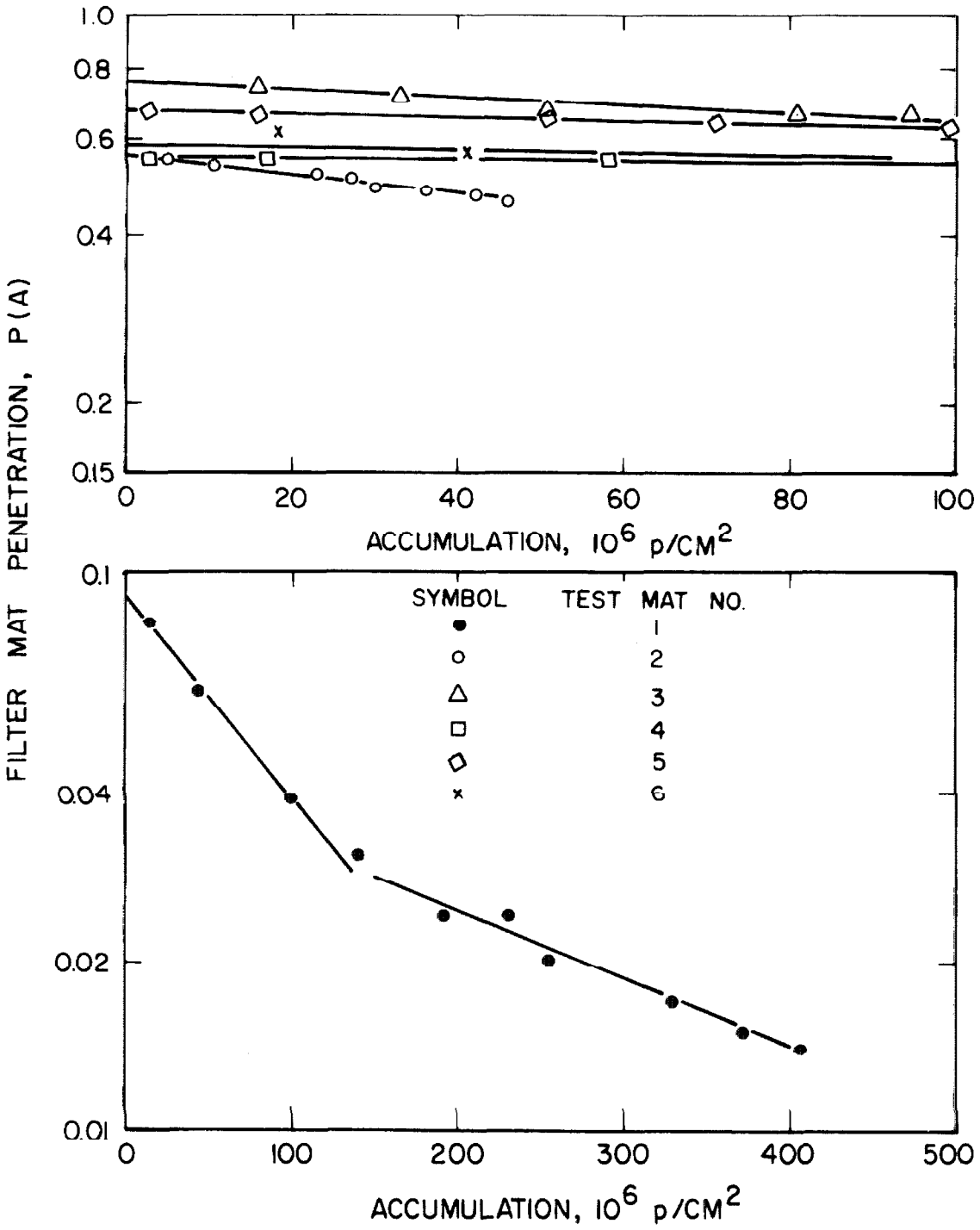

Figure 3-3. Penetration Decrease as a Result of Solid Particle Accumulation in Tests 1-6

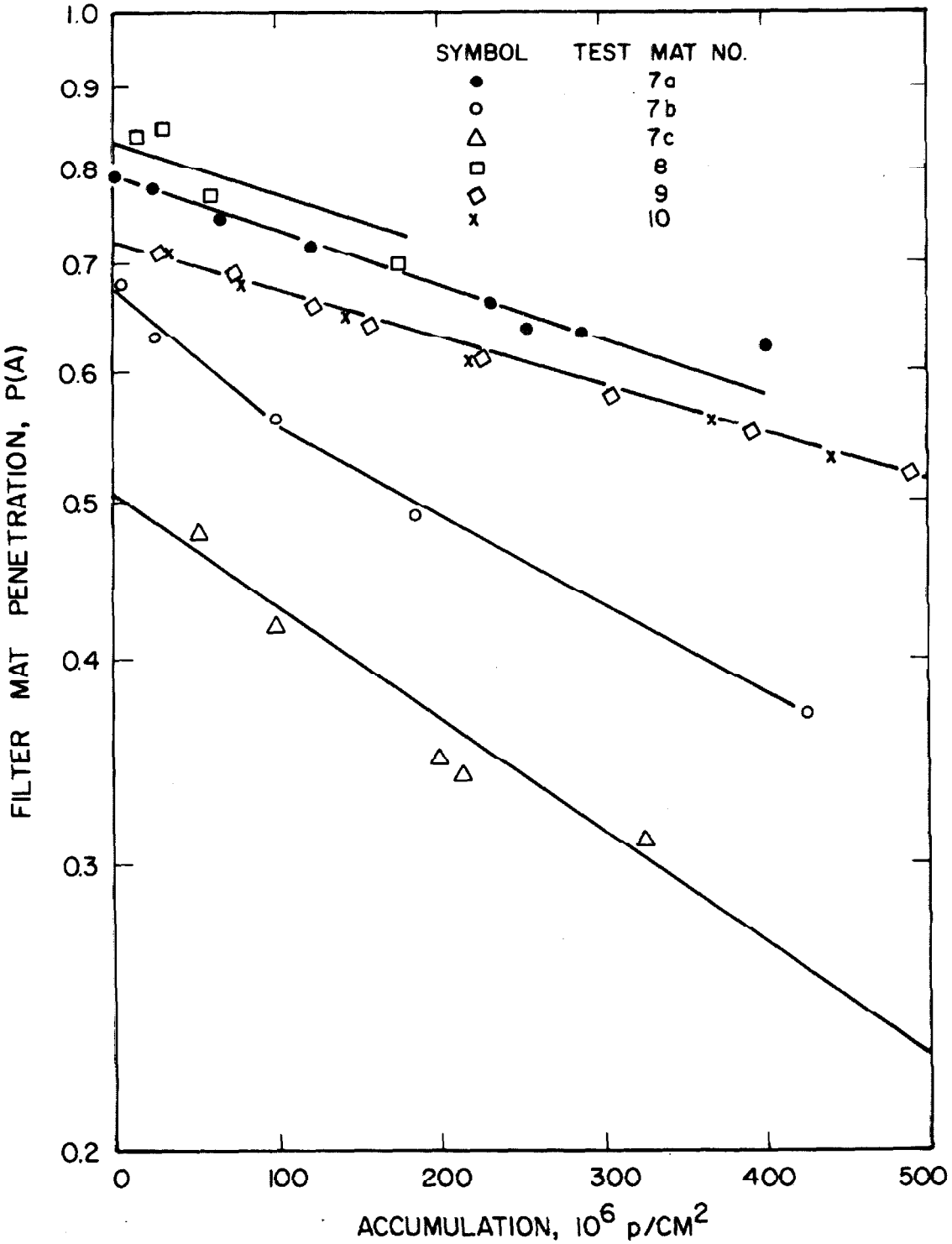

Figure 3-4. Penetration Decrease as a Result of Solid Particle Accumulation in Tests 7a-10

TABLE 3-3

Filter Penetration and Particle Accumulation

Test Filter No.	P(0)[a]	P(A)[b]	S[c] 10^{-9} cm^2/p
1	0.09	0.045	6.9
2	0.56	0.45	4.3
3	0.76	0.64	1.8
4	0.56	0.54	0.60
5	0.67	0.62	0.68
6	0.58	0.54	0.60
7a	0.79	0.73	0.78
7b	0.68	0.59	1.40
7c	0.50	0.43	1.60
8	0.89	0.69	2.54
9	0.71	0.67	0.60
10	0.72	0.67	0.70

a. P(0) = penetration at start of test, determined from extrapolation of penetration-accumulation plot to zero accumulation; dimensionless.
b. P(A) = penetration at accumulation (A) equal to 100 x 10^6 p/cm^2 filter face area, for all tests except no.2, taken at 50 x 10^6 p/cm^2; dimensionless.
c. $S = A^{-1}\ln(P(0)/P(A))$.

particle size was 0.6 microns in diameter. Concentration seemed to vary somewhat from test to test, and was not reported for data shown in Figure 1-3. Accumulation was calculated from an estimated inlet concentration of 10^6 p/cm^3. Values of S were calculated at each of four velocities from the penetrations shown in Table 3-4. The average value of S estimated from the LaMer data was 0.51 x 10^{-9} cm^2/p, or slightly lower than that found in the present experiments.

D. Initial Filter Penetration and Fiber Efficiency

The initial aerosol penetration, P(0), through each of the 12 test filters was determined by extrapolation of accumulation-penetration plots to zero accumulation as shown in Figures 3-3 and 3-4. Initial values are shown in Table 3-5. The principal variable in 9 of the 12 filter mat tests was the relative amount of fiber per unit area. The velocity was constant in these nine tests (at 13.78 cm/sec) so that the initial filter fiber efficiency, η (0), should remain approximately constant. Under these conditions:

$$P(0) \sim \exp(-L\alpha) \qquad (3\text{-}3)$$

Initial penetration was plotted against the relative fiber weight per unit area ($L\alpha$) as shown in Figure 3-5. Test filters 7a-7c were thin and had nearly constant deposition throughout. A straight line was passed through these three points and zero, as shown (black dots).

Points for test mats 4, 6, and 8 lie near this line. Points for test mats 2, 3, and 5 fall somewhat further away. For example, the experimental penetration for test mat 2 was about 55%, but according to its physical characteristics ($L\alpha$) and the assumed line in Figure

TABLE 3-4

Filter Penetration and Accumulation
Estimated from LaMer Data

Velocity cm/sec	Time min	Conc.,[a] p/cm^3	P(0)[b]	P(A)[c]	A[d] $10^9 p/cm^2$	S[e] $10^{-9} cm^2/p$
28	1	10^6	0.12	0.045	1.55	0.63
13	1	10^6	0.13	0.085	0.70	0.61
4.7	1	10^6	0.125	0.11	0.25	0.51
2.5	3	10^6	0.135	0.12	0.39	0.28

a. Concentration not reported, estimated from reference 68, p. 26.
b. Initial penetration, dimensionless.
c. Penetration estimated from Figure 1-3 at time indicated in Col. 2.
d. Accumulation
e. $S = A^{-1} \ln(P(0)/P(A))$.

TABLE 3-5

Initial Filter Penetration

Test Filter No.	Initial Penetration P(0)	$\eta(0)^a$	$\eta^*(0)^b$	$\eta_c(0)^c$
1	0.0915	0.191	0.072	0.167
2	0.560	0.069	0.053	0.061
3	0.760	0.061	0.051	0.057
4	0.560	0.164	0.123	0.156
5	0.670	0.094	0.078	0.088
6	0.580	0.117	0.099	0.110
7a	0.791	0.182	0.163	0.175
7b	0.685	0.165	0.137	0.154
7c	0.505	0.171	0.124	0.153
8	0.890	0.125	0.117	0.122
9	0.710	0.167	0.166	0.159
10	0.720	0.248	0.210	0.238

a. Filter fiber efficiency from equation (1-6).
b. Filter fiber efficiency from thin-bed approximation, equation (3-5).
c. $\eta_c(0) = \eta(0)/(1 + 4.5\alpha)$, from Chen (23).

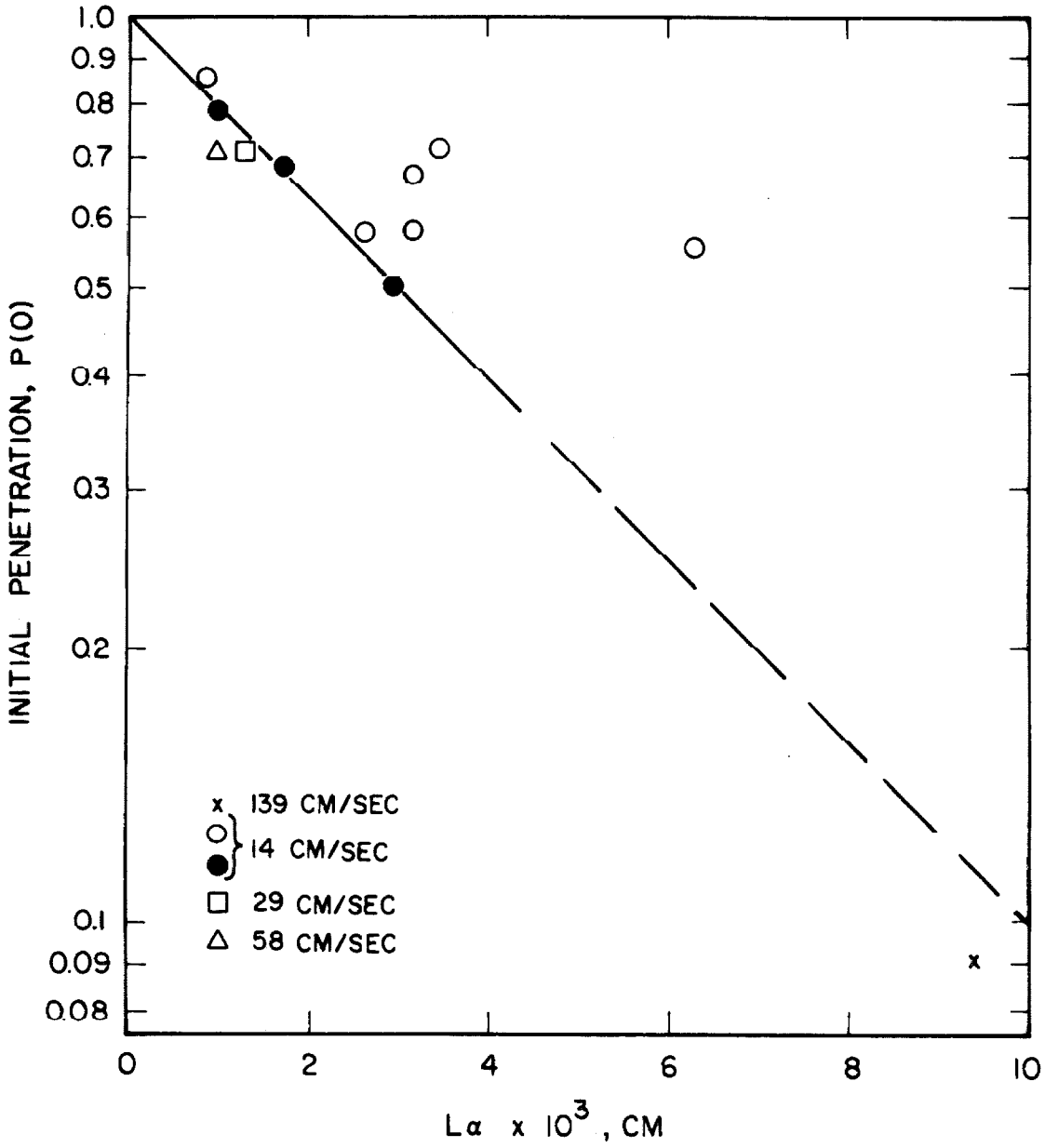

Figure 3-5. Initial Filter Penetration

3-5, it should have had a penetration of about 25%. Penetration for mats 3 and 5 was also higher than would have been predicted. These same three tests also had lower initial resistance than would have been predicted from experimental data on the remaining mats, as shown in Figure 3-2. Initial data for resistance and penetration of test mats 2, 3, and 5 may be slightly in error.

Initial filter penetration is related to initial filter fiber efficiency through the parameters of the filter mat:

$$\eta(0) = \frac{\pi a}{2 \alpha L} \ln (1/P(0)) . \qquad (1\text{-}6)$$

The average initial filter fiber efficiency, $\eta(0)$, is 0.173, as calculated from the straight line shown in Figure 3-5. Initial fiber efficiencies were also calculated for each individual test, as shown in Table 3-5. The average value of $\eta(0)$ was 0.128 for the 9 test mats (tests 2-8) operated at 13.78 cm/sec (range 0.061 to 0.175).

The initial filter fiber efficiency was also calculated by a thin-bed approximation:

$$\eta^*(0) = (1 - P(0)) \text{ Area test mat/Area fiber} \qquad (3\text{-}4)$$

or

$$\eta^*(0) = (1 - P(0)) (0.0302)/\text{Filter weight} \qquad (3\text{-}5)$$

as shown in Appendix 3-4. Values of $\eta^*(0)$ are shown in Table 3-5. For the thin beds used in these studies (tests 7a, 8, 9, and 10), the two methods for calculation of initial fiber efficiency produced about

the same value. As fiber weight increases, the thin bed approximation can be seen to be a less effective estimate of fiber efficiency when compared to that determined from the exponential form.

The last column in Table 3-5 presents the values of the corrected initial single fiber efficiency ($\eta_c(0)$) calculated from the empirical form developed by Chen (21):

$$\eta_c(0) = \eta(0)/(1 + 4.5\,\alpha) . \qquad (3\text{-}6)$$

This correction is discussed in Chapter V.

Values of the initial filter fiber efficiency ($\eta(0)$) for test numbers 2 through 8 were plotted against α . Because of the scatter of the data, no clear relationship between the initial fiber efficiency and α was apparent. Further discussions of initial filter fiber efficiency and initial single fiber efficiency for these tests are contained in Chapter V, as are the comparisons with theory and some previous experiments.

E. Effect of Particle Accumulation on Filter Resistance

Fiber filtration of an aerosol containing solid particles produces an increase in filter resistance proportional to the accumulation of particles. By assuming the drag force on each deposited particle contributes equally to the total resistance, the increased filter resistance was estimated as:

$$\delta \Delta p = (S_p \mu U_o a_p) A . \qquad (1\text{-}42)$$

Experimental resistances were plotted at several values of accumulation for each test, as shown in Figures 3-6 and 3-7. The slopes of these

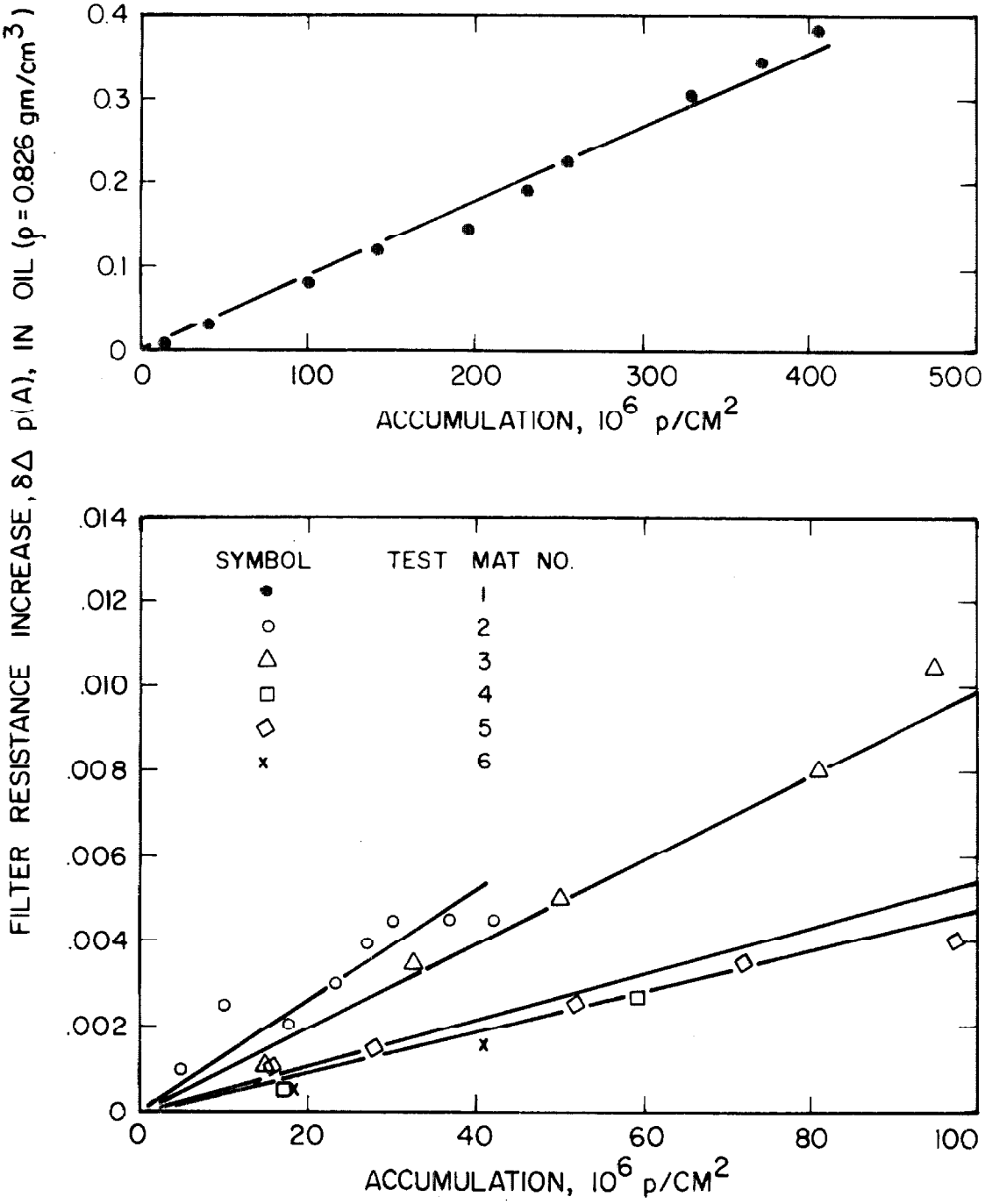

Figure 3-6. Resistance Decrease as a Result of Solid Particle Accumulation in Tests 1-6

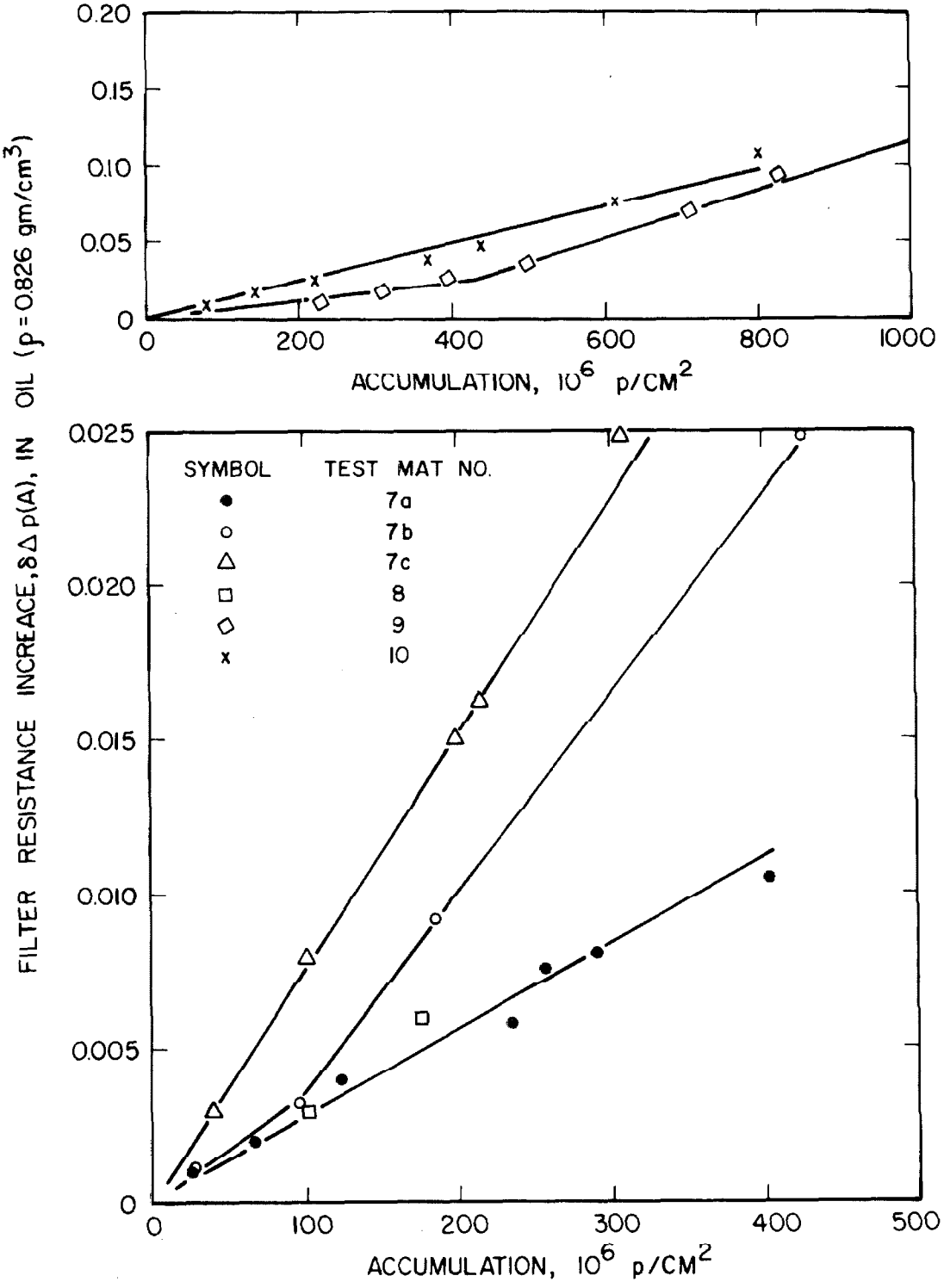

Figure 3-7. Resistance Increase as a Result of Solid Particle Accumulation in Tests 7a-10

lines ($\delta \Delta p/A$) and the calculated resistance coefficients (S_p) are presented in Table 3-6. The average value of S_p was 0.70 with a range from 0.33 to 1.64.

Resistance coefficients are plotted as a function of filter fiber fraction (α) in Figure 3-8. The coefficient appears to be proportional to α for 10 out of the 12 tests. Resistance coefficients for test numbers 2 and 3 lie about twice as high as would have been predicted from the data of the remaining 10 tests. The reason for this discrepancy is not known. Tests 3, 4, 5, and 6 represented a replicate series, and data for test number 3 did not agree with data for the others in the set. The discrepancy between the data for tests 2 and 3 and the data for the other 10 tests is assumed to be due to experimental error. Data for the 10 tests were plotted to estimate a relationship between resistance coefficient and fiber fraction. A straight line was drawn among the 10 points, using as a basis the data for test nos. 7a, 7b, and 7c, and zero, as being the most reliable points. No attempt was made to apply statistical curve-fitting techniques. For the 10 tests (excluding tests 2 and 3), the dashed line shown in Figure 3-8 is represented by:

$$S_p = 33 \alpha \qquad (3\text{-}7)$$

in the range $0.007 < \alpha < 0.035$. The resistance coefficient does not seem to be strongly influenced by filter depth ($0.11 \leq L \leq 0.29$ cm) or filtering velocity ($13.8 \leq U_o \leq 139$ cm/sec). Observations quoted in Chapter I, Section D4b indicated that the rate of resistance rise might be proportional to fiber fraction. This appears to be correct for this

TABLE 3-6

Resistance Increase as a Result of Particle Accumulation

Test Filter No.	$\delta\Delta p/A$[a]	S_p[b]
1	80×10^{-11}	1.00
2	13×10^{-11}	1.64
3	9.7×10^{-11}	1.23
4	4.6×10^{-11}	0.58
5	5.0×10^{-11}	0.63
6	4.6×10^{-11}	0.58
7a	3.0×10^{-11}	0.38
7b	3.5×10^{-11}	0.44
7c	7.5×10^{-11}	0.95
8	3.0×10^{-11}	0.38
9	5.7×10^{-11}	0.34
10	11.0×10^{-11}	0.33

a. slope of resistance rise- accumulation plot; inches of petroleum gage oil (sp.g. 0.826) per deposited particle per cm^2 of filter face area; calculated at accumulation (A) of 10^8 p/cm^2, except test no. 2 at 4×10^7 p/cm^2.

b. $S_p = \delta\Delta p/A(\mu U_o a_p)$, dimensionless.

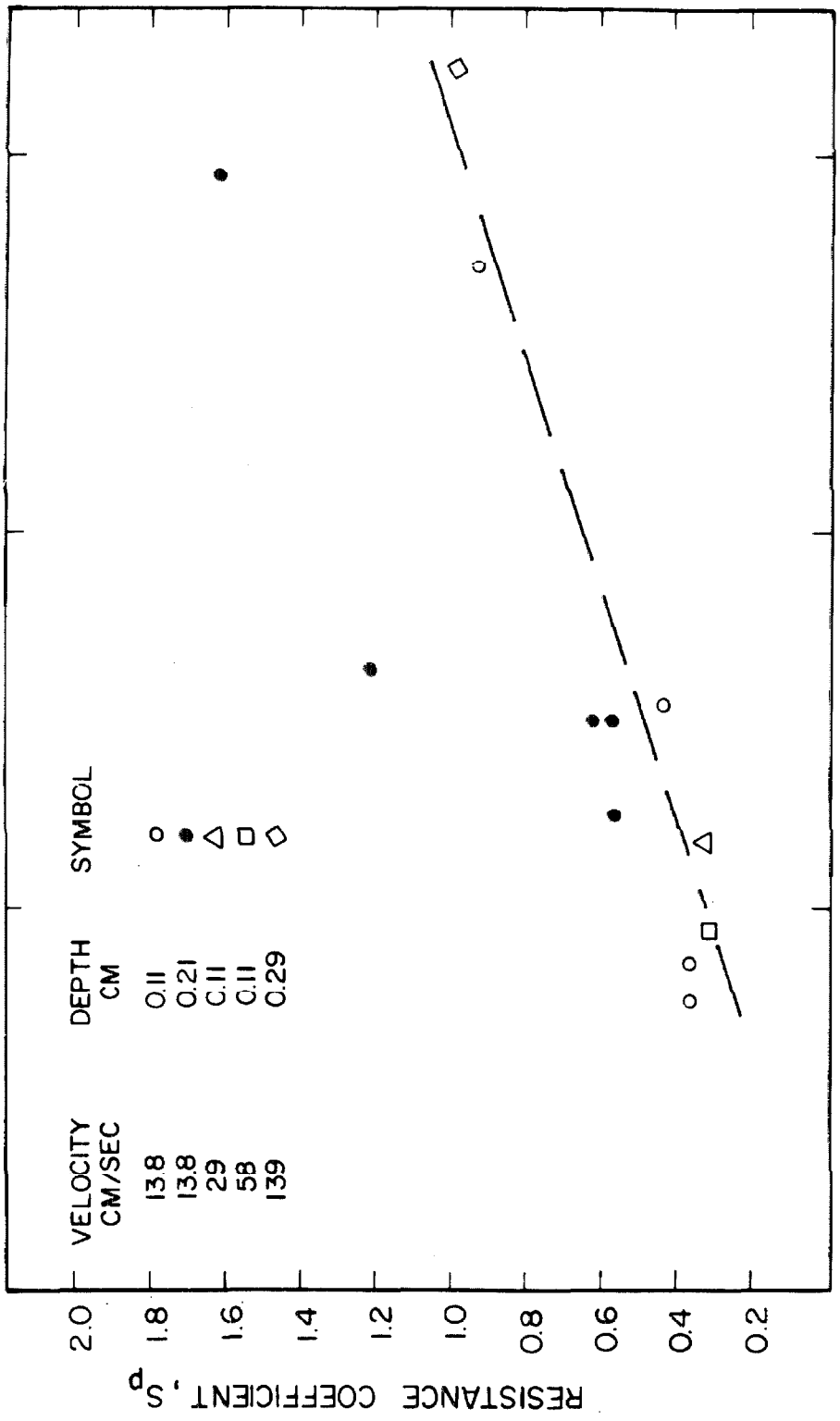

Figure 3.8. Variation of Resistance Coefficient (S_p) with Fiber Fraction (α).

study. A more compact filter (higher α) produces a higher resistance per unit of accumulated material.

An analytical solution for the drag on one or more particles attached to a fiber in slow viscous flow has not been obtained. The velocity near the fiber is lower than the free stream velocity, and is a function of the fiber diameter. The coefficient S_p may be a function of the fiber and particle diameters, but these effects were not investigated in the present study.

Resistance coefficients were computed from the data of LaMer shown in Figure 1-4. Values of accumulation were assumed from Table 3-4 at one minute. The resistance rise was estimated at one minute, as shown in Table 3-7. The average value of S_p is 13.6 or twenty times higher than the average value found in the present study. The estimated resistance coefficient based on an extrapolation of empirical equation (3-7) is 4.2 at a value of α of 0.128 reported in the LaMer study.

TABLE 3-7

Filter Resistance and Accumulation
Estimated from LaMer Data

Velocity cm/sec	A^a $10^9 p/cm^2$	$\delta \Delta p^b$	$S_p{}^c$
28	1.55	2.15	10.1
13	0.70	0.55	12.2
4.7	0.25	0.10	18.5

a. Accumulation, particles/cm^2 of filter face area, taken from Col. 6, Table 3-4.
b. Increase in filter resistance resulting from accumulation of particles, cm nitrobenzene (ρ_f = 1.2 gm/cm^3), taken from Figure 1-4 at one minute.
c. $S_p = \delta \Delta p / A(\mu U_o a_p)$, dimensionless, a_p = 0.3 microns.

IV.

SINGLE FIBER TEST RESULTS AND DISCUSSION

A. Single Fiber Data

Seven single glass fibers were taken from bulk filter media and mounted as shown in Figure 2-5. Aerosol samples were taken before a fiber was installed in the aerosol tunnel, to estimate particle concentration. Each fiber was then exposed to aerosol flow and removed for analysis of deposit. Accumulated particles were photographed. The numbers of individual particles were counted on a known length of fiber (81¼ microns). Operating conditions and test results are indicated in Table 4-1. Particle count data for each test are given in Appendix 4-1.

At the conclusion of a test run, a cumulative record of events was used to construct a graph of the time variation of particle concentration. Cumulative records are given in Appendix 4-2.

The fiber efficiency, η (Z), and aerosol particle concentration, $N_o(t)$, were both slowly varying functions of time. The fiber efficiency was calculated from the rate of change of particle deposition on the fiber (p/cm of fiber-sec):

$$\eta(Z) = \frac{d(2aZ)}{dt} \cdot \frac{1}{2aU_o N_o(t)} \qquad (4\text{-}1)$$

To obtain the efficiency of the fiber as a function of time, the cumulative number of particles per unit length of fiber (i.e., 2aZ) was plotted against cumulative exposure time (data of column 5 was plotted as a function of data in column 2, Appendix 4-1). A smooth curve was drawn among the points and the slope was obtained graphically

TABLE 4-1

Single Fiber Test Results

Fiber No. (1)	Fiber Diam. (2)	Velocity cm/sec (3)	Slope Time min (4)	Slope[a] (5)	Conc. $N_9(t)$ p/cm^3 (6)	Accumul. (2) 10^6p/cm^2 (7)	$\eta(Z)$ (8)	$\eta(0)$ (9)	S^b 10^{-9}cm^2/p (10)
4[c]	9.6	13.8	100	48.9	1118	3.0	0.0525	0.051	0.5
			200	64.5	1333	10.5	0.0580		
			300	69.8	1412	16.2	0.0591		
			400	76.0	1497	23.2	0.0609		
5[c]	8.7	13.8	60	46.9	782	4.0	0.0840	0.077	2.0
			135	57.8	823	9.2	0.0983		
			221	66.4	873	14.8	0.1060		
			300	76.7	915	19.7	0.1172		
			420	97.5	976	32.1	0.1270		
6[d]	9.7	29	120	126	975	14.2	0.076	0.074	0
			220	128	1041	26.6	0.072		
7[e]	11.0	58	60	198	970	10.3	0.0527	0.051	0
			121	215	1035	21.2	0.0535		
8	10.4	13.8	61	56.3	1010	3.0	0.0650	0.065	0.7
			189	73.0	1065	12.2	0.0800		
			400	83.0	1158	30.3	0.0835		

TABLE 4-1 (cont'd)

Fiber No. (1)	Fiber Diam. (2)	Velocity cm/sec (3)	Slope Time min (4)	Slope[a] (5)	Conc. $N_0(t)$ p/cm^3 (6)	Accumul. (Z) 10^6p/cm^2 (7)	$\eta(Z)$ (8)	$\eta(0)$ (9)	S^b 10^{-9}cm^2/p (10)
9	8.5	13.8	30	23.0	821	1.3	0.0400	0.040	1.8
			180	28.9	713	5.5	0.0580		
			480	40.2	836	18.3	0.0688		
10	9.2	13.8	61	70.0	888	3.8	0.104	0.100	1.8
			184	96.5	944	15.0	0.134		
			336	121	1025	33.1	0.155		

a. Slope, p/cm fiber- min; $d(2aZ)/dt = 60U_0N_0(t)\eta(t)$.
b. $\eta(Z) = \eta(0) + SZ$.
c. Alternate exposures with test filter no. 8.
d. Alternate exposures with test filter no. 9.
e. Alternate exposures with test filter no. 10.

at two or more points on the curve. The calculated slopes and the times at which they were obtained are presented in Table 4-1 (columns 5 and 4, respectively). The fiber efficiency was then calculated from equation (4-1), using a value of $N_o(t)$ taken from the graph of time variation of particle concentration. The values of $N_o(t)$ used in computations are shown in column 6, Table 4-1.

Accumulation (Z, p/cm^2 of fiber) (column 7, Table 4-1) was calculated from the particle count per unit length of fiber divided by the measured clean fiber size (column 2). The estimation of local accumulation by using the clean fiber diameter in the cross-section represents an approximation. The cross-section available for deposition is a function of the amount of deposit, as can be seen in the photographs of the deposits presented in section D, below.

B. Effect of Particle Accumulation on Single Fiber Efficiency

The general form of the assumption for the variation of local fiber efficiency with local accumulation was:

$$\eta(Z) = \eta(0) + S Z \qquad (1\text{-}28)$$

Figure 4-1 shows the relationship between $\eta(Z)$ and Z as determined from the data of columns 7 and 8 of Table 4-1. The variation in single fiber efficiency is approximately linear for accumulations up to 33×10^6 p/cm^2 of fiber (the limit of observations). There is a tendency for the data points at the highest accumulations to be slightly low. The apparent reduction in fiber efficiency represented by these low points may be the result of the experimental difficulty of seeing all particles in heavy deposits.

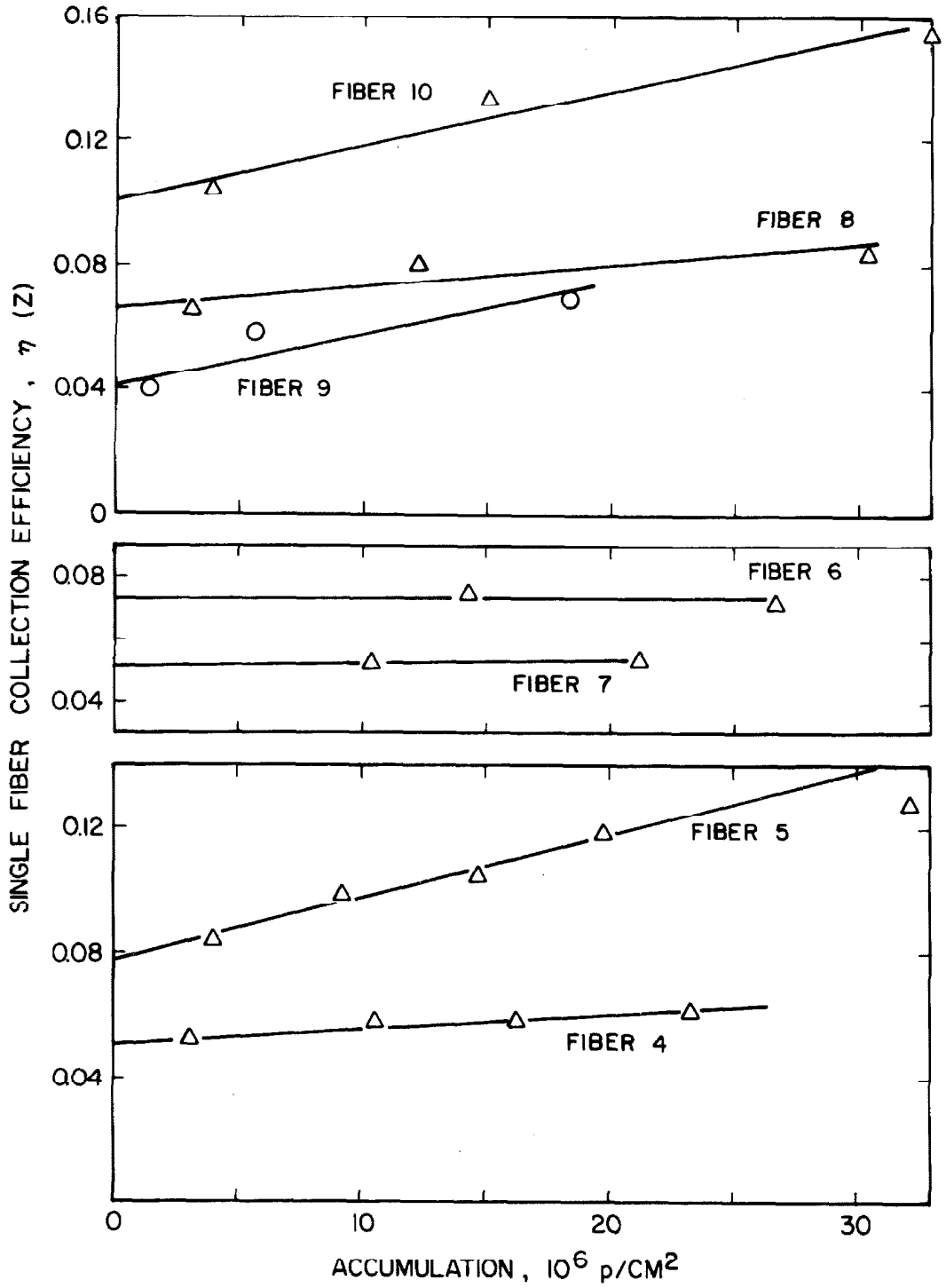

Figure 4-1. Variation of Single Fiber Efficiency with Accumulation

The slopes of the lines (S) in Figure 4-1 were computed as shown in column 10 of Table 4-1. The average value of S for 5 fibers operated at 13.78 cm/sec was about 1.36×10^{-9} cm^2/p, with a range from 0.5 to 2.0×10^{-9} cm^2/p. The average value of S derived from 10 filter mat tests was 1.13×10^{-9} cm^2/p with a range from 0.6 to 2.5×10^{-9} cm^2/particle. The average value of the single fiber efficiency accumulation coefficient is practically the same as the coefficient derived from filter mat accumulation studies.

C. Initial Single Fiber Efficiency

Values of $\eta(Z)$ were extrapolated to zero accumulation as shown in Figure 4-1. Initial single fiber efficiency from this extrapolation is shown in column 9 of Table 4-1. The average initial single fiber efficiency for 5 fibers operated at 13.78 cm/sec was 0.066 with a range from 0.04 to 0.10. Fibers tested at 29 and 58 cm/sec had efficiencies within the same range (0.074, 29 cm/sec and 0.051, 58 cm/sec). The velocity effect was not extensively studied. Comparisons of single fiber efficiency and filter fiber efficiency are given in Chapter V.

D. Deposit Structure and Changes with Time

A photographic record was made of the deposition of 1.305-micron polystyrene latex aerosol particles on single glass fibers. Representative photographs of the development of particle deposits on fiber number 5 are presented in Figures 4-2 and 4-3. Figure 4-2(a) shows the bare fiber before the initial exposure to aerosol flow (measured 8.7 microns). Figures 4-2, (b) and (c) show the particle deposits in the same region after 60 and 135 minutes, respectively. The

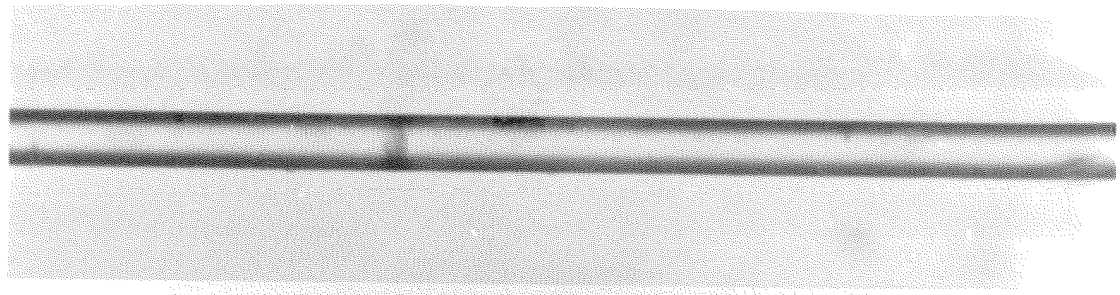

(a) 0 minutes

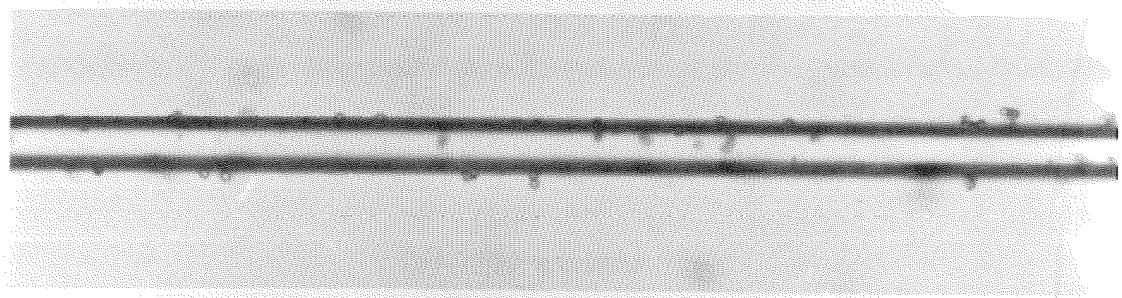

(b) 60 minutes

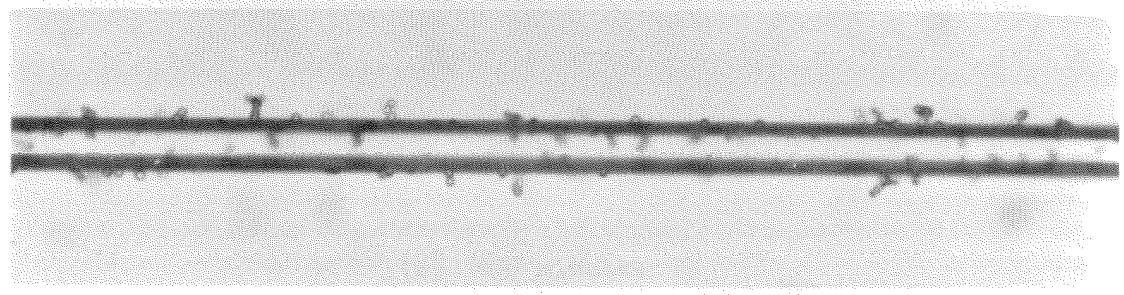

(c) 135 minutes

Figure 4.2. Deposits of 1.305-micron Polystyrene Latex Spheres on 8.7-micron Diameter Glass Fiber Operated at 13.8 cm/sec for 0, 60, and 135 minutes at an Approximate Concentration of 1000 p/cm^3 (Single Fiber 5).

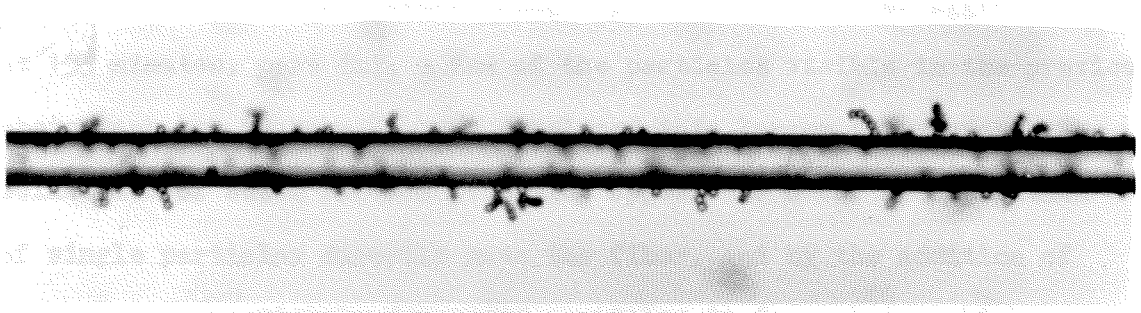

(a) 221 minutes

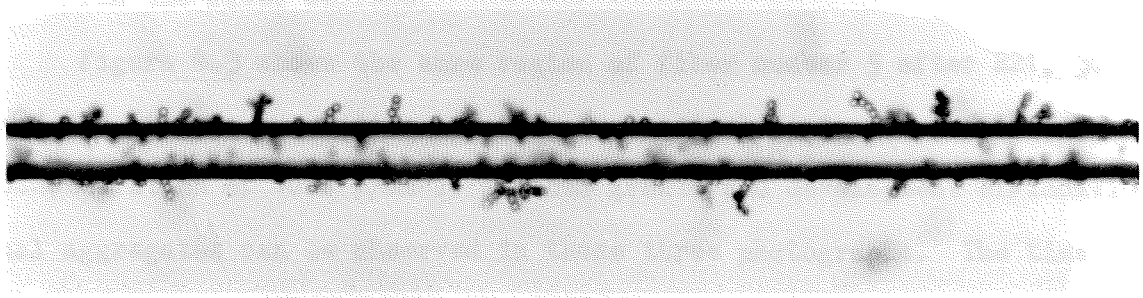

(b) 300 minutes

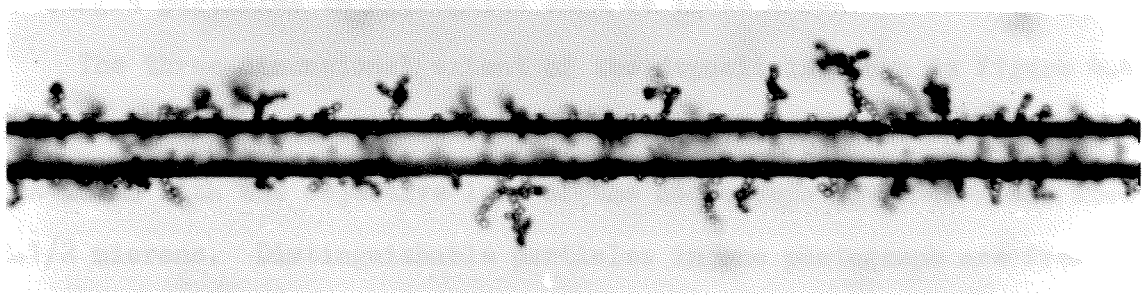

(c) 420 minutes

Figure 4-3. Deposits of 1.305-micron Polystyrene Latex Spheres on 8.7-micron Diameter Glass Fiber Operated at 13.8 cm/sec for 221, 300, and 420 minutes at an Approximate Concentration of 1000 p/cm^3 (Single Fiber 5).

average particle concentrations during exposure were 771 and 809 p/cm^3, respectively. At 60 minutes, part (b), much of the fiber remains bare. Deposition consists of several single particles and a few aggregates. At 135 minutes, part (c), a few of the particles visible in the previous photograph can be seen to have developed into larger structures. The collection of solid aerosol particles appears to occur by deposition of single particles directly onto the fiber, and by the addition of particles to previously deposited particles to form chains which branch out from the fiber surface.

Figure 4-3 shows the same region of fiber number 5 after 221, 300 and 420 minutes cumulative exposure, respectively, at an approximate concentration of 1000 p/cm^3. Further growth and development of individual aggregates can be observed in these three photographs. The time variation of aggregate size has been obtained from counts of the number of single particles in aggregates such as those shown.

The three-dimensional extent of the deposit is shown in Figure 4-4 (single fiber 5 at 300 minutes exposure). Each successive photograph was taken with the objective lens of the microscope moved downward about 2-1/2 microns. Distinguishable particles in one photograph are frequently out-of-focus or invisible in the next one.

Typical photomicrographs above indicate that the deposit begins with single particles and progresses by formation of doublets, triplets, and higher order multiplets. Physical form of these deposits appears to be primarily chain-like. Aggregates build up and outward from fibers as long straight and branched chains.

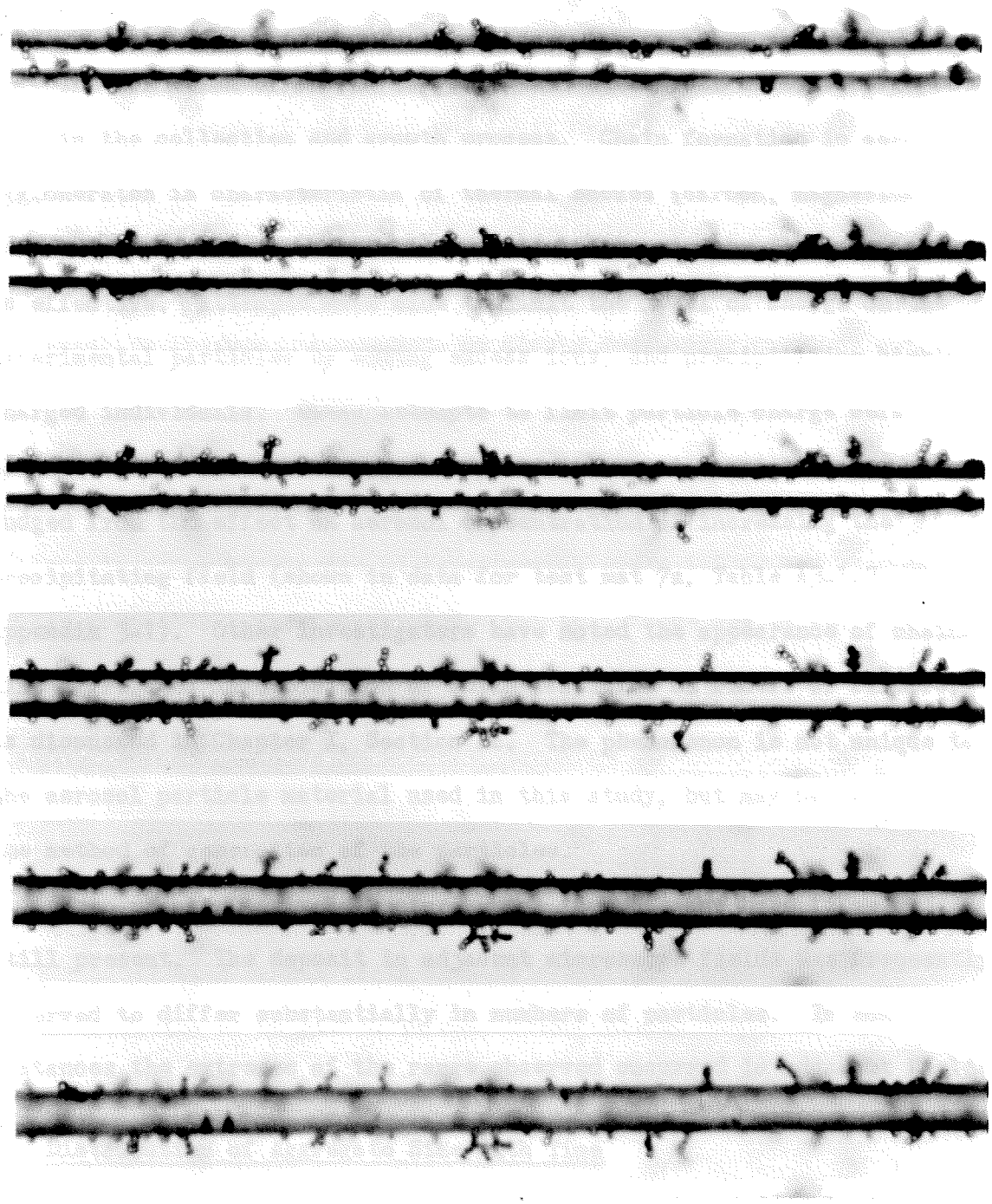

Figure 4.4. Through-focus Series of Photographs of Deposit of 1.305-micron Polystyrene Latex Spheres on 8.7-micron Diameter Glass Fiber Operated at 13.8 gm/sec for 300 minutes at an Approximate Concentration of 1000 p/cm^3 (Single Fiber 5).

The formation of chains suggests that electrical effects have some part in the collection and growth process. Chain formation in aerosol agglomerates is characteristic of thermal smokes (carbon, magnesium oxide, titanium oxide, etc.) where particle charging by flame ionization is effective. Attempts were made to limit the level of charge on the experimental particles by adding excess ions, and precipitating highly charged individuals. These attempts to limit particle charge were only partly effective. Some charge was present on most particles as can be judged from the effect on aerosol concentration of increasing the precipitating field (shown in data for test mat 7a, Table A3-1-7, Appendix 3-1). Other investigators have noted the appearance of chain-like aggregates in deposition of solid particles on fibers or filters, as discussed in Chapter I, Section D2. The phenomenon is not unique to the aerosol particle material used in this study, but may be related to the method of generation of the particles.

Even when extensive structures were formed, some bare fiber was still present. The deposit in adjacent microscope fields was frequently observed to differ substantially in numbers of particles. In some instances the extremes of the range observed occurred in adjacent fields.

E. Distribution of Aggregate Size with Time

Accumulation was measured on single fibers by counting individual particles of each aggregate in each microscopic field. The number of individual particles in a single aggregate was recorded (j). The distribution of aggregate size ($1 \leq j < 50$) at each analysis time is presented in Appendix 4-3 for each fiber.

The number of particles per unit area of size j was calculated from the microscope field size and fiber diameter. The counts per unit area for aggregate sizes $j = 1,2,3$, and 4 were plotted as a function of time for each fiber. Curves for single fiber numbers 9 and 10 are shown in Figures 4-5 and 4-6. The rate of change of the number of aggregates of size j $(1 \leq j \leq 4)$ seems to be slowly decreasing on fiber number 9. On fiber 10, the rate of change of number of aggregates of size j seems to approach zero after an initial growth. The reason for the differences in structure growth on the various fibers is not known. The change in slope may be due to experimental error introduced when the fiber preparation was removed for analysis. There may be electrostatic effects on the deposit which promote or limit deposition.

F. Effect of Velocity on Deposit Structure

The structure or geometry of particle deposits on a fiber probably control the changing collection efficiency (Chapter I, Section D1). The effect of aerosol velocity on deposit structure was briefly investigated with single fiber numbers 6 and 7. These fibers were tested at velocities of 29 and 58 cm/sec, respectively, while the remaining five fibers were operated at 13.8 cm/sec. Particle accumulation coefficients (S) were observed to be practically zero for single fibers 6 and 7 (Figure 4-1). The coefficient S was not shown to be a function of velocity in filter mat tests (Table 3-3, filter numbers 1, 9, and 10).

Photographs of the particle deposits on single fiber numbers 6 and 7 were examined and compared to deposits on fibers tested at lower velocity. Figure 4-7(a) shows the deposit on single fiber 6

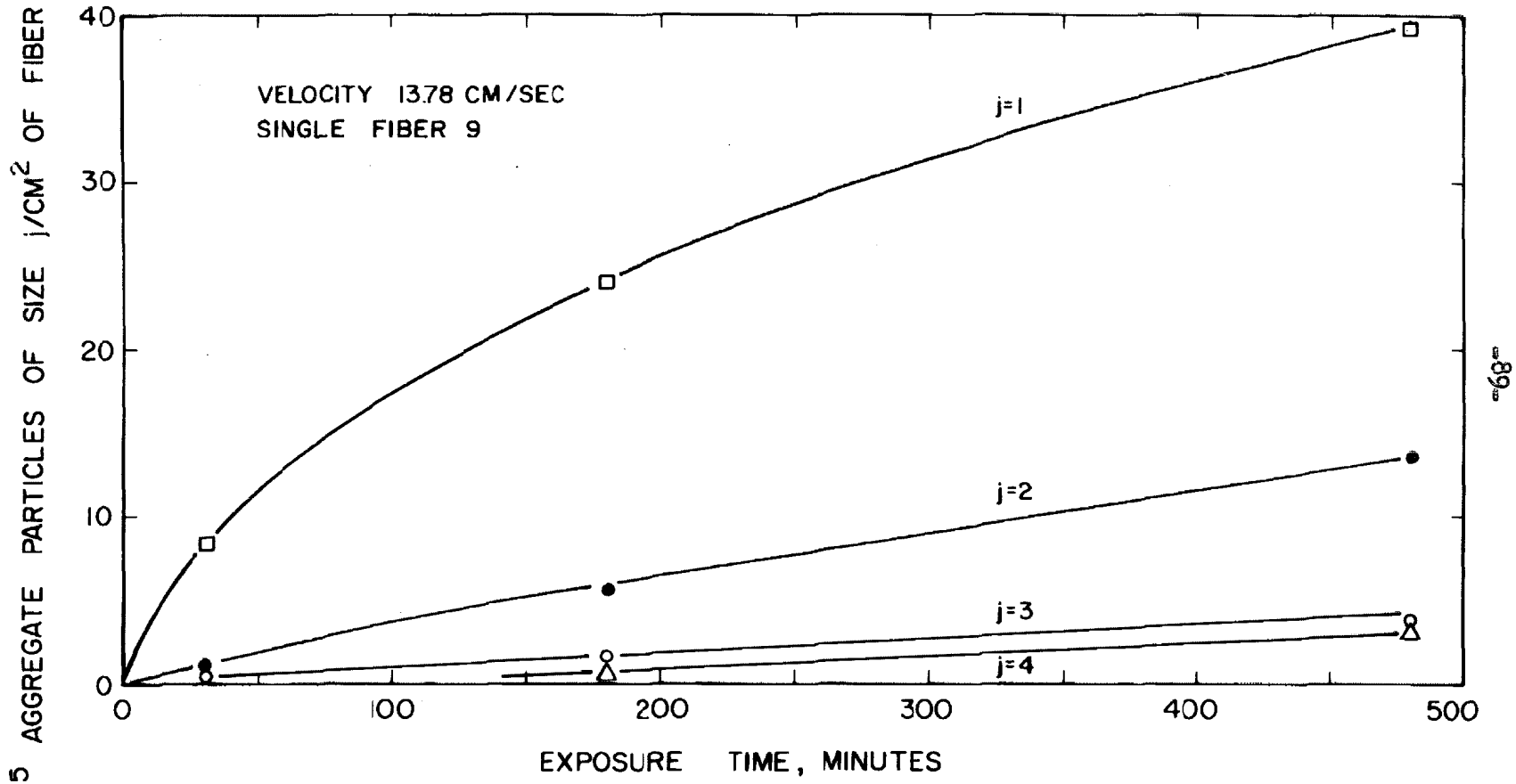

Figure 4.5. Cumulative Number of Aggregates of Size j = 1, 2, 3, 4 on Single Fiber 9 at Various Test Intervals

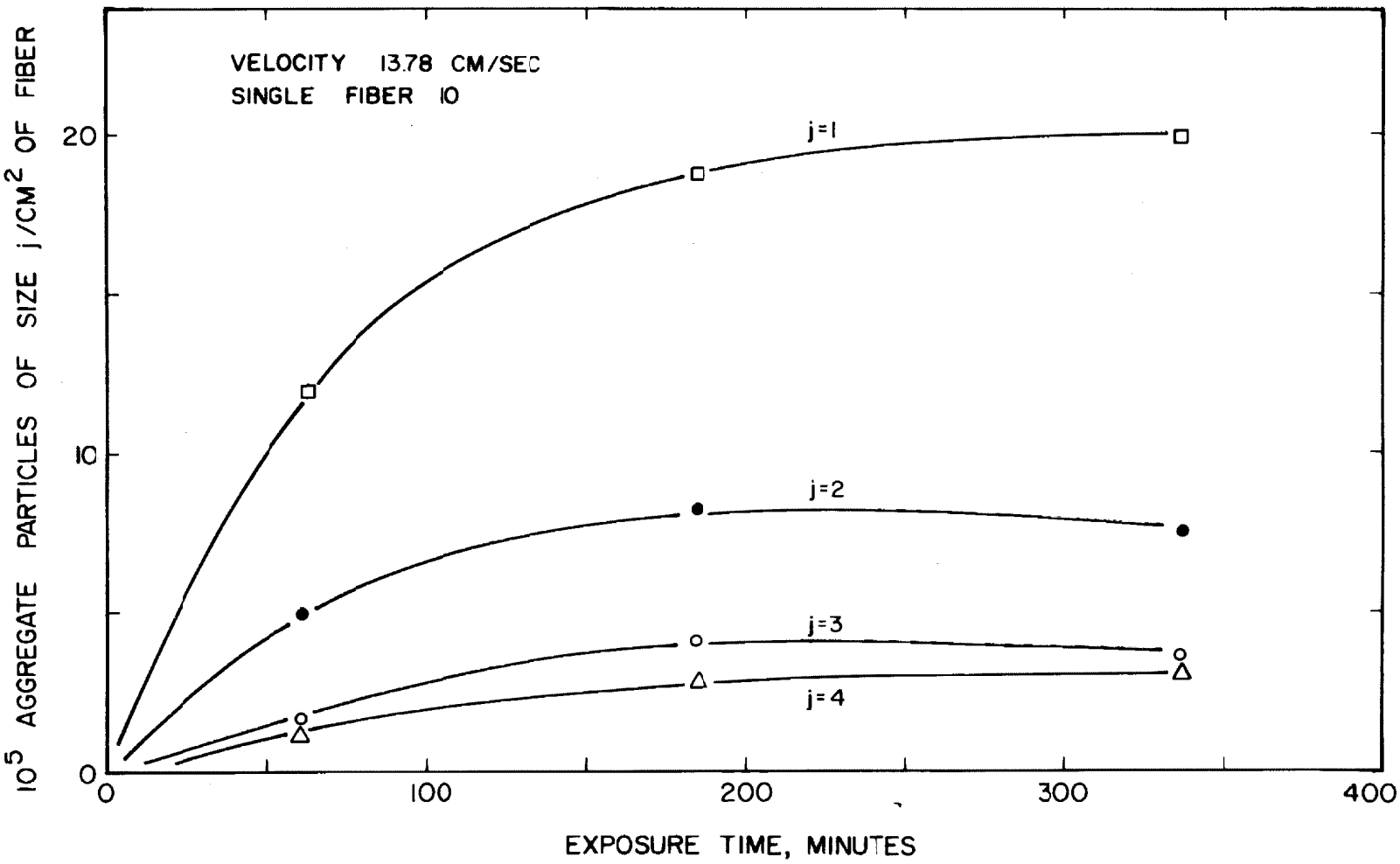

Figure 4.6. Cumulative Number of Aggregates of Size j = 1, 2, 3, 4 on Single Fiber 10 at Various Test Intervals

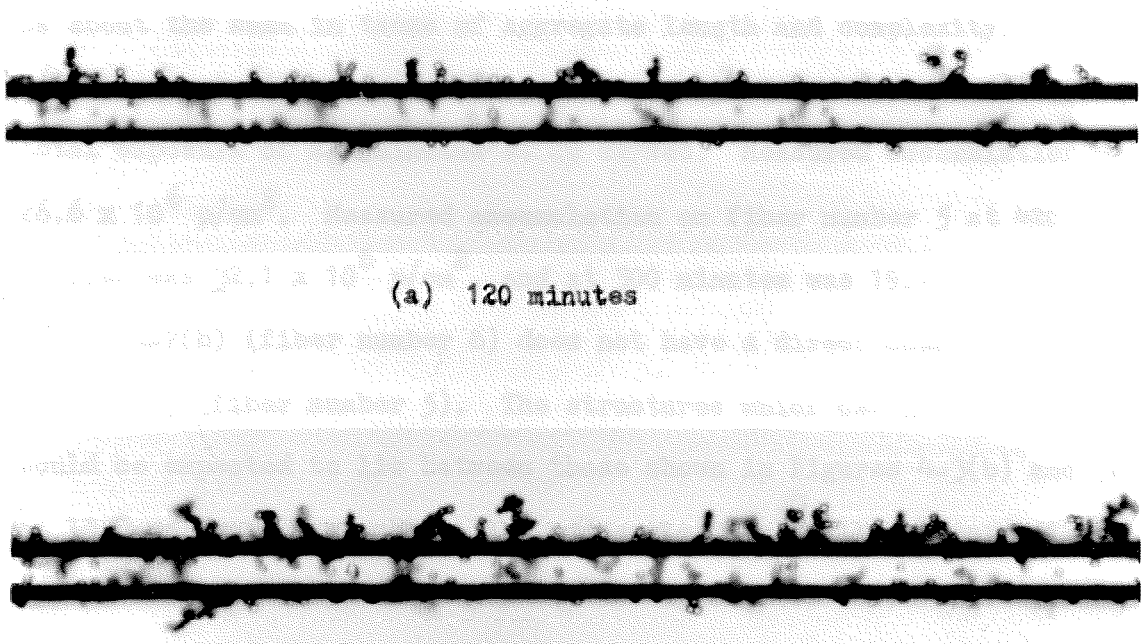

(a) 120 minutes

(b) 220 minutes

Figure 4-7. Deposits of 1.305-micron Polystyrene Latex Spheres on 9.7-micron Diameter Glass Fiber Operated at 29 cm/sec for 120 and 220 minutes at an Approximate Concentration of 1000 p/cm^3 (Single Fiber 6).

after 120 minutes exposure at 29 cm/sec (accumulation 14.2 x 10^6 p/cm^2; Table 4-1). This figure may be compared to Figure 4-3(a) showing an approximately equal accumulation (14.8 x 10^6 p/cm^2) on single fiber 5 after 221 minutes exposure at 13.8 cm/sec (i.e., one-half of the velocity at twice the time). The deposits in these two figures appear to be about the same in terms of aggregate length and complexity.

Figure 4-7(b) shows the accumulated deposit on fiber 6 after a total exposure of 221 minutes at 29 cm/sec. Measured accumulation was 26.6 x 10^6 p/cm^2. Measured accumulation on fiber number 5 at 420 minutes was 32.1 x 10^6 p/cm^2, and at 300 minutes was 19.7 x 10^6 p/cm^2. Figure 4-7(b) (fiber number 6) does not have a direct counterpart in Figure 4-3 (fiber number 5). The structures which develop at 29 cm/sec would be expected to lie between those shown in Figures 4-3(b) and (c) at 13.8 cm/sec. Many chain-like aggregates are still evident. There appears to be a slight tendency for the aggregates to be shorter and more compact at the higher velocity.

Figure 4-8 shows the deposit structures on fiber number 7 after operation for 60 and 121 minutes at 58 cm/sec. Measured accumulations at these times were 10.3 x 10^6 p/cm^2 and 21.1 p/cm^2, respectively. Based on approximately equal accumulations, it is possible to compare Figures 4-8(a) and (b) (fiber number 7) with Figures 4-2(c) (fiber 5 at 135 minutes, accumulation 9.25 x 10^6 p/cm^2) and 4-3(b) (fiber 5 at 300 minutes, accumulation 19.7 x 10^6 p/cm^2), respectively. Again, there seems to be a slight tendency for more compact deposits to form at the higher velocity of 58 cm/sec.

(a) 60 minutes

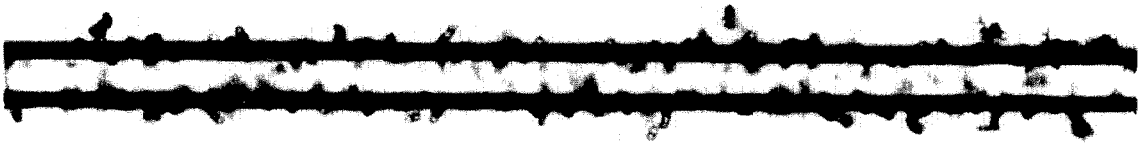

(b) 121 minutes

Figure 4.8. Deposits of 1.305-micron Polystyrene Latex Spheres on 11.0-micron Diameter Glass Fiber Operated at 58 cm/sec for 60 and 121 minutes at an Approximate Concentration of 1000 p/cm^3 (Single Fiber 7).

The effect of increased velocity on deposit structure seems to be slight over the range $13.8 \leq U_0 \leq 58$ cm/sec. Deposits formed at velocities of 29 and 58 cm/sec appear shorter and with more complex aggregates when compared on the basis of equal accumulation to deposits formed at a velocity of 13.8 cm/sec.

Aggregate size distributions may be compared at approximately equal accumulations as shown in Figure 4-9 for fibers 5 and 7. There seems to be a qualitative similarity between the two distributions of aggregates for these two fibers. The effect of velocity on deposit structure does not seem to be of major importance within the limited range investigated in this study. Values of zero obtained for particle accumulation coefficients (S) of fibers 6 and 7 do not appear to be related to any obvious changes in deposit structure.

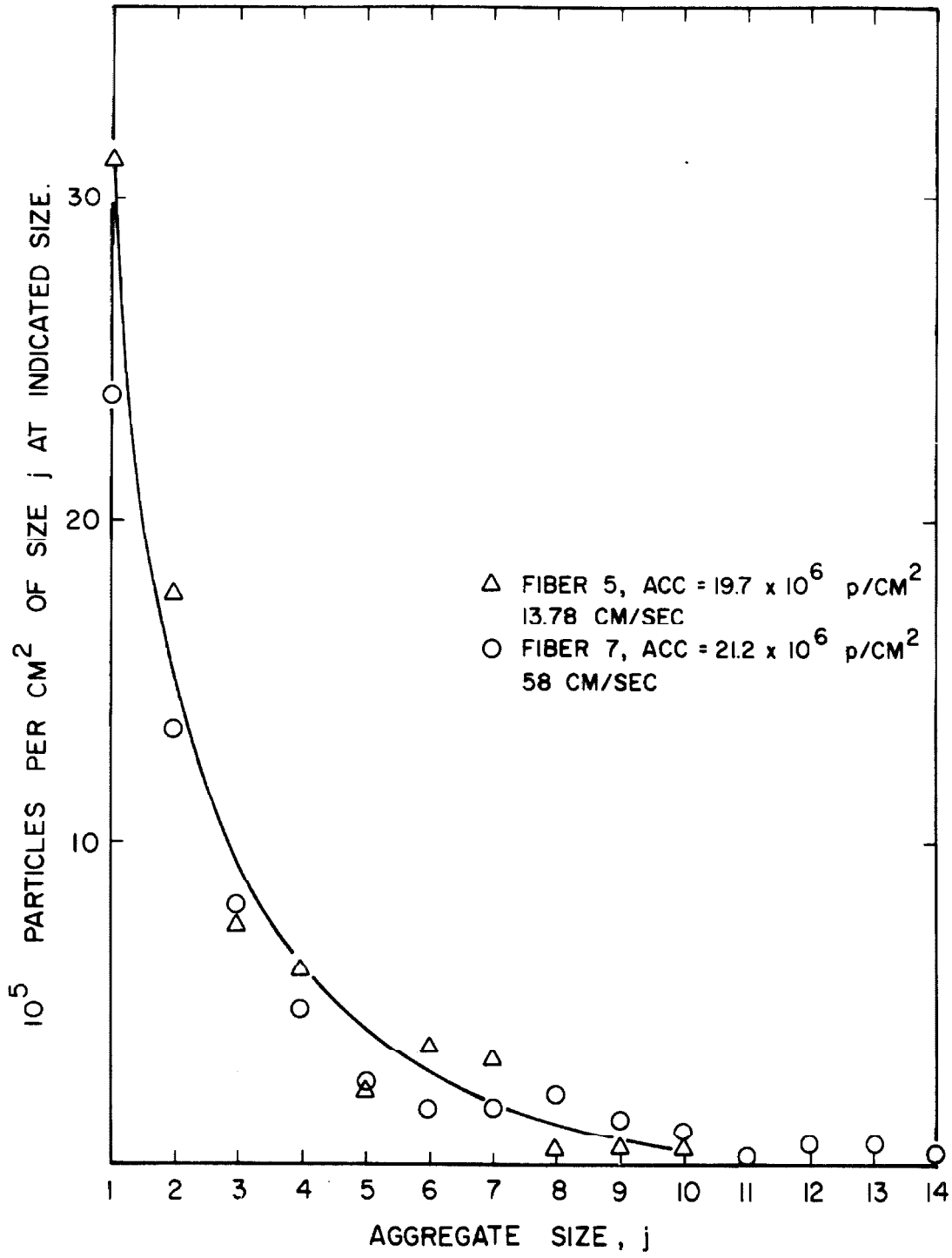

Figure 4-9. Effect of Velocity on Deposit Structure (Single Fibers 5 and 7) as Measured by Aggregate Size Distribution at Approximately Equal Accumulation

V.

COMPARISONS OF INITIAL FILTER FIBER AND SINGLE FIBER EFFICIENCIES WITH THEORY AND PREVIOUS INVESTIGATIONS

A. Comparison of Initial Filter Fiber Efficiency with Theory and Previous Investigations

The initial filter fiber efficiency, $\eta(0)$, and calculated values of the impaction parameter (I) and Peclet number (Pe) are given in Appendix 5-1. Figure 5-1 shows curves of the theoretical solution for deposition of particles by diffusion and direct interception on an isolated cylindrical fiber, as recently presented by Friedlander (33). Values of η RPe and $RPe^{1/3}$ are shown in Appendix 5-1 for the test mats used in this study. These points are plotted in Figure 5-1. They are up to one order of magnitude higher than the theoretical curve for $Re = 10^{-1}$ (for U_o = 13.78 cm/sec, Re = 0.087). Friedlander presents values of the filtration results for DOP (oil smoke) from Chen (23) and for sulfuric acid droplets from Wong and Johnstone (40). The general area occupied by the results of Wong is indicated in Figure 5-1. The results of Chen are reasonably close to the theoretical prediction shown.

At a value of the independent variable, $RPe^{1/3}$, of 5.5, the average value of the dependent variable, η RPe, was 10^3, 6×10^2, and 1.1×10^2 for the average of filter fiber tests, single fiber tests, and Friedlander theory, respectively.

Results of previous experiments with polystyrene latex by Stern

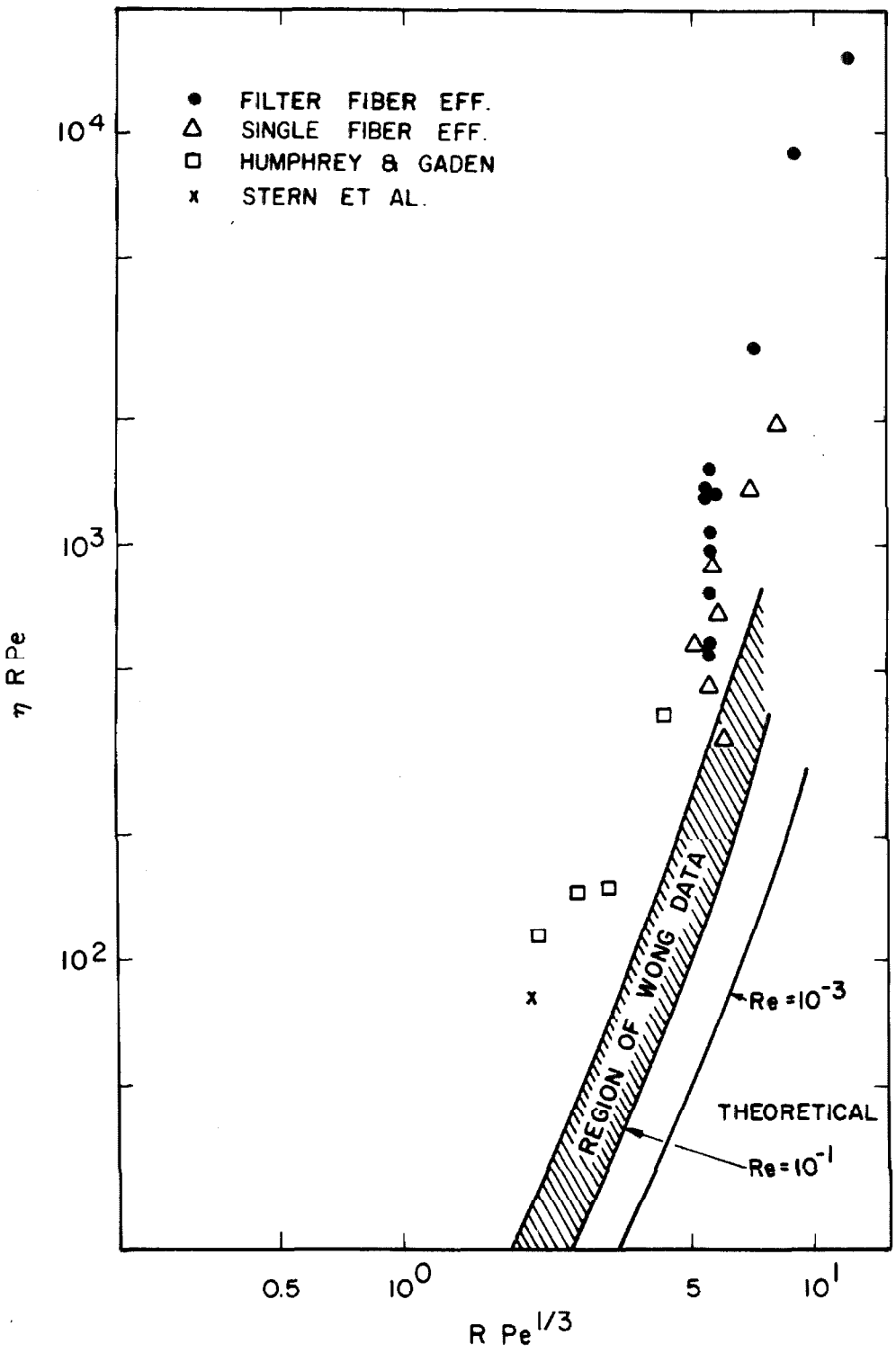

Figure 5-1. Comparison of Initial Fiber Efficiency with Theory and Previous Investigations

et al. (45), and with bacterial spores by Humphrey and Gaden (44), are also shown in Figure 5-1, as taken from Friedlander and Pasceri (31). Results of several investigations with solids seem to lie up to an order of magnitude higher than the theory predicts. Results of other studies with liquid droplets tend to confirm the theoretical analysis.

The difference in collection of solid and liquid particles may be a consequence of higher particle charge on solids generated by spraying. Limited tests were conducted during the present study to assess the effect of particle charge. They seemed to indicate that charge was not affecting filter collection significantly.

The results of the present study were also compared to Wong's experiments (40) in terms of the impaction parameter. These results were higher than the equivalent values presented by Wong. Test mat numbers 1, 9, and 10 were operated at increased velocity (139, 29, and 58 cm/sec, respectively). Fiber efficiency is somewhat higher at these velocities, but no clear trend is apparent. No consistent effects of impaction were observed in the two tests at the highest velocities. Direct interception was the controlling mechanism for particle collection in most of the present tests.

B. Comparison of Initial Single Fiber Efficiency with Theory and Previous Investigations

The initial single fiber efficiency and calculated values of the interception and impaction groups, and the Peclet number are presented in Appendix 5-2. The experimental single fiber efficiency was plotted as a function of the interception parameter (R). The theoretical

values were also plotted for the fibers used in this study, from the solution for the direct interception of spherical particles on isolated cylindrical fibers (33). The experimental points were more than 10 times higher than the theoretical prediction.

Data from these single fiber tests were also compared to the solution for diffusion of particles of finite diameter suggested by Friedlander, and some results of previous investigations of Chen, and Wong and Johnstone, as shown in Figure 5-1. Results of the present tests were found to lie within and slightly higher than the Wong data. Quantitative agreement is only fair among all experimental studies, as has been pointed out for filter mat studies above.

C. Comparison of Initial Single Fiber Efficiency and Initial Filter Fiber Efficiency

The efficiency of a single cylindrical fiber for collection of aerosol particles has been obtained analytically or numerically from a consideration of the forces acting on the particle, or from its thermal motion in equilibrium with the gas. To test these solutions in fiber filters, one assumes a regular array of cylinders which interact with the aerosol independently, obtaining the relationship between filter fiber efficiency (η (0)) and filter mat penetration (N_L/N_o):

$$\eta(0) = \frac{\pi a}{2 \alpha L} \ln (N_o/N_L) . \qquad (1-6)$$

Adjacent fibers are assumed to cause the flow field near a fiber to contract and produce a slightly higher collection efficiency. In a series of careful experiments, Chen (23) varied the value of α and

determined the filter fiber efficiency, $\eta(0)$, from measured values of mat penetration. He plotted values of $\eta(0)$ against α and found empirically that the efficiency at the zero intercept, $\eta_c(0)$, was related to $\eta(0)$ determined from his experiments, by:

$$\eta(0) = \eta_c(0)(1 + 4.5\alpha) \qquad (3.6)$$

for $0.015 \leq \alpha \leq 0.08$.

Filter fiber efficiencies from the present study (Table 3.5) were plotted against α. The scatter in the data was larger than the variation in $\eta(0)$ with α, for $0.007 \leq \alpha < 0.035$. The average initial filter fiber efficiency for 9 test mats operated at 13.78 cm/sec was 0.12 with a range from 0.052 to 0.175. The average initial single fiber efficiency for 5 fibers operated at 13.78 cm/sec was 0.066 with a range from 0.04 to 0.10. Fiber efficiencies determined from filter tests were higher than single isolated fiber efficiencies. The variations in results from the two kinds of tests, and the small number of tests, limit the conslusions that may be drawn.

VI.

SUMMARY AND CONCLUSIONS

A. Principal Results of this Research

1. The filtration of solid aerosol particles produces deposits on the filter fibers. The deposits project from the fibers and act as additional collecting surfaces to promote further capture. The total collection efficiency of the fiber then depends upon the amount of accumulated material, as well as the collection efficiency of the bare fiber. Local fiber collection efficiency was assumed to be represented by an expansion in terms of the local accumulation (Z, p/cm^2 of fiber) as:

$$\eta(Z) = \eta(0) + S Z \qquad (1\text{-}28)$$

and the higher order terms were neglected. The accumulation coefficient (S) was assumed to be a constant related to the structure and area of deposited particles and their particle capture efficiency. Single isolated 10-micron glass fibers were exposed to known concentrations of 1.305-micron polystyrene particles in an aerosol tunnel of novel design. Single fibers were periodically removed and the resulting particle deposit structures were photographed and counted. Particle accumulation coefficient (S) was computed from these data. The average value of this coefficient for five fibers tested at 13.8 cm/sec was found to be 1.36×10^{-9} cm^2/p for local accumulations $Z \leq 33 \times 10^6$ p/cm^2 of fiber area. For example, if $Z = 20 \times 10^6$ p/cm^2

after time t, the efficiency of removal would be increased by 0.0272 or 2.72 percent.

2. As material deposits on fibers in a filter, the overall filter collection efficiency increases. The relative amount of material escaping capture in the filter (penetration = 1-efficiency) decreases as a function of the accumulation of deposited material. By using the expression for the local fiber efficiency given above, a function was derived to describe the change in filter penetration as a result of accumulation:

$$P(A) = P(0) \exp(-SA) \qquad (1\text{-}33)$$

where A is the accumulation of deposited particles for the whole filter (p/cm^2 of filter face area). The penetration and accumulation can be obtained from periodic measurements of the inlet and outlet particle concentrations, if filter velocity is kept constant:

$$A = U_o N_o \Delta t \, \bar{E} \qquad (1\text{-}37)$$

where $\bar{E}$ is the average filter efficiency during the time interval Δt. Filter mats were cut from a lap of 10-micron fiber and tested in the aerosol tunnel with 1.305-micron polystyrene particles. Particle concentrations were measured and accumulation was calculated by equation (1-37). The average value of the particle accumulation coefficient (S) obtained in these studies was 1.8×10^{-9} cm^2/p for $A \leqslant 5 \times 10^8$ p/cm^2 of filter face area. The coefficients determined from single fiber tests and filter mat tests were found to be in fair agreement, considering the experimental difficulties. The coefficient

S did appear to be reasonably constant in both types of tests.

3. The rate of accumulation of material in a fiber filter depends upon the filter efficiency, and the efficiency, in turn, depends in part upon the accumulated deposit at any time. The variation of filter penetration as a function of accumulation is given above by equation (1-33). The accumulation of material within the filter can be expressed by an equation of continuity of material as:

$$\frac{dA}{dt} = U_o N_o (1 - P(A)) . \qquad (1-34)$$

This equation can be integrated, using the previous expression for P(A) and the condition that A = 0 at t = 0, to yield:

$$A = U_o N_o t + S^{-1} \ln [(1 - P(0))/(1 - P(A))] . \qquad (1-35)$$

Note that filter performance changes which are proportional to particle accumulation will generally be non-linear when plotted as functions of time only, if filter efficiency is changing. This effect is particularly noticeable in the case of filter air-flow resistance, as discussed below. Plots of particle accumulation as functions of time were observed to be concave upward, in keeping with the general form of equation (1-35).

4. The deposits formed during filtration of solid particles produce an increase in filter air-flow resistance. The structures of deposited particles develop and grow out from the filter fibers, adding to the fiber drag. It was assumed that the resulting drag on the deposit in the filter would be proportional to the accumulation

of particles (A) and the drag on a single particle, in the following form:

$$\delta \Delta p = (S_p \mu U_o a_p) A \qquad (1\text{-}42)$$

The particle resistance coefficient (S_p) is unknown because the drag on multiple particle aggregates resting on fibers has not been solved. The resistance of experimental filters was observed as a function of accumulation. Values of the coefficient (S_p) were determined. It was found in the majority of tests that the coefficient was a function of fiber fraction, of the form:

$$S_p = 33 \alpha \qquad (3\text{-}7)$$

for $0.007 < \alpha < 0.035$. The coefficient was not a function of filtering velocity ($13 < U_o < 140$ cm/sec) or filter depth ($0.11 \leq L \leq 0.29$ cm) in the ranges studied. Effects of particle size and fiber size were not investigated. Graphs of filter resistance-increase as a function of accumulation were generally linear. The general form of the resistance increase as a function of time should be concave upward, as long as the filter efficiency is changing with accumulation. When efficiency approaches unity, the resistance increase should be proportional to operating time.

5. The initial filter fiber efficiencies were obtained from extrapolation of accumulation-efficiency plots to zero accumulation. These efficiencies were compared to a theoretical solution for the diffusion of particles of finite diameter presented by Friedlander (33). Values of the efficiencies obtained in this study were observed

to be up to one order of magnitude higher than predicted by the Friedlander theory. The theory appears to be practically confirmed by some careful experiments of Chen (23), and Wong and Johnstone (40) using liquid droplets. Nearly all reported experimental results obtained using solid particles were observed to be substantially higher than predicted by the theory. There seems to be a significant difference in the experimental fiber filtration efficiency for solid and liquid particles. This difference is probably a result of particle electrostatic charge arising during the generation of solid particles by spraying liquid suspensions. Further investigation is required. Initial single fiber efficiencies were also obtained from extrapolation of accumulation-efficiency plots to zero accumulation. These efficiencies were found to lie within and below the range of filter fiber efficiencies on the Friedlander theoretical plot.

6. Initial air-flow resistance of test filters was used to calculate an experimental filter medium resistivity:

$$K_o' = \frac{\Delta P}{L} \cdot \frac{a^2}{\mu U_o} \qquad (1\text{-}20)$$

The experimental values were compared to some theoretical solutions for the resistivity of fibrous media. Theoretical resistivity ($K_0(\alpha)$) is a function of fiber fraction only for slow viscous flow. Theoretical solutions are of the form:

$$K_o(\alpha) = 8\alpha/(-\ln\alpha - C_o) \qquad (3\text{-}2)$$

for $\alpha << 1$. The coefficient C_o has been determined analytically by Kuwabara (13) as 3/2, and by Happel and Brenner (12) as 1. Langmuir (9) obtained:

$$K_o(\alpha) = \gamma 4\alpha/(-\ln\alpha - 3/2) \qquad (6\text{-}1)$$

with $1 < \gamma < 2$ to account for fiber orientation. Experimental resistivities were plotted as a function of fiber fraction and equation (3-2) was used to calculate C_o. The experimental value of C_o was about 1/2. The value of γ was not obtained in this study. In general, the Happel-Brenner and Kuwabara solutions yielded resistivities which were slightly high. No attempt was made to relate the theoretical solutions to results of several other experimental studies reported in the literature.

B. Applications of the Results

1. The results of this study can be applied directly to the design of filter systems to achieve an optimum balance between installation and capital costs, and operating and filter replacement costs. In practice, a filter system is designed and installed based on filter manufacturers recommended air-flow. Filters are then operated until they "clog", that is, until filter resistance rises to some undesirable value. Filters then must be replaced or cleaned. Filters used for collection of solid aerosol particles do not exhibit any migration of collected material to the outlet side during normal operation. A fibrous filter does not release any of its accumulated material in the form of "breakthrough" common in adsorption and

liquid filtration. In general, filter efficiency is adequate for the designated task at the start of filtration, and the increase in filter efficiency as a result of accumulation is of no consequence. The governing economic consideration is filter "life" or the time required for the resistance to increase a certain amount. The results of the present research show that filter resistance resulting from accumulation is proportional to the accumulation and the particle drag:

$$\delta \Delta p = (S_p \mu U_o a_p) A. \qquad (1\text{-}42)$$

Since A is a function of U_o, the clogging resistance is approximately proportional to the square of the filtering velocity. For example, a two-fold increase in the size of the initial installation of a filter system should produce approximately a four-fold increase in filter life. The relative economics of increasing the size of a filter system as opposed to more frequent filter changes depend upon capital charges and other considerations unique to the given system. It should be possible to optimize system design velocity with the information resulting from this study. The effect of velocity on filter efficiency has been summarized in Chapter I.

2. The accumulating deposit on single glass fibers was observed as a function of time. Chain aggregates of particles formed and grew out from the fibers. The development of aggregates was photographed and their sizes were measured. Information on aggregate size as a function of operating variables should be useful in the development of a theory of particle deposition effects in fiber filters.

3. Filters composed of layers of graded fiber sizes are used to separate the polydisperse atmospheric aerosol into size fractions (4, 5, 6, 7, 8). After operating the filter for a day or more, the amount of deposited material on each of the graded fiber layers is determined. The particle size separated by each layer is obtained by prior calibration with monodispersed particles. The relative fraction of material on each layer is presumed to be proportional to the frequency of occurrence of the calibrated particle size in the atmospheric aerosol. The results of the present study indicate that accumulation effects are probably of importance in the interpretation of graded fiber filter results. The accumulation of material in the filter produces a higher efficiency, and this may tend to indicate a larger particle size than is actually present (5, 6, 7).

C. Further Studies

1. Accumulation effects on single fibers were investigated with 1.305-micron diameter aerosol particles of polystyrene latex, spray-dried from a suspension. The chain-like form of particle deposit structures suggests that further study is required with solid particles having known electrostatic charge, so that contributions of this effect can be isolated. Other aerosol particle materials and different particle sizes should also be investigated.

2. The single fibers used in this study were 10-micron diameter glass fibers taken at random from bulk fiber glass media. They were not treated in any way. Further study of the effect of fiber size, surface condition, and surface treatment is required. Fibers coated

with molecular layers of evaporated metals or carbon should prove useful in the study of fiber charge effects. Thin layers of conducting materials should continue to permit the microscopic observation of the deposit while providing known electrical or thermal boundaries. Effects of hydrophobic, hydrophilic, and adhesive coatings can be studied with the single fiber technique developed for this investigation. The method can in principle be extended to other obstacle geometries as well, e.g. spheres of varying diameter.

3. The study of accumulation effects on the performance of commercial filter media has been limited to a few studies with polydisperse aerosols. To provide useful engineering data, it would be of value to investigate commercial filter performance as a function of accumulation with monodisperse solid particles.

APPENDIX 2-1

DETAILS OF AEROSOL TEST APPARATUS

APPENDIX 2-1

DETAILS OF AEROSOL TEST APPARATUS

A2-1-1 Introduction

A general description of the experimental apparatus used for this study has been presented in Chapter II. The following sections contain more details about the construction and operation of the aerosol generators, the charge neutralization devices, and the aerosol tunnel.

A2-1-2 Aerosol Generation

Figure A2-1-1 is a photograph of apparatus for the generation of monodispersed solid aerosol particles. Four major components are illustrated. From right to left, they are (1) a silica gel drying column, (2) a compressed air regulator valve, air saturator and mist droplet eliminator, (3) a sprayer with a particle suspension reservoir and (4) a drying section connected to a tee containing an air ion source.

In operation, a suspension of monodispersed solid particles in liquid was atomized by the sprayer shown in Figure A2-1-2*. Filtered compressed air was regulated and then saturated with water in a steel pipe bottle (2 in. diam. x 18 in. long) by means of a porous dip tube. The air then passed through a droplet eliminator (same sized pipe packed with aluminum wool), and through a hose to the sprayer. During the operation of model I (II) generator, pressure was regulated

---

* Slightly modified from a design kindly furnished for this study by Dr. P.K. Mueller, Chief, Air and Industrial Hygiene Laboratory, Dept. of Public Health, State of California, Berkeley, California.

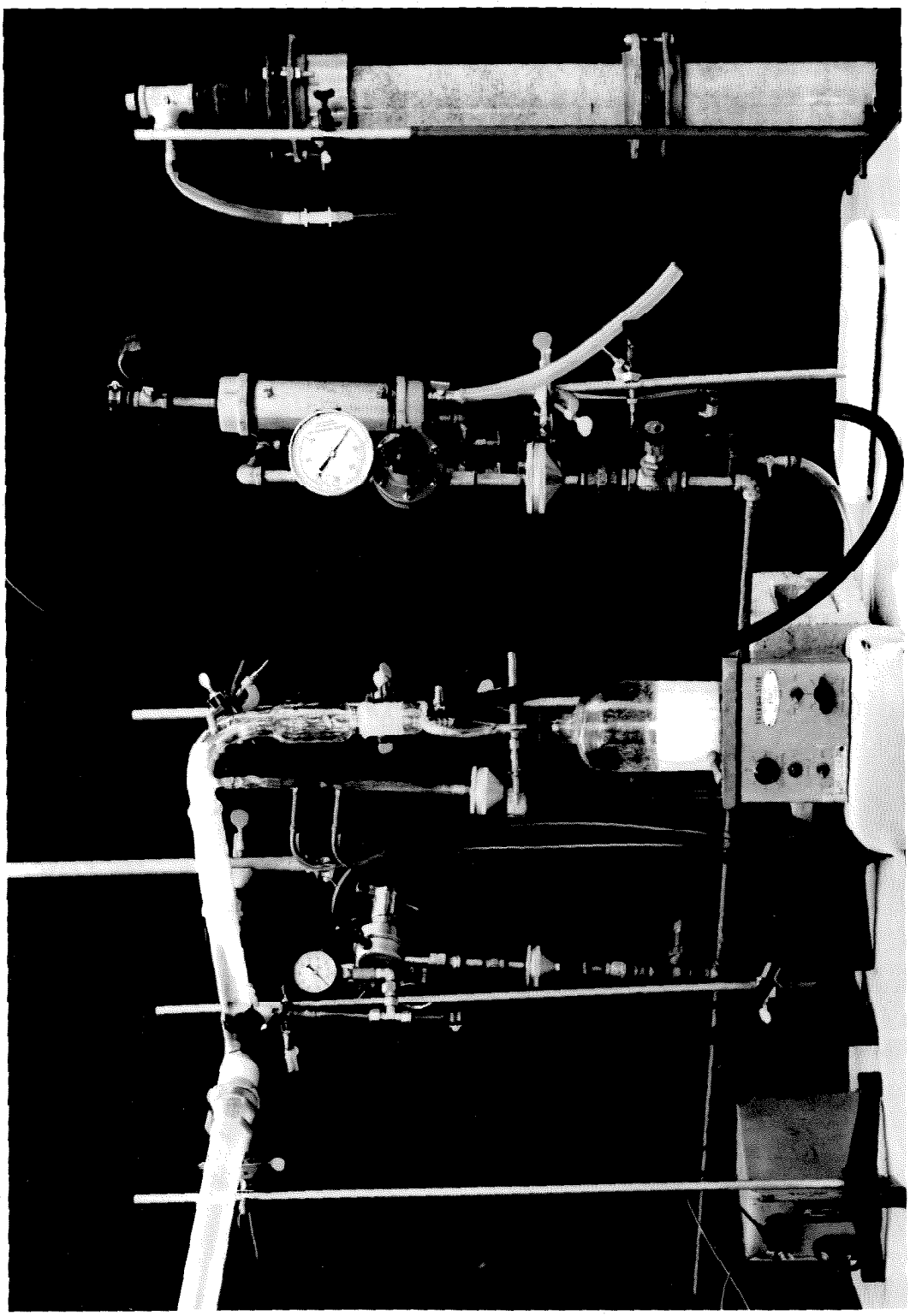

Figure A2-1-1. Photograph of Apparatus for Aerosol Generation

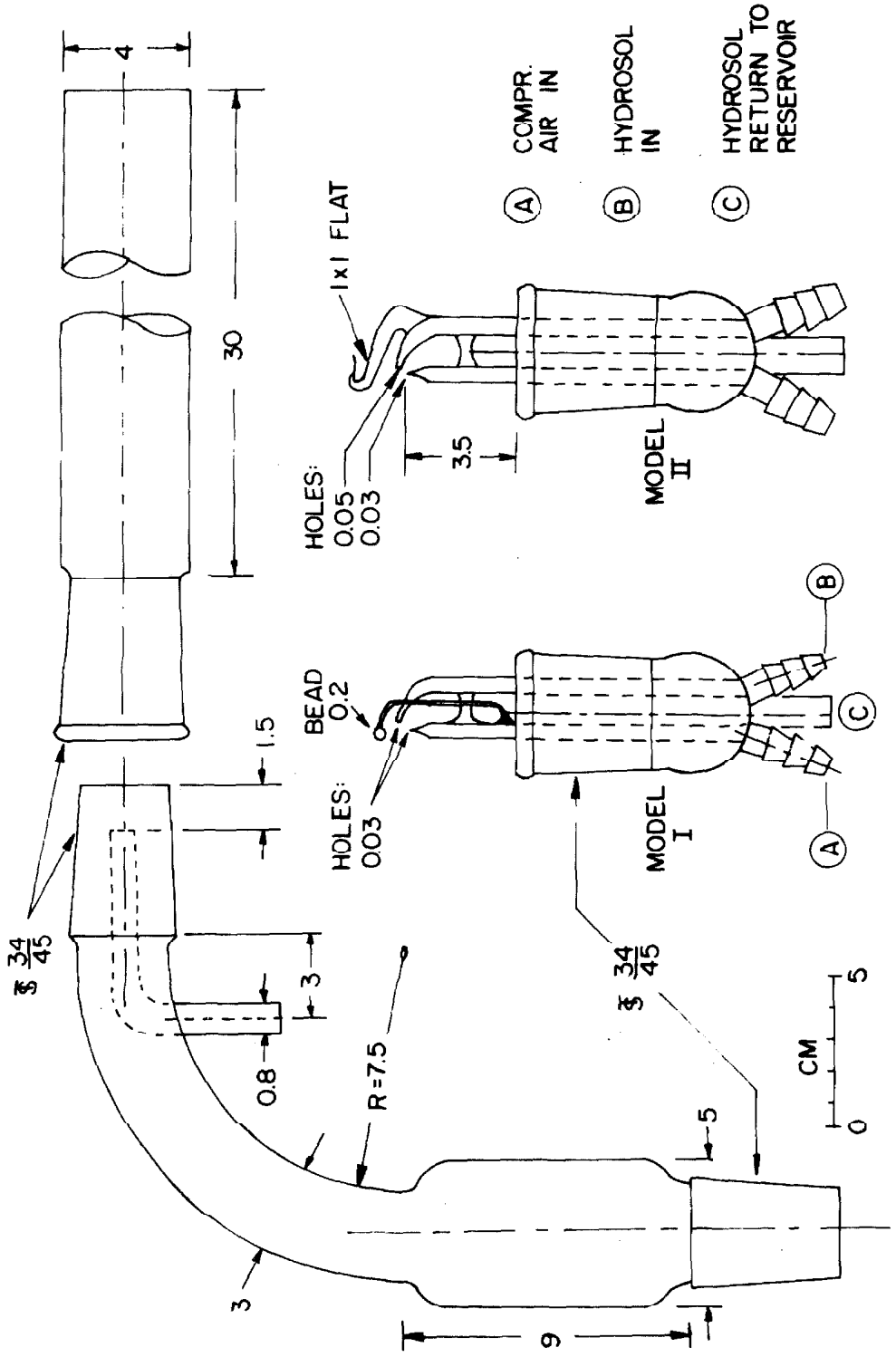

Figure A2-1-2. Aerosol Generator

to 30 (60) psig; sprayer air volume was 7 (13.7) lpm at laboratory temperature and pressure.

Liquid was supplied to the sprayer from the one-liter bottle located on a magnetic stirrer shown just below the generator, as shown in Figure A2-1-1. Stock suspensions of Dow Polystyrene Latex Particles* were diluted with distilled, demineralized, and membrane filtered water. Dilutions ranged from 10^3:1 to 50:1 in the various tests.

The suspension was conducted from the reservoir bottle to the sprayer through a glass tube. The high velocity compressed air jet aspirated a stream of the hydrosol and atomized it by shear and by impaction on the adjacent surface. Most of the suspension deposited on the walls of the enlarged section of the elbow shown in Figure A2-1-2. A fine mist passed upward through the elbow to the drying section. The sprayer had a liquid feed rate of about 50 cm^3/min at an air pressure of 60 psig. About 1 cm^3/min was aerosolized, the remainder passing back to the storage reservoir by gravity through a return tube. Ten cm^3/hr of dilution water was added to the reservoir to compensate in part for evaporation losses caused by the sprayer compressed air.

Dried air (33.3 lpm) was admitted through the smaller tube at the top of the elbow shown in Figure A2-1-2. This air had been pumped through the silica gel column and then membrane filtered and

---

* 1.305-microns diameter, standard deviation 0.0158-microns, Run No. LS-464-E, kindly furnished for these studies by Bioproducts Dept., The Dow Chemical Co., Midland, Michigan (L.J. Lippie).

metered. An aerosol of the monodispersed polystyrene latex spheres formed as the mist droplets evaporated in the straight tube section.

A2-1-3 Aerosol Charge Reduction

The mist was charged to an unknown extent in the spraying process. As water evaporated, the charge was transferred to the small solid particles contained in some of the droplets. To reduce the charge on the particles they were mixed with a stream of bipolar air ions in the tee section shown in Figure A2-1-1. Bipolar air ions were produced by a sonic jet ionizer modified from a design by Whitby (77). The ionizer was constructed from a one-half inch nylon tee as shown in Figure A2-1-3. A brass plate with a 0.040 inch orifice was held by the compression nut in one leg of the tee. The opposite leg held a one-half inch diameter nylon rod drilled to hold a tungsten needle (0.040 inch diameter). The needle was located 0.070 inch behind the orifice. Filtered, regulated compressed air was furnished at 30 psig through the third leg of the tee. Sonic flow was obtained at the orifice (27.6 lpm).

A corona discharge was maintained from the needle to the orifice by a 15 kv. luminous tube transformer regulated to 2.5 kv.a.c. Bipolar ions were removed from the corona discharge by the escaping air and ejected into the aerosol stream. A glass tube followed, as shown in Figure A2-1-1, to permit the air ions and particles to mix.

A2-1-4 Electrostatic Precipitator

To reduce the likelihood of highly charged particles reaching the aerosol tunnel, the aerosol stream was next passed through a low

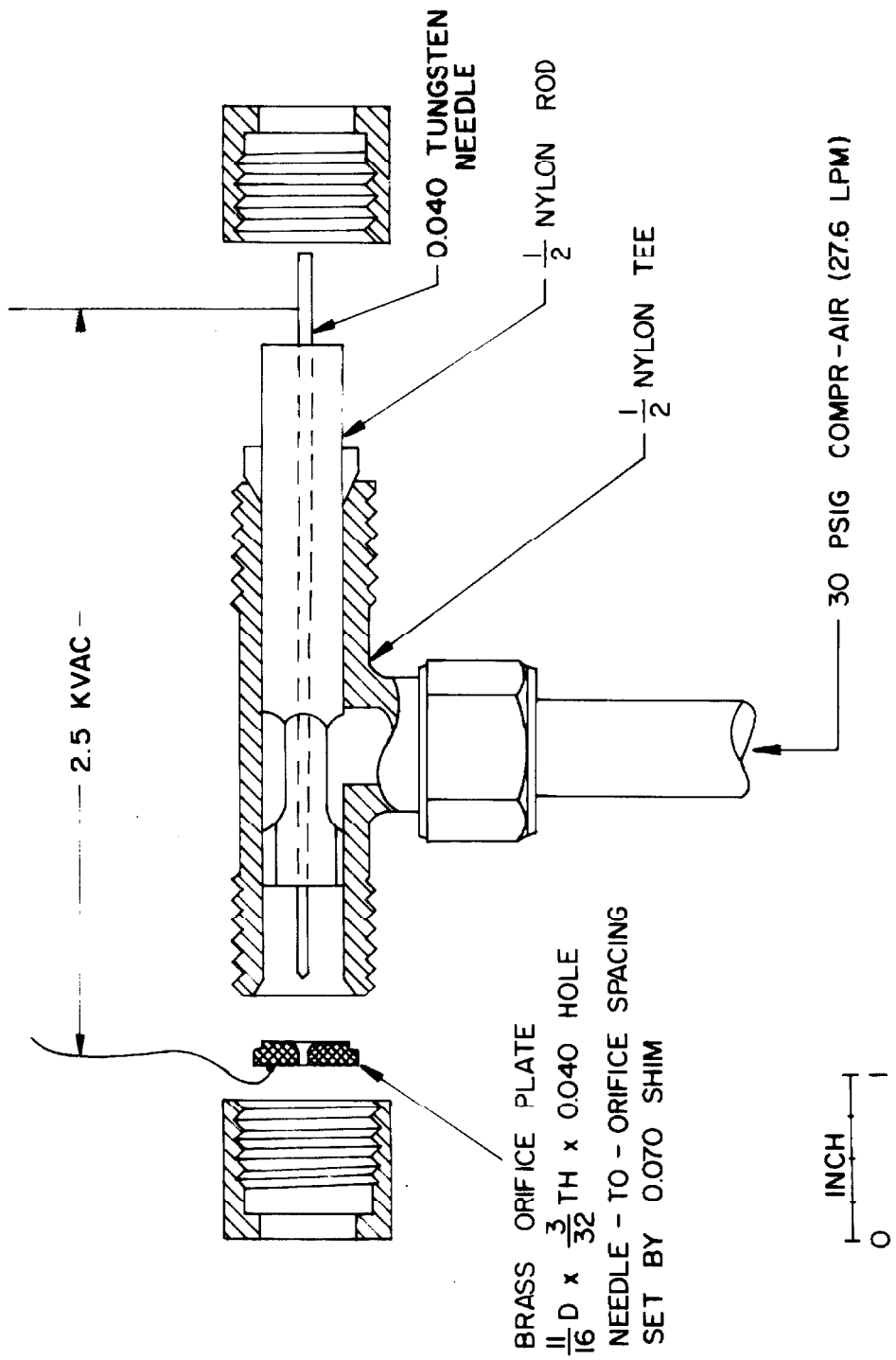

Figure A2-1-3. Sonic Jet Ionizer

voltage electrostatic precipitator shown at the top of Figure A2-1-4. The precipitator was formed by a 1-1/8 inch outside diameter copper tube 60 inches long held by two Teflon insulators in the center of a 2-inch (i.d.) copper tube. Plastic cones were placed in either end of the central tube to promote smooth air flow. The central tube was maintained at a negative potential with respect to the outer tube by means of a d.c. supply* (0, 170 to 1530 v.d.c. in 85 volt steps). The outer tube was grounded through a ten megohm resistor. The voltage drop was measured by a high impedance recording voltmeter.**

Gap spacing on the precipitator was approximately one cm. Operating voltage on the central electrode was usually 170 v.d.c. to cause precipitation of highly charged particles only. To maintain a reasonable aerosol concentration, it was necessary to accept some aerosol charge. The equilibrium charge on one micron aerosol particles is about 3 electron charges (78). Some study of charge effects on filtration was attempted by changing the precipitator voltage and observing filter efficiency during tests on filter number 7a. The average charge per particle was not measured directly.

A2-1-5 Aerosol Tunnel Assembly

A schematic diagram of the aerosol tunnel constructed for this study has been included as part of Figure 2-1. A photograph of the tunnel assembly is shown in Figure A2-1-4. The tunnel consisted of

---

* J-F High Voltage D.C. Supply, Model 409A, Ser. 411, John Fluke Mfg. Co., Inc., Seattle, Washington.
** 0 to 10 millivolt servo/riter, Model FWS, S/N FWS 1325, Texas Instruments, Inc., Houston, Texas.

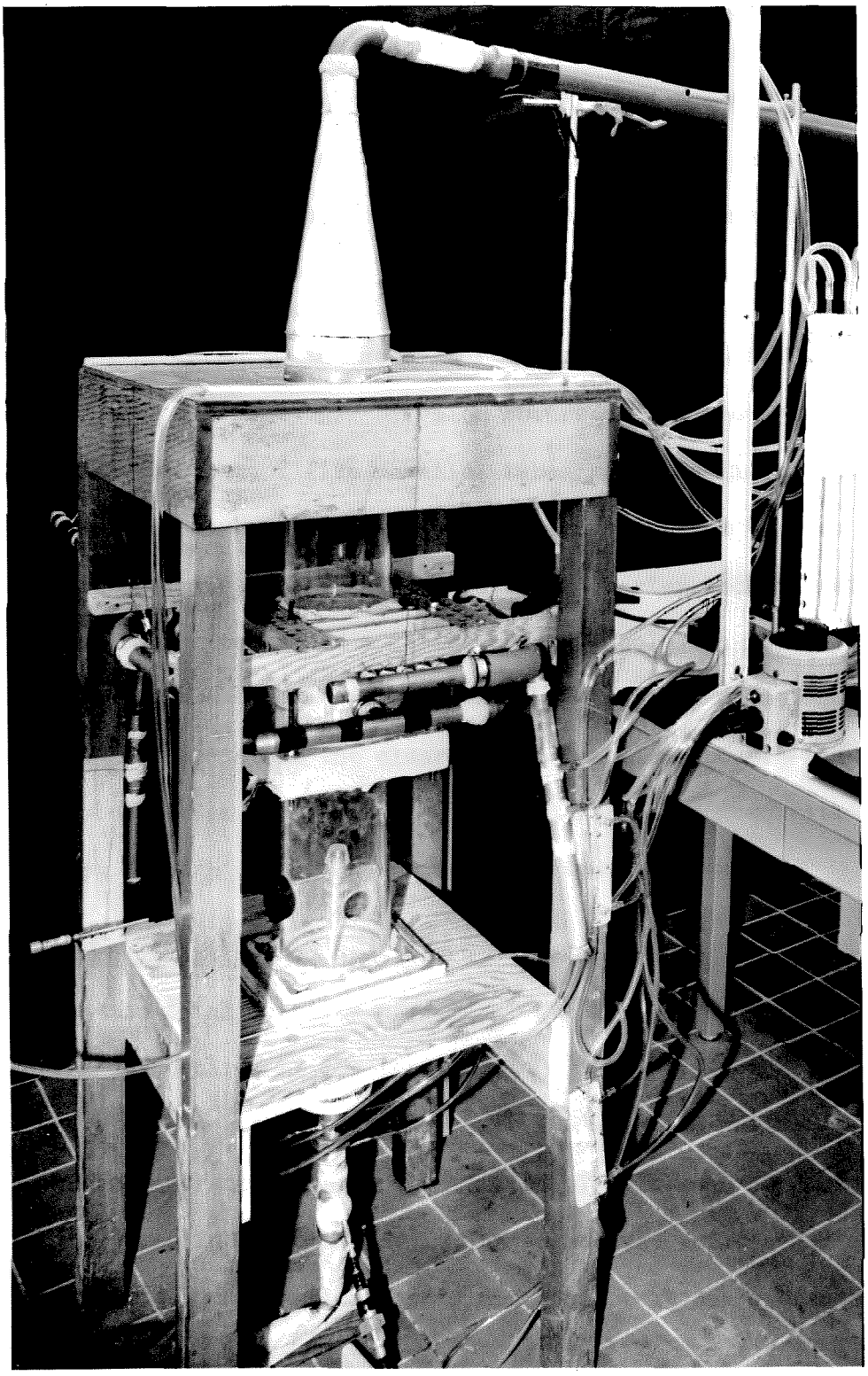

Figure A2-1-4. Photograph of Aerosol Tunnel

six major components; (1) dilution and mixing section (2) extraction section, (3) upstream sampling section, (4) contraction, (5) test section, and (6) downstream sampling section. Components were bolted together by means of plywood flanges and sealed against air leakage with a mastic sealing compound. These parts are discussed below.

A2-1-6 Aerosol Dilution Section

Aerosol produced by the generator entered the top of the aerosol tunnel through an expansion. Dilution occurred by introduction of air through two banks of five parallel tubes shown in Figure A2-1-5. Air was admitted through filters to manifolds connected to each end of the two tube banks. Each of the five one-quarter inch diameter tubes in each bank contained a series of small holes in its top surface, facing the oncoming aerosol stream. Jets of dilution air mixed with the aerosol in the clear plastic section above. The total diluted stream containing the desired aerosol concentration then passed through the grid formed by the two tube banks.

A2-1-7 Aerosol Extraction Section

Since the total quantity of aerosol at this point in the tunnel was more than required at the test section, the excess amount was extracted at the section shown in Figure A2-1-6. The wall of the tunnel at the extraction section consisted of a 16-mesh screen* (4 inches long by 6 inches diameter). The screen was enclosed by an annular pipe (8 inch diameter) containing four exit ports connected

---

* Copper Radar Screen, 16 mesh, 0.010 inch wire diameter, kindly furnished for these studies by the Industrial Wire Products Corp., Los Angeles, Calif.

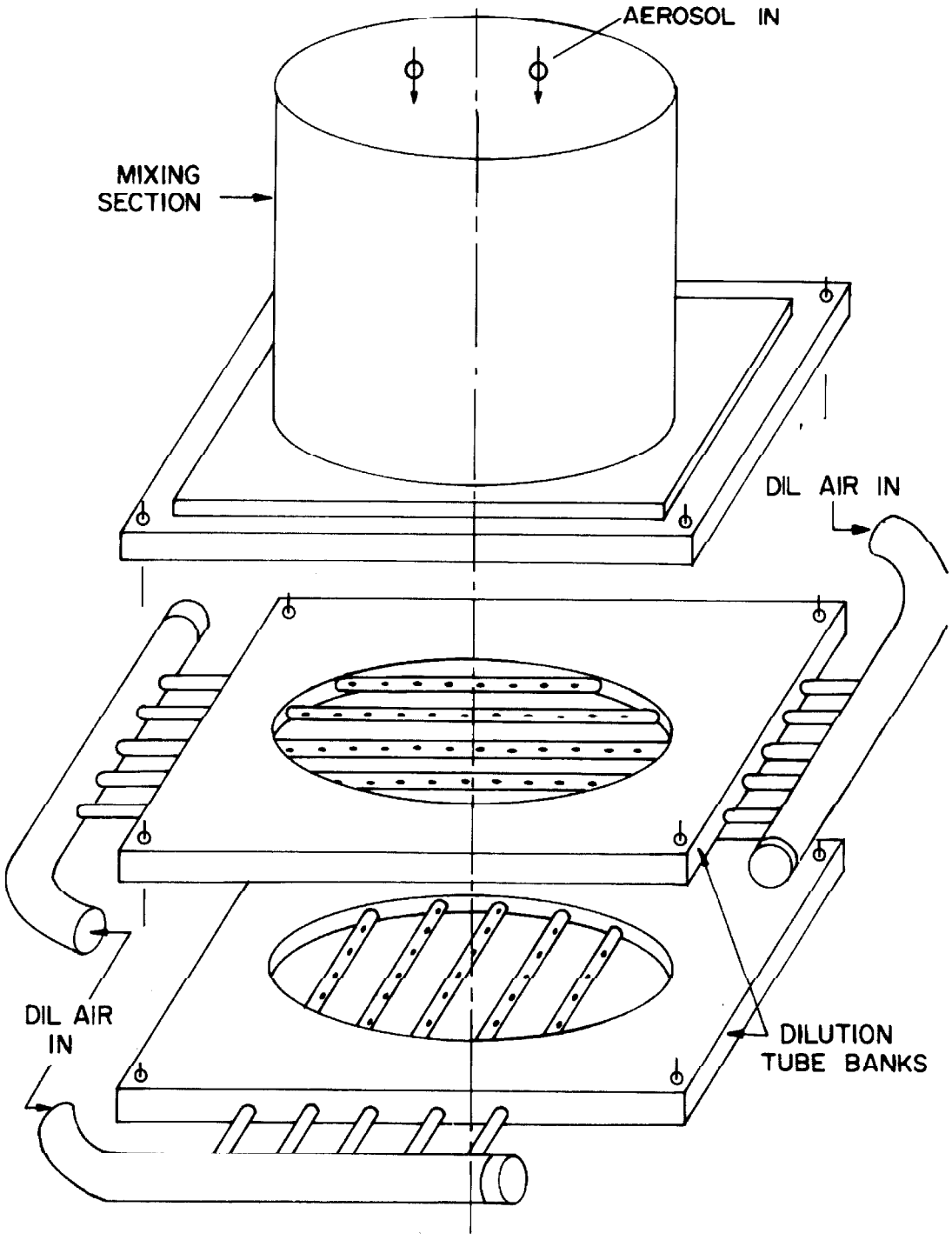

Figure A2-1-5. Aerosol Dilution Section

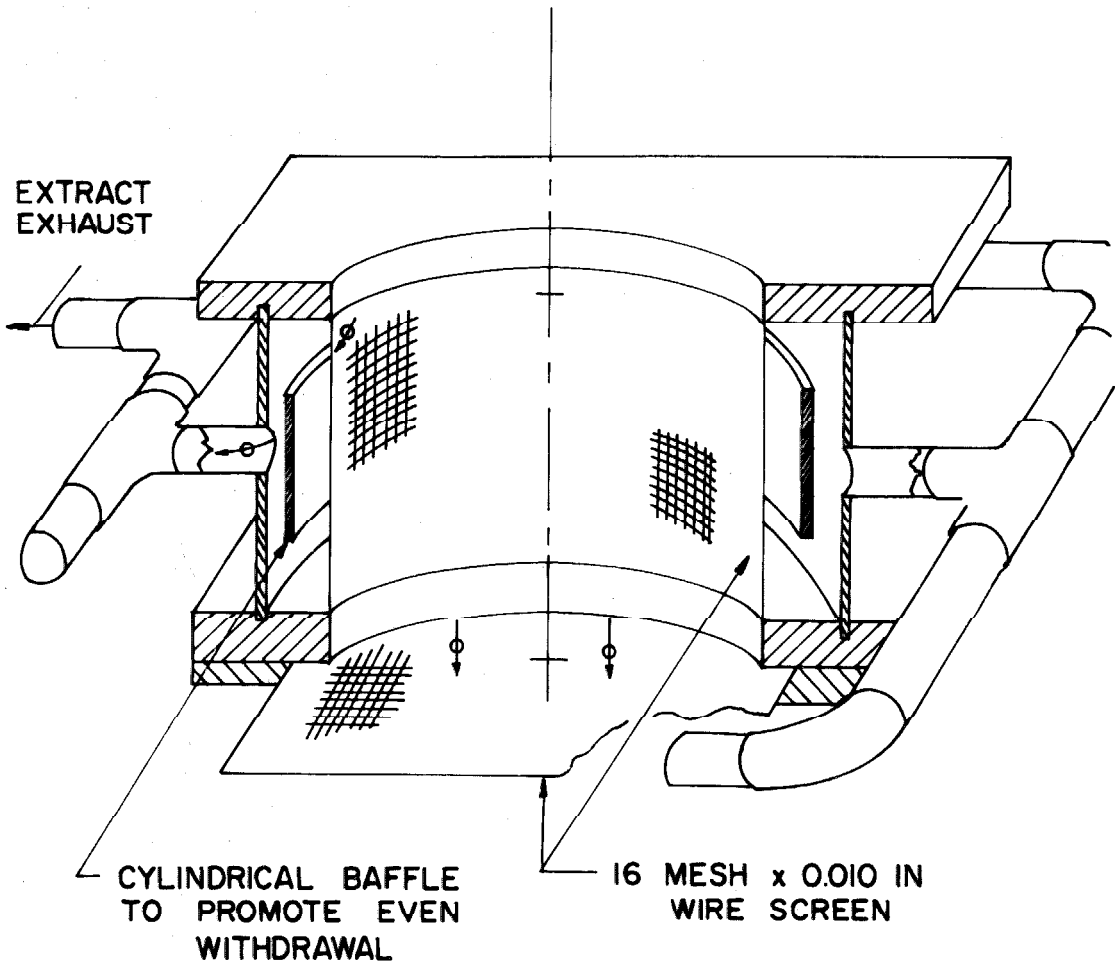

Figure A2-1-6. Aerosol Extraction Section

to a common exhaust. Extracted aerosol was metered and discharged through an exhaust line. Aerosol remaining in the tunnel passed through a single wire screen to promote uniform flow.

A2-1-8 Upstream Aerosol Sampling Section

A sample for particle concentration analysis was taken isokinetically from the clear plastic tube (12 inches long by 6 inches diameter) visible in the lower center of Figure A2-1-4. An upstream sampling probe containing a 25mm circle of membrane filter* was inserted through a hole in the plastic tube and held in place by means of a rubber stopper. A metered amount of aerosol was drawn through the probe and particles deposited on the filter. Sample analysis is discussed in Chapter II. The probe design (Model III) consisted of a standard solder union for 7/8-inch (o.d.) copper tubing modified as shown in Figure A2-1-7. Exterior fairing was made from styrene plastic rod. Earlier models (I, II) are also shown in outline in Figure A2-1-7. A calibrated glass capillary flowmeter was used to regulate flow rate to an exhaust pump.

A2-1-9 Tunnel Contraction

Aerosol remaining in the tunnel after passing the upstream sampler then passed through a 16:1 contraction to the tunnel test section. The contraction is illustrated in Figure 2-3. Offset dimensions (x' along the centerline and R' the radial distance) used for the construction of the wooden pattern are given in Table A2-1-1.

---

* Type HA, Grid Marked, 0.45-micron nominal pore size, Millipore Filter Corp., Bedford, Mass.

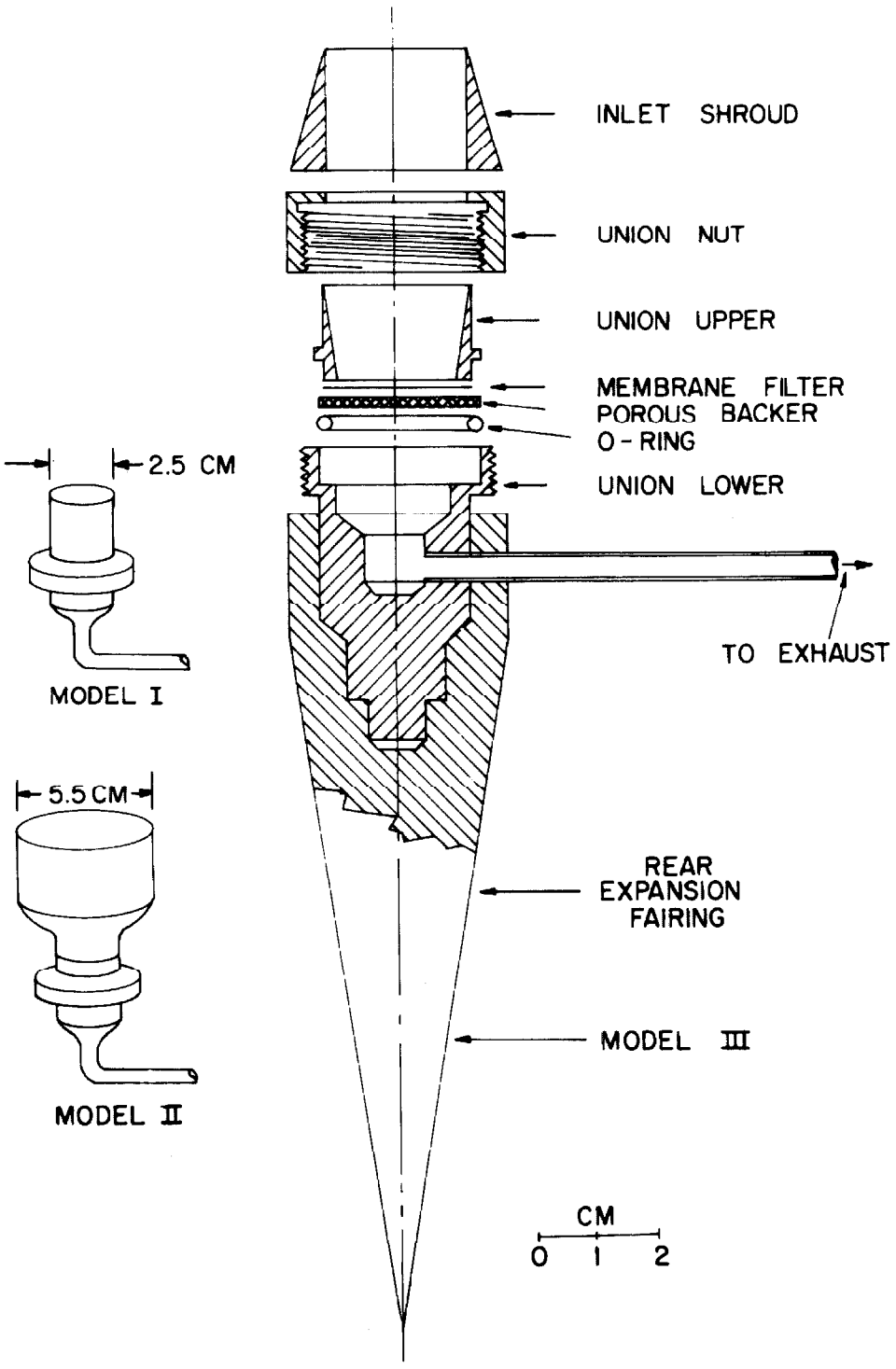

Figure A2-1-7. Upstream Aerosol Sampling Probe

TABLE A2-1-1

Aerosol Tunnel Contraction Offsets

Centerline Dist. (x') inches	Radius (R') inches
0	0.75
0.9915	0.765
2.232	0.90
3.003	1.05
3.54	1.20
3.99	1.35
4.38	1.50
4.68	1.65
4.965	1.80
5.22	1.95
5.43	2.10
5.68	2.25
5.91	2.40
6.132	2.55
6.45	2.70
6.825	2.85
7.125	2.925
7.80	3.00

The contraction reduced the tunnel diameter from 6 inches to 1-1/2 inches in a length of 7.8 inches.

A2-1-10 Tunnel Test Section

Aerosol passed from the end of the contraction into a 1-1/2-inch diameter tube as shown in Figure 2-4. Filter mats and single fiber experiments were held in a modified 1-1/2-inch union as discussed in Chapter II.

A2-1-11 Downstream Aerosol Sampling Section

A downstream sample was taken after the aerosol passed through the test section. A small probe located in the center of the downstream tube conducted a sample of the aerosol to an external filter holder as shown in Figure A2-1-8. The holder consisted of a copper tubing union modified to hold a 25 mm circle of membrane filter. The external location was required because of space limitations in the tunnel. The remaining aerosol then passed through an orifice meter to an exhauster in a laboratory hood.

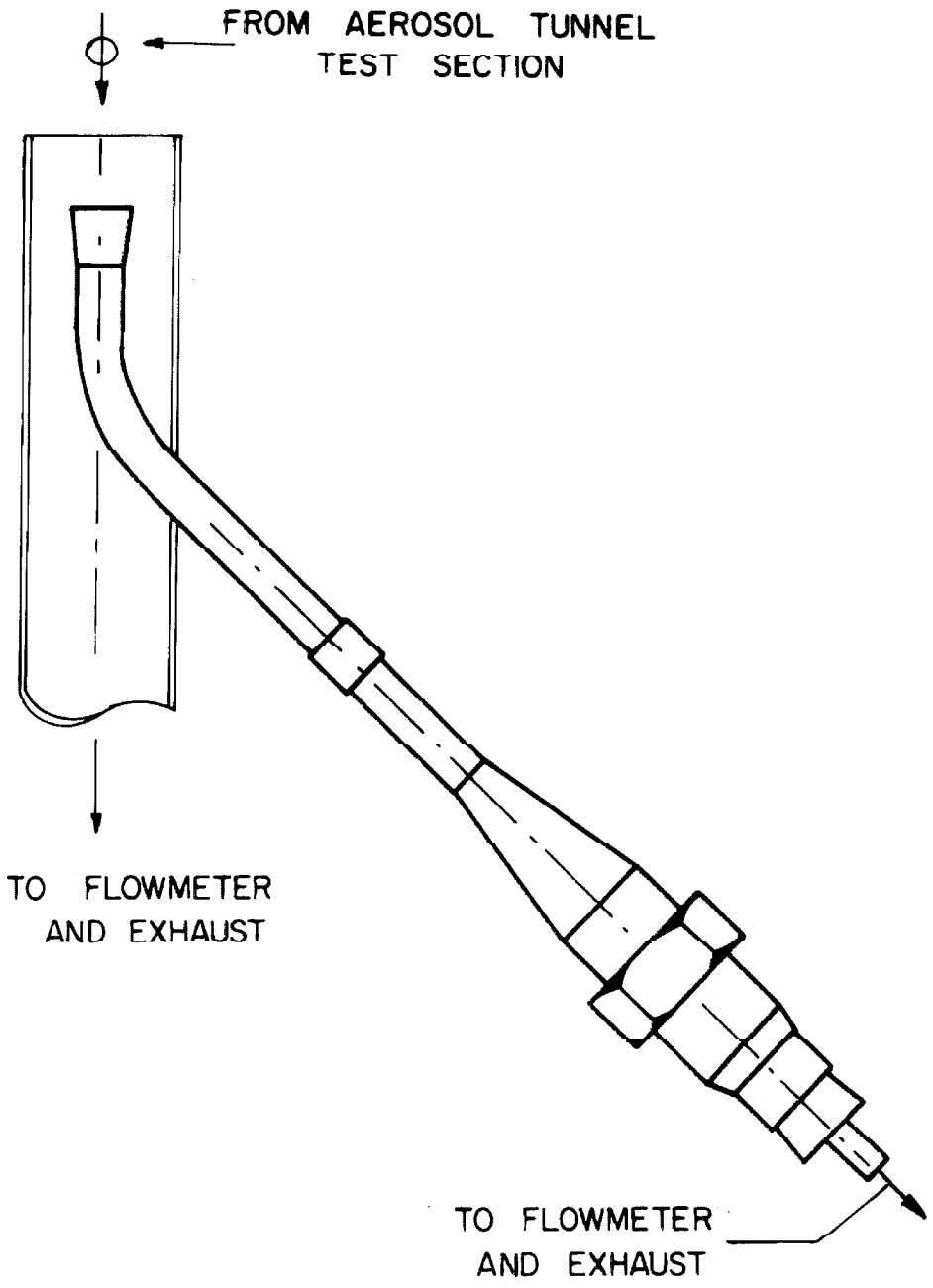

Figure A2-1-8. Downstream Aerosol Sampling Probe

APPENDIX 3-1

FIBER FILTER TEST DATA

TABLE A3-1-1

Test Data for Filter No. 1

Cum. Time min.	Resist.[a] in oil	Particle Concentration p/cm^3		Efficiency	Remarks[b]
		Inlet	Outlet		
0	1.40	-	-	-	On
132	1.40	-	-	-	Stop - start
169	1.40	7.96	0.750	0.9114	10m(-) (-)
184	1.41	-	-	-	Stop - start
249	1.41	9.10	0.717	0.9212	20m(-) (-)
354	1.42	-	-	-	-
370	1.42	14.00	0.998	0.9288	20m(-) (-)
384	1.43	-	-	-	Stop - start
473	1.44	-	-	-	-
488	1.43	-	-	-	-
518	1.43	-	-	-	Res. above on vertical manometer
533	1.429	-	-	-	Res. below on 10:1 inclined manometer
548	1.430	-	-	-	-
560	-	20.6	1.203	0.9415	20m(0.032)(0.013)
571	1.433	-	-	-	-
608	1.434	-	-	-	Stop - start
653	1.451	-	-	-	-
688	1.464	-	-	-	-
703	-	23.9	1.064	0.9555	20m(-) (-)

TABLE A3-1-1 (Cont'd)

Test Data for Filter No. 1

Cum. Time min.	Resist.[a] in oil	Particle Concentration p/cm³ Inlet	Particle Concentration p/cm³ Outlet	Efficiency	Remarks[b]
715	1.469	-	-	-	-
758	1.472	-	-	-	-
793	1.481	-	-	-	-
818	1.477	-	-	-	Stop - start New suspension
842	-	27.8	1.073	0.9602	20m(0.064)(0.04)
854	1.486	-	-	-	-
882	1.489	-	-	-	-
957	1.495	-	-	-	Stop - start
985	1.504	-	-	-	-
997	-	28.4	0.869	0.9694	20m(-) (-)
1010	1.507	-	-	-	Stop - start
1026	1.510	-	-	-	-
1091	1.517	-	-	-	-
1156	1.529	-	-	-	-
1176	1.531	-	-	-	-
1188	-	23.8	0.555	0.9768	20m(0.04)(0)
1231	1.538	-	-	-	-
1276	1.550	-	-	-	-
1296	1.554	-	-	-	-
1307	-	22.6	0.531	0.9765	20m(-)(-)

TABLE A3-1-1 (Cont'd)

Test Data for Filter No. 1

Cum. Time min.	Resist.[a] in oil	Particle Concentration p/cm^3		Efficiency	Remarks[b]
		Inlet	Outlet		
1321	1.567	-	-	-	-
1381	1.575	-	-	-	Stop -start
1420	1.575	-	-	-	-
1480	1.584	-	-	-	-
1493	-	15.55	0.362	0.9767	20m(0.025)(0)
1535	1.591	-	-	-	-
1595	1.595	-	-	-	-
1693	1.612	-	-	-	-
1735	1.616	-	-	-	-
1750	1.620	-	-	-	-
1761	-	7.09	0.178	0.9749	20m(0.016)(0)
1775	1.628	-	-	-	-
1780	1.632	-	-	-	Stop-start New suspension
1808	1.634	-	-	-	-
1819	-	24.9	0.46	0.9816	20m(-) (-)
1838	1.642	-	-	-	-
1863	1.649	-	-	-	-
1908	1.653	-	-	-	-
1968	1.667	-	-	-	-
2028	1.683	-	-	-	-

TABLE A3-1-1 (Cont'd)

Test Data for Filter No. 1

Cum. Time min.	Resist.[a] in oil	Particle Concentration p/cm^3		Efficiency	Remarks[b]
		Inlet	Outlet		
2068	1.685	-	-	-	-
2138	1.705	-	-	-	-
2150	-	22.9	0.398	0.9827	20m(0.042)(0)
2168	1.716	-	-	-	Stop - start
2173	1.72	-	-	-	Change to vertical manometer
2178	1.72	-	-	-	On over night
2488	1.76	-	-	-	-
2507	1.76	-	-	-	-
2519	-	15.9	0.241	0.9848	20m(-) (-)
2544	1.76	-	-	-	-
2643	1.78	-	-	-	-
2678	1.78	-	-	-	Stop test.

a. Resistance, inches of petroleum gage oil (sp.g. 0.826).

b. Numbers in ( ) are fraction of particle count composed of more than one particle,(Inlet)(Outlet); operating velocity 139 cm/sec; probe I; numbers beside m are sampling times, min; Gen. I at 30 psig.

TABLE A3-1-2

Test Data for Filter No. 2

Cum. Time min.	Resist.[a] in oil	Particle Concentration p/cm³		Efficiency	Remarks[b]
		Inlet	Outlet		
0	0.070	-	-	-	On
10	-	58.6	33.0	0.436	10m(-) (-)
35	-	60.6	31.5	0.480	10m(-) (-)
64	0.071	61.0	35.8	0.411	10m(-) (-)
109	0.071	-	-	-	-
161	0.071	61.9	34.4	0.446	10m(-) (-)
184	0.071	-	-	-	Stop - start
209	0.071	-	-	-	-
258	0.072	61.7	31.0	0.497	10m(-) (-)
314	0.072	-	-	-	-
355	0.072	91.3	44.1	0.516	10m(-) (-)
389	0.0725	-	-	-	-
469	0.073	91.0	46.0	0.495	10m(-) (-)
493	0.072	-	-	-	Stop - start
602	0.072	-	-	-	-
624	0.072	76.2	42.2	0.447	10m(-) (-)
636	0.072	-	-	-	Stop - start
695	0.072	-	-	-	-
765	0.072	-	-	-	Stop - start
783	0.073	63.1	30.6	0.515	10m(-) (-)
894	0.0735	-	-	-	-

TABLE A3-1-2 (Cont'd)

Test Data for Filter No. 2

Cum. Time min.	Resist.[a] in oil	Particle Concentration p/cm^3 Inlet	Particle Concentration p/cm^3 Outlet	Efficiency	Remarks[b]
999	0.074	39.4	21.2	0.461	10m(-) (-)
1047	0.0745	-	-	-	Stop - start
1103	0.0745	-	-	-	Stop - start
1225	0.0745	-	-	-	-
1284	0.074	-	-	-	-
1328	0.0745	13.38	9.42	0.295	10m(-) (-)
1346	0.0745	-	-	-	Stop - start New suspension
1367	0.075	75.8	38.5	0.491	10m(-) (-)
1384	0.0755	-	-	-	-
1401	0.0755	-	-	-	-
1448	0.0765	-	-	-	-
1466	0.0765	75.0	38.3	0.489	10m(-)(-)
1476	0.074	-	-	-	Stop - start Air on at night
1516	0.0740	-	-	-	-
1538	0.0745	72.5	38.9	0.464	10m(-) (-)
1583	0.0745	-	-	-	Stop - start
1663	0.0745	-	-	-	-
1726	0.0745	65.4	29.5	0.549	10m(-) (-)
1778	0.0745	-	-	-	-

TABLE A3-1-2 (Cont'd)

Test Data for Filter No. 2

Cum. Time min.	Resist. in oil [a]	Particle Concentration p/cm³ Inlet	Particle Concentration p/cm³ Outlet	Efficiency	Remarks [b]
1823	0.0745	-	-	-	-
1853	0.0740	60.1	28.0	0.535	10m(-) (-)
1876	0.0740	-	-	-	Stop test.

a. Resistance, inches of petroleum gage oil (sp.g. 0.826).

b. Numbers in ( ) are fraction of particle count composed of more than one particle, (Inlet)(Outlet); operating velocity 13.78 cm/sec; Probe I,II; numbers beside m are sampling times, min; Gen. I at 30 psig.

TABLE A3-1-3

Test Data for Filter No. 3

Cum. Time min.	Resist.[a] in oil	Particle Concentration p/cm^3		Efficiency	Remarks[b]
		Inlet	Outlet		
0	0.0355	-	-	-	On
12	0.0355	851	519	0.390	2m(0.127)(0.106)
22	0.0355	810	600	0.260	2m(0.10)(0.10)
28	0.0355	-	-	-	Stop - start
31	0.0355	611	498	0.185	2m(0.099)(0.093)
42	0.0355	818	630	0.230	2m(0.114)(0.109)
53	0.0360	-	-	-	-
62	0.0360	942	557	0.409	2m(0.116)(0.075)
68	0.0365	-	-	-	-
82	-	923	568	0.385	2m(0.132)(0.102)
88	0.0365	-	-	-	Stop - start on Probe I
105	0.0365	-	-	-	Stop - start
117	-	795	581	0.269	2m,dn (0.088)
120	0.0370	-	-	-	9m,up (0.14)
123	-	795	649	0.183	2m,dn (0.090)
129	0.0370	-	-	-	-
154	0.0375	-	-	-	-
161	-	804	602	0.250	2m,dn (0.056)
164	0.0380	-	-	-	10m,up (0.133)
168	-	804	606	0.253	2m,dn (0.060)

TABLE A3-1-3 (Cont'd)

Test Data for Filter No. 3

Cum. Time min.	Resist[a] in oil	Particle Concentration p/cm³ Inlet	Particle Concentration p/cm³ Outlet	Efficiency	Remarks[b]
170	0.0385	-	-	-	-
209	0.0390	-	-	-	-
221	-	820	547	0.333	2m,dn (0.103)
224	0.0395	-	-	-	10m,up (0.127)
229	-	820	557	0.320	2m,dn (0.077)
234	0.0395	-	-	-	-
249	0.0400	-	-	-	-
264	0.0400	-	-	-	Stop - start
272	-	853	549	0.356	2m,dn (0.070)
275	0.0405	-	-	-	10m,up (0.14)
279	-	853	542	0.346	2m,dn (0.069)
281	0.040+	-	-	-	-
375	0.0425	-	-	-	-
392	-	850	568	0.331	2m,dn (0.077)
395	0.0430	-	-	-	10m,up (0.116)
399	-	850	522	0.350	2m,dn (0.067)
401	0.0435	-	-	-	-
420	0.0440	-	-	-	-
440	0.0445	-	-	-	-
452	-	783	521	0.334	2m,up (0.069)
455	0.0445	-	-	-	10m,dn (0.118)

TABLE A3-1-3 (Cont'd)

Test Data for Filter No. 3

Cum. Time min.	Resist.[a] in oil	Particle Concentration p/cm³ Inlet	Particle Concentration p/cm³ Outlet	Efficiency	Remarks[b]
459	-	783	568	0.274	2m,up (0.076)
510	0.0460	-	-	-	Stop - start
520	0.0465	-	-	-	-
527	-	784	-	-	near wall (0.059)
533	-	888	-	-	center (0.068)
539	-	839	-	-	far wall (0.066)
549	0.0465	-	-	-	-
552	-	839	468	0.441	2m,up (0.065)
555	0.0465	-	-	-	10m,dn (0.123)
559	-	839	571	0.319	2m,up (0.065)
561	0.0470	-	-	-	-
572	0.0470	-	-	-	Stop test.

a. Resistance, inches of petroleum gage oil (sp.g. 0.826).

b. Numbers in ( ) are fraction of particle count composed of more than one particle, (Inlet)(Outlet); operating velocity 13.78 cm/sec; Probe II used for first 88 min., Probe I for remainder of test; numbers beside m are sampling times, min; Gen. I at 30 psig.

TABLE A3-1-4

Test Data for Filter No. 4

Cum. Time min.	Resist.[a] in oil	Particle Concentration p/cm3		Efficiency	Remarks[b]
		Inlet	Outlet		
0	0.0275	-	-	-	On
15	-	64	38.1	0.404	20m(0.015)(0.039)
32	0.0275	-	-	-	-
52	-	60.5	44.4	0.266	20m(0.035)(0.04)
81	0.0275	-	-	-	-
92	-	61.1	32.6	0.466	20m(0.019)(0.035)
104	0.0275	-	-	-	-
151	0.0275+	-	-	-	-
162	-	52.9	32.8	0.379	20m(0.025)(0.029)
177	0.0275+	-	-	-	-
180	-	-	-	-	Stop - start New suspension
186	0.0275+	-	-	-	-
197	-	(325)	164.1	(0.505)	20m(0.06)(0.136)
212	0.0275+	-	-	-	-
234	-	317	174.1	0.450	15m(0.087)(0.125)
248	0.0275+	-	-	-	-
271	0.0280	-	-	-	-
277	-	330	181.6	0.450	10m(0.084)(0.09)
291	0.0280	-	-	-	-
294	-	309	182.0	0.410	5m(0.047)(0.059)

TABLE A3-1-4 (Cont'd)

Test Data for Filter No. 4

Cum. Time min.	Resist.[a] in oil	Particle Concentration p/cm^3		Efficiency	Remarks[b]
		Inlet	Outlet		
302	0.0280	-	-	-	Stop - start New suspension
321	0.0280	-	-	-	-
324	-	695	392	0.435	3m(0.064)(0.087)
337	0.0285	-	-	-	3m(0.064)(0.083)
400	-	-	-	-	Stop(estimated times below)
400	0.0295	-	-	-	On
452	0.0300+	-	-	-	-
602	0.0325	-	-	-	Stop - start
770	0.0350	-	-	-	-
772	-	977	550	0.437	3m(0.072)(0.118)
779	0.0350	-	-	-	Stop test.

a. Resistance, inches of petroleum gage oil (sp.g. 0.826).

b. Numbers in ( ) are fraction of particle count composed of more than one particle, (Inlet)(Outlet); operating velocity 13.78 cm/sec; Probe I; numbers beside m are sampling time, min; Gen. I at 30 psig.

TABLE A3-1-5

Test Data for Filter No. 5

Cum. Time min.	Resist.[a] in oil	Particle Concentration p/cm³		Efficiency	Remarks[b]
		Inlet	Outlet		
0	0.031+	-	-	-	On
15	-	83.0	51.6	0.377	10m(0.037)(0.023)
22	0.031+	-	-	-	-
40	-	81.7	57.0	0.302	10m(0.026)(0.029)
57	0.031+	-	-	-	Stop - start
74	-	93.5	75.0	0.194	10m(0.012)(0.025)
93	0.0315	-	-	-	-
99	-	93.5	73.7	0.210	10m(0.016)(0.029)
110	0.0315	-	-	-	Stop - start New suspension
128	0.0320	-	-	-	-
131	-	474	298	0.370	5m(0.089)(0.075)
147	0.0320	-	-	-	-
151	-	482	291	0.397	5m(0.056)(0.066)
164	0.0320	-	-	-	-
171	-	437	276	0.369	5m(0.037)(0.085)
191	-	469	266	0.431	5m(0.067)(0.066)
200	0.0325-	-	-	-	Stop - start New suspension
219	0.0325	-	-	-	-
222	-	960	620	0.354	3m(0.069)(0.087)
234	0.0325+	-	-	-	-

TABLE A3-1-5 (Cont'd)

Test Data for Filter No. 5

Cum. Time min.	Resist.[a] in oil	Particle Concentration p/cm^3 Inlet	Particle Concentration p/cm^3 Outlet	Efficiency	Remarks[b]
236	-	982	637	0.352	3m(0.090)(0.092)
243	0.0325+	-	-	-	Stop - start
275	0.0325	-	-	-	-
278	-	1010	672	0.335	3m(0.084)(0.072)
299	0.0330-	-	-	-	-
310	-	1014	663	0.347	3m(0.06)(0.066)
313	0.0330	-	-	-	-
331	0.0330+	-	-	-	-
356	0.0335-	-	-	-	-
358	-	1075	635	0.408	3m(0.065)(0.080)
422	0.0340	-	-	-	-
424	-	925	636	0.312	3m(0.057)(0.08)
486	0.0350	-	-	-	-
494	-	921	560	0.392	3m(0.054)(0.064)
498	0.0350+	-	-	-	-
536	0.0360	-	-	-	-
538	-	874	537	0.344	3m(0.048)(0.072)
566	0.0360	-	-	-	Stop - start
587	0.0360	-	-	-	-
590	-	909	660	0.274	3m(0.061)(0.09)
624	0.0365	-	-	-	Stop - start

TABLE A3-1-5 (Cont'd)

Test Data for Filter No. 5

Cum. Time min.	Resist.[a] in oil	Particle Concentration p/cm³ Inlet	Particle Concentration p/cm³ Outlet	Efficiency	Remarks[b]
683	0.0365+	-	-	-	-
686	-	855	607	0.289	3m(0.041)(0.086)
858	0.0390	-	-	-	-
860	-	884	586	0.337	3m(0.044)(0.047)
866	0.040-	-	-	-	Stop-new suspension. Gen.I at 60 psig. Add saturator and larger silica gel column.
925	0.0405-	-	-	-	-
928	-	1119	784	0.299	3m(0.094)(0.102)
946	0.0415	-	-	-	-
998	0.0430	-	-	-	-
1104	0.0490	-	-	-	-
1125	0.0495	-	-	-	-
1128	-	1510	751	0.503	3m(0.07)(0.091)
1135	0.0495	-	-	-	-
1221	0.0540	-	-	-	-
1269	0.0565	-	-	-	-
1282	-	1606	601	0.626	3m(0.086)(0.088)
1302	0.0560	-	-	-	-
1463	0.0650	-	-	-	-
1488	-	1161	484	0.416	3m(0.106)(0.071)

TABLE A3-1-5 (Cont'd)

Test Data for Filter No. 5

Cum. Time min.	Resist.[a] in oil	Particle Concentration p/cm³ Inlet	Particle Concentration p/cm³ Outlet	Efficiency	Remarks[b]
1491	0.0645	-	-	-	-
1586	0.0675+	-	-	-	-
1625	0.0695-	-	-	-	-
1630	-	796	313	0.607	3m(0.088)(0.06)
1634	0.0685	-	-	-	Stop - start New suspension
1644	-	717	293	0.591	3m(0.072)(0.047)
1650	0.0690	-	-	-	-
2395	0.1005	-	-	-	-
2404	-	882	322	0.636	3m(0.048)(0.032)
2409	0.0920	-	-	-	note decr. res.
2414	0.0920	-	-	-	-
2713	0.1066	-	-	-	-
2720	0.1065	-	-	-	-
2722	-	793	221	0.721	3m(0.031)(0.035)
2725	0.0985	-	-	-	note decr. res.
2728	0.099-	-	-	-	Stop test.

a. Resistance, inches of petroleum gage oil(sp.g. 0.826)

b. Numbers in ( ) are fraction of particle count composed of more than one particle, (Inlet)(Outlet); operating velocity 13.76 cm/sec; Probe I; numbers beside m are sampling times, min; Gen. I at 30 psig, except as noted changed to 60 psig.

TABLE A3-1-6

Test Data for Filter No. 6

Cum. Time min.	Resist.[a] in oil	Particle Concentration p/cm³ Inlet	Particle Concentration p/cm³ Outlet	Efficiency	Remarks[b]
0	0.0330	-	-	-	On
10	-	243	169	0.303	3m(0.027)(0.032)
21	0.0330	-	-	-	-
24	-	290	174	0.400	3m(0.032)(0.033)
35	0.0330	-	-	-	-
40	-	258	188.5	0.269	3m(0.025)(0.036)
68	0.0330	-	-	-	-
72	-	283	185	0.344	3m(0.023)(0.031)
95	0.0335	-	-	-	-
98	-	287	130	0.546	3m(0.023)(0.019)
128	0.0335+	-	-	-	-
130	-	253	141	0.444	3m(0.024)(0.027)
158	0.0335+	-	-	-	-
162	-	303	161	0.468	3m(0.022)(0.021)
178	0.0340	-	-	-	-
182	-	319	146	0.542	3m(0.016)(0.026)
186	.0330	-	-	-	Stop-start note decr. res.
208	-	248	184	0.258	3m(0.016)(0.022)
278	0.0330+	-	-	-	-
282	-	288	171	0.406	3m(0.023)(0.022)
319	0.0340	-	-	-	Stop - start

TABLE A3-1-6 (Cont'd)

Test Data for Filter No. 6

Cum. Time min.	Resist.[a] in oil	Particle Concentration p/cm^3 Inlet	Particle Concentration p/cm^3 Outlet	Efficiency	Remarks[b]
338	-	239	138	0.413	3m(0.016)(0.019)
436	0.0340+	-	-	-	-
440	-	273	138	0.495	3m(0.048)(0.026)
451	0.0345	-	-	-	Stop - start New suspension
458	-	423	204	0.517	3m(0.040)(0.043)
469	0.0345	-	-	-	-
472	-	381	210	0.448	3m(0.028)(0.043)
488	0.0345+	-	-	-	-
634	0.0355	-	-	-	-
657	0.0360	-	-	-	-
662	-	508	237	0.534	3m(0.044)(0.05)
690	0.0370	-	-	-	-
728	-	619	248	0.599	3m(0.035)(0.044)
796	0.0385	-	-	-	-
798	-	540	240	0.528	3m(0.071)(0.039)
801	0.0385+	-	-	-	Turn ions off 0 k.v. at 30 psig
814	-	805	428	0.469	3m(0.059)(0.028)
823	0.0390	-	-	-	ions still off
826	-	837	425	0.492	3m(0.044)(0.06)
831	0.0390	-	-	-	Turn ions on at 2.5 k.v. a.c.

TABLE A3-1-6 (Cont'd)

Test Data for Filter No. 6

Cum. Time min.	Resist.[a] in oil	Particle Concentration p/cm³ Inlet	Particle Concentration p/cm³ Outlet	Efficiency	Remarks[b]
840	-	492	334	0.320	3m(0.042)(0.05)
843	0.0390+	-	-	-	Stop - start Add suspension
1500	0.0460	-	-	-	Blown manometer on bed resistance
1576	0.0480+	-	-	-	-
1582	-	848	316	0.627	3m(0.044)(0.052)
1594	0.0475	-	-	-	note decr. res. ions off at 30 psig.
1602	-	1130	397	0.649	3m(0.083)(0.052)
1610	0.0475+	-	-	-	Ions on, 2.5 k.v. a.c.
1629	0.0480	-	-	-	-
1632	-	916	415	0.546	3m(0.039)(0.055)
1636	0.0480	-	-	-	Stop test.

a. Resistance, inches of petroleum gage oil(sp.g. 0.826).

b. Numbers in ( ) are fraction of particle count composed of more than one particle, (Inlet)(Outlet); Operating velocity 13.76 cm/sec; Probe I; Generator model II operated at 60 psig; Ionizer on at 30 psig and 2.5 k.v. a.c., except as noted; no electrostatic precipitator.

TABLE A3-1-7

Test Data for Filter No. 7a

Cum. Time min.	Resist.[a] in oil	Particle Concentration p/cm^3		Efficiency	Remarks[b]
		Inlet	Outlet		
0	0.0085	-	-	-	On, collector ESP at 1530 v.d.c.
12	-	30.2	26.1	0.136	3m(0.087)(0.089)
25	0.0085	-	-	-	-
28	-	38.4	28.4	0.261	3m(0.067)(0.082)
64	0.0085	-	-	-	-
68	-	38.4	29.2	0.239	3m(0)(0.079)
85	0.0085	-	-	-	-
88	-	32.8	26.4	0.195	3m(0.04)(0.096)
109	0.0085	-	-	-	Reduce collector ESP to 170v.d.c. (-).
116	-	682	517	0.240	3m(0.057)(0.078)
165	0.0085+	-	-	-	-
172	-	670	535	0.201	3m(0.071)(0.073)
176	0.0085+	-	-	-	-
337	0.0095	-	-	-	-
390	0.010-	-	-	-	-
394	-	856	666	0.222	3m(0.08)(0.083)
420	0.010+	-	-	-	-
424	-	724	630	0.129	3m(0.071)(0.081)
432	0.010+	-	-	-	Stop - start
454	-	960	640	0.313	3m(0.053)(0.079)

TABLE A3-1-7 (Cont'd)

Test Data for Filter No. 7a

Cum. Time min.	Resist.[a] in oil	Particle Concentration p/cm³ Inlet	Particle Concentration p/cm³ Outlet	Efficiency	Remarks[b]
482	0.0105-	-	-	-	-
484	-	990	647	0.345	3m(0.083)(0.098)
498	0.0105	-	-	-	-
502	-	995	725	0.272	3m(0.089)(0.116)
513	0.0105	-	-	-	Stop - start New suspension
522	-	608	448	0.262	3m(0.062)(0.088)
531	0.0105	-	-	-	-
534	-	586	407	0.307	3m(0.043)(0.055)
542	0.0105+	-	-	-	-
1127	0.014	-	-	-	-
1140	-	979	651	0.335	3m(0.084)(0.104)
1153	0.0140	-	-	-	-
1156	-	936	596	0.363	4m(0.098)(0.122)
1218	0.0140+	-	-	-	-
1222	-	1105	752	0.320	3m(0.109)(0.127)
1299	0.0145	-	-	-	Stop - start New suspension
1311	0.0160-	-	-	-	-
1316	-	591	399	0.325	3m(0.05)(0.099)
1412	0.0160	-	-	-	-
1416	-	619	311	0.400	3m(0.052)(0.068)

TABLE A3-1-7 (Cont'd)

Test Data for Filter No. 7a

Cum. Time min.	Resist.[a] in oil	Particle Concentration p/cm³		Efficiency	Remarks[b]
		Inlet	Outlet		
1420	0.0160	-	-	-	Change collector ESP to 510 v. d.c.(-).
1431	0.0160	-	-	-	-
1436	-	176	100	0.431	3m(0.06)(0.09)
1441	0.0160	-	-	-	Change collector ESP to 1020v. d.c.(-).
1454	-	53	38	0.283	3m(0.077)(0.091)
1461	0.0160	-	-	-	Change collector ESP to 1530 v. d.c.(-).
1470	-	32.8	19.5	0.403	3m(0.08)(0.072)
1478	0.0160	-	-	-	Change collector ESP to 0 v. d.c.
1520	-	1172	658	0.440	3m(0.06)(0.09)
1527	0.0165-	-	-	-	Collector ESP on at 170v. d.c.(-).
1537	0.0165	-	-	-	Turn ions off, 0 k.v. at 30 psig.
1540	-	1015	621	0.388	3m(0.065)(0.066)
1545	0.0165	-	-	-	Change collector ESP to 0 v. d.c. ions still off, 0 k.v. at 30 psig.
1556	-	1350	1011	0.250	3m(0.059)(0.114)

TABLE A3-1-7 (Cont'd)

Test Data for Filter No. 7a

Cum. Time min.	Resist.[a] in oil	Particle Concentration p/cm³ Inlet	Particle Concentration p/cm³ Outlet	Efficiency	Remarks[b]
1560	0.0165	-	-	-	Collector ESP on at 170 v. d.c.(-), ions on at 2.5k.v. a.c. at 30 psig.
1591	0.0165	-	-	-	Ions off, 0 k.v. at 30 psig, collector ESP off, 0v. d.c., inner collector electrode grounded.
1738	0.0190	-	-	-	-
1766	-	1707	1057	0.380	3m(0.08)(0.108)
1773	0.0190	-	-	-	Stop test.

a. Resistance, inches of petroleum gage oil(sp.g. 0.826).

b. Numbers in ( ) are fraction of particle count composed of more than one particle (Inlet)(Outlet); operating velocity 13.76 cm/sec; Probe I; numbers beside m are sampling times, min; Generator model II at 60 psig; Ionizer on at 30 psig and 2.5 k.v. a.c., except as noted; collecting electrostatic precipitator (ESP) on at 170 v. d.c. center tube negative, except as noted.

TABLE A3-1-8

Test Data for Filter No. 7b

Cum. Time min.	Resist.[a] in oil	Particle Concentration p/cm³ Inlet	Particle Concentration p/cm³ Outlet	Efficiency	Remarks[b]
0	0.0195+	-	-	-	On, Ions off, at 30 psig.
16	-	1013	769	0.310	3m(0.081)(0.118)
21	0.0195+	-	-	-	Ions on 2.5 k.v. a.c., at 30 psig.
40	-	743	455	0.387	3m(0.09)(0.10)
69	0.020	-	-	-	-
76	-	836	526	0.370	3m(0.075)(0.09)
97	0.0205	-	-	-	-
102	-	680	486	0.285	3m(0.06)(0.084)
123	0.0205	-	-	-	-
255	0.0220	-	-	-	-
268	0.0230	-	-	-	Stop - start
317	0.0230	-	-	-	Stop - start
334	0.0230	-	-	-	-
350	-	1627	729	0.552	3m(0.088)(0.09)
368	0.0245	-	-	-	-
370	-	1335	688	0.484	3m(0.077)(0.105)
420	0.0255+	-	-	-	-
422	-	1079	644	0.404	3m(0.085)(0.093)
450	0.0270	-	-	-	-
452	-	1118	630	0.436	3m(0.098)(0.112)

TABLE A3-1-8 (Cont'd)

Test Data for Filter No. 7b

Cum. Time min.	Resist.[a] in oil	Particle Concentration p/cm^3		Efficiency	Remarks[b]
		Inlet	Outlet		
490	0.0285	-	-	-	-
492	-	1263	592	0.532	3m(0.093)(0.095)
500	0.0290	-	-	-	Stop - start New suspension
511	0.0295	-	-	-	-
844	0.0465	-	-	-	-
847	0.0465	-	-	-	Stop - start
860	0.0465	-	-	-	-
866	-	1332	482	0.638	3m(0.075)(0.093)
868	0.0420	-	-	-	note decr. res.
925	0.0445	-	-	-	-
930	-	1322	497	0.624	3m(0.110)(0.094)
942	0.0450	-	-	-	Stop

a. Resistance, inches petroleum gage oil(sp.g. 0.826).

b. Numbers in ( ) are fraction of particle count composed of more than one particle, (Inlet)(Outlet); operating velocity 13.78 cm/sec; Probe I; numbers beside m are sampling times, min; Generator model II at 60 psig; Ionizer at 30 psig and 2.5 k.v. a.c. except as noted; collecting electrostatic precipitator on at 170 v. d.c. center tube negative.

TABLE A3-1-9

Test Data for Filter No. 7c

Cum. Time min.	Resist.[a] in oil	Particle Concentration p/cm³ Inlet	Particle Concentration p/cm³ Outlet	Efficiency	Remarks[b]
0	0.0380	-	-	-	On
20	-	618	312	0.495	3m(0.062)(0.10)
31	0.0380	-	-	-	-
36	-	559	364	0.348	3m(0.048)(0.069)
64	0.0385	-	-	-	-
119	0.0395	-	-	-	-
122	-	-	327	-	3m(0.066)(0.062)
200	0.0410	-	-	-	-
269	0.0425	-	-	-	-
276	-	613	292	0.523	3m(0.037)(0.078)
310	0.0435+	-	-	-	-
318	-	695	309	0.555	3m(0.072)(0.046)
331	0.0440	-	-	-	-
491	0.0485+	-	-	-	-
506	0.0490	-	-	-	-
510	-	806	286	0.645	3m(0.082)(0.068)
522	0.0490+	-	-	-	-
526	-	845	311	0.632	3m(0.055)(0.098)
605	0.0525	-	-	-	-
610	-	927	346	0.644	3.1m(0.05)(0.072)

TABLE A3-1-9 (Cont'd)

Test Data for Filter No. 7c

Cum. Time min.	Resist.[a] in oil	Particle Concentration p/cm³ Inlet	Particle Concentration p/cm³ Outlet	Efficiency	Remarks[b]
624	0.0530	-	-	-	Add 50 cc H_2O to suspension
641	0.0540	-	-	-	-
646	-	768	246	0.679	3m(0.081)(0.064)
655	0.0540	-	-	-	Stop - start New suspension
663	0.0545	-	-	-	-
666	-	518	188	0.638	3m(0.082)(0.057)
676	0.0545	-	-	-	-
1270	0.0775	-	-	-	-
1276	-	898	258	0.712	3m(0.077)(0.054)
1278	0.0710+	-	-	-	Note decr. res.
1309	0.073	-	-	-	-
1316	-	1037	276	0.734	3m(0.10)(0.094)
1351	0.0745	-	-	-	-
1394	0.0780	-	-	-	-
1419	0.0805	-	-	-	-
1430	-	1215	309	0.746	3m(0.062)(0.091)
1434	0.0790	-	-	-	Note decr. res.
1440	-	-	-	-	Stop test.

TABLE A3-1-9 (Cont'd)

Test Data for Filter No. 7c

Cum. Time min.	Resist.[a] in oil	Particle Concentration p/cm³		Efficiency	Remarks[b]
		Inlet	Outlet		

a. Resistance, inches petroleum gage oil (sp.g. 0.826).

b. Numbers in ( ) are fraction of particle count composed of more than one particle, (Inlet)(Outlet); operating velocity 13.78 cm/sec; Probe I; numbers beside m are sampling times, min; Generator model II at 60 psig; Ionizer at 30 psig and 2.5 k.v. a.c. except as noted; collecting electrostatic precipitator on at 170 v. d.c. center tube negative.

TABLE A3-1-10

Test Data for Filter No. 8 and Single Fiber Nos. 1 Through 5

Cum. Time[a] min.	Resist.[b] in oil	Particle Concentration p/cm3 Inlet[c]	Particle Concentration p/cm3 Outlet[c]	Efficiency[c]	Remarks[d]
(0)	-	-	-	-	On single fiber 1
(20)	-	-	-	-	Stop s.f. 1
0	0.0070[e]	-	-	-	On filter mat 8
21	-	55.5*	51*	0.08*	-
51	-	56.5*	51*	0.10*	Stop - start New suspension
78	-	263	240	0.088	3m(0.028)(0.045)
92	-	74.5*	67.5*	0.09*	-
110	-	-	-	-	Off f.m. 8
(20)	-	-	-	-	Single fiber 1 continued
(40)	-	-	-	-	Stop s.f. 1 loose upon removal
110	-	-	-	-	Filter mat 8 continued
178	-	282	260	0.075	3m(0.054)(0.051)
198	-	82.5*	72.5*	0.12*	Off f.m. 8
(0)	-	-	-	-	On single fiber 2
(20)	-	-	-	-	Stop s.f. 2. Loose upon removal
(0)	-	-	-	-	On single fiber 3
(30)	-	-	-	-	Stop s.f. 3 Fiber loose

TABLE A3-1-10 (Cont'd)

Test Data for Filter No. 8 and Single Fiber Nos. 1 through 5

Cum. Time[a] min.	Resist.[b] in oil	Particle Concentration p/cm³ Inlet[c]	Particle Concentration p/cm³ Outlet[c]	Efficiency[c]	Remarks[d]
198	-	100*	88*	0.12*	Filter mat 8 cont'd
233	-	100*	90*	0.10*	Off f.m. 8
(0)	-	-	-	-	On single fiber 4
(30)	-	-	-	-	Off s.f. 4
233	-	-	-	-	Filter mat 8 cont'd
256	-	26*	23*	0.12*	-
258	-	372	318	0.145	3m(0.044)(0.044)
263	-	26.5*	23*	0.13*	-
270	-	-	-	-	Off f.m. 8
(30)	-	-	-	-	Single fiber 4 continued
(60)	-	-	-	-	Off s.f. 4
270	-	-	-	-	Filter mat 8 cont'd
300	-	26*	22.5*	0.14*	-
321	-	28*	22.5*	0.19*	Off f.m. 8 New suspension
321	-	32*	27*	0.16*	Filter mat 8 cont'd
354	-	1255	1051	0.161	3m(0.063)(-)
358	-	-	-	-	Off f.m. 8
(60)	-	-	-	-	Single fiber 4 continued
(80)	-	-	-	-	Off s.f. 4

TABLE A3-1-10 (Cont'd)

Test Data for Filter No. 8 and Single Fiber Nos. 1 through 5

Cum. Time[a] min.	Resist.[b] in oil	Particle Concentration p/cm^3 Inlet[c]	Particle Concentration p/cm^3 Outlet[c]	Efficiency[c]	Remarks[d]
358	-	-	-	-	Filter mat 8 cont'd
387	-	29.5*	25.5*	0.14*	-
392	-	1080	954	0.125	3m(0.044)(0.078)
397	-	-	-	-	Off f.m. 8
(80)	-	-	-	-	Single fiber 4 continued
(100)	-	-	-	-	Off s.f. 4
397	-	31*	27*	0.13*	Filter mat 8 cont'd
447	-	30*	26*	0.13*	-
493	-	31*	27*	0.13*	-
496	-	1168	995	0.147	3m(0.065)(0.10)
500	-	-	-	-	Off f.m. 8
(100)	-	-	-	-	Single fiber 4 continued
(120)	-	-	-	-	Off s.f. 4
500	-	30*	27*	0.10*	Filter mat 8 cont'd
534	-	33*	28*	0.15*	-
540	-	1225	1010	0.176	3m(0.039)(0.096)
544	-	-	-	-	Off f.m. 8
(120)	-	-	-	-	Single fiber 4 continued
(140)	-	-	-	-	Off s.f. 4

TABLE A3-1-10 (Cont'd)

Test Data for Filter No. 8 and
Single Fiber Nos. 1 through 5

Cum. Time[a] min.	Resist.[b] in oil	Particle Concentration p/cm³ Inlet[c]	Particle Concentration p/cm³ Outlet[c]	Efficiency[c]	Remarks[d]
544	-	-	-	-	Filter mat 8 cont'd
608	-	30*	25*	0.17*	-
628	-	1268	975	0.230	3m(0.056)(0.075)
637	-	-	-	-	Off f.m. 8
(140)	-	-	-	-	Single fiber 4 continued
(180)	-	-	-	-	Off s.f. 4
637	-	-	-	-	Filter mat 8 cont'd
671	-	27.5*	22.3*	0.19*	Stop - change tubing to aerosol photometer.
671	-	-	-	-	Filter mat 8 cont'd
695	-	72*	59*	0.18*	-
704	-	1349	927	0.312	3m(0.056)(0.11)
711	-	-	-	-	Off f.m. 8
(180)	-	-	-	-	Single fiber 4 continued
(200)	-	-	-	-	Off s.f. 4
711	-	-	-	-	Filter mat 8 cont'd
716	-	70.5*	57.5*	0.19*	-
726	-	1358	975	0.283	3m(0.042)(0.086)
730	-	-	-	-	Off f.m. 8

TABLE A3-1-10 (Cont'd)

Test Data for Filter No. 8 and
Single Fiber Nos. 1 through 5

Cum. Time[a] min.	Resist.[b] in oil	Particle Concentration p/cm^3 Inlet[c]	Particle Concentration p/cm^3 Outlet[c]	Efficiency[c]	Remarks[d]
(200)	-	-	-	-	Single fiber 4 continued
(241)	-	-	-	-	Off s.f. 4
730	-	-	-	-	Filter mat 8 cont'd
737	-	67.5*	56.5*	0.16*	-
746	-	1353	910	0.328	3m(0.04)(0.76)
750	-	-	-	-	Off f.m. 8
(241)	-	-	-	-	Single fiber 4 continued
(300)	-	-	-	-	Off s.f. 4
750	-	-	-	-	Filter mat 8 cont'd
772	-	67.5*	58*	0.14*	-
776	-	1425	1058	0.258	3m(0.044)(0.094)
782	-	-	-	-	Off f.m. 8
(300)	-	-	-	-	Single fiber 4 continued
(420)	-	-	-	-	Stop s.f. 4
782	0.0095	-	-	-	Filter mat 8 cont'd New suspension
791	-	30.8*	23.6*	0.235*	-
830	-	43*	34.6*	0.19*	Stop - start
870	-	36*	29*	0.19*	-

TABLE A3-1-10 (Cont'd)

Test Data for Filter No. 8 and Single Fiber Nos. 1 through 5

Cum. Time[a] min.	Resist.[b] in oil	Particle Concentration p/cm^3 Inlet[c]	Particle Concentration p/cm^3 Outlet[c]	Efficiency[c]	Remarks[d]
876	-	965	595	0.384	3m(0.064)(0.101)
886	-	-	-	-	Off f.m. 8
(0)	-	-	-	-	On single fiber 5
(60)	-	-	-	-	Off s.f. 5
886	-	-	-	-	Filter mat 8 cont'd
909	-	34*	26.5*	0.22*	-
916	-	886	637	0.281	3m(0.056)(0.078)
919	-	-	-	-	Off f.m. 8
(60)	-	-	-	-	Single fiber 5 continued
(135)	-	-	-	-	Off s.f. 5
919	-	-	-	-	Filter mat 8 cont'd
945	0.0120	28.2*	22.5*	0.20*	-
964	-	825	600	0.273	3m(0.045)(0.076)
966	-	-	-	-	Off f.m. 8
(135)	-	-	-	-	Single fiber 5 continued
(221)	-	-	-	-	-
966	-	-	-	-	Filter mat 8 cont'd
986	-	27.5*	22.5*	0.18*	-
994	-	750	645	0.140	3m(0.072)(0.077)
997	-	-	-	-	Off f.m. 8

TABLE A3-1-10 (Cont'd)

Test Data for Filter No. 8 and Single Fiber Nos. 1 through 5

Cum. Time[a] min.	Resist.[b] in oil	Particle Concentration p/cm^3 Inlet[c]	Particle Concentration p/cm^3 Outlet[c]	Efficiency[c]	Remarks[d]
(221)	-	-	-	-	Single fiber 5 continued
(300)	-	-	-	-	Off s.f. 5
997	0.0120	-	-	-	Filter mat 8 cont'd
1027	-	30*	25*	0.17*	-
1036	-	976	682	0.300	3m(0.056)(0.112)
1038	-	-	-	-	Off f.m. 8
(300)	-	-	-	-	Single fiber 5 continued
(420)	-	-	-	-	Off s.f.5
1038	-	-	-	-	Filter mat 8 cont'd
1073	0.0130*	29.5*	24*	0.19*	-
1082	-	952	664	0.302	3m(0.049)(0.119)
1084	-	-	-	-	Stop f.m. 8
(420)	-	-	-	-	Single fiber 5 continued
(540)	-	-	-	-	Stop s.f. 5

TABLE A3-1-10 (Cont'd)

Test Data for Filter No. 8 and
Single Fiber Nos. 1 through 5

Cum. Time[a] min.	Resist.[b] in oil	Particle Concentration p/cm³ Inlet[c]	Particle Concentration p/cm³ Outlet[c]	Efficiency[c]	Remarks[d]

a. Cumulative times shown in ( ) are for single fiber tests, cumulative times shown without ( ) are for filter mat 8 test.

b. Resistance, inches of petroleum gage oil (sp.g. 0.826).

c. Numbers marked with asterisks are light scattering photometer readings and the filter efficiency calculated from these readings: efficiency = 1- (Out/In).

d. Numbers in ( ) are fraction of particle count composed of more than one particle, (Inlet)(Outlet); operating velocity 13.78 cm/sec; Probe III; numbers beside m are sampling times, min; Generator model II at 60 psig; Ionizer on at 30 psig and 2.5 k.v. a.c.; collecting electrostatic precipitator on at 170 v. d.c. center tube negative.

e. Initial resistance estimated from filter weight and initial resistance of filter no. 7a.

TABLE A3-1-11

Test Data for Filter No. 9 and Single Fiber No. 6

Cum. Time[a] min.	Resist.[b] in oil	Particle Concentration p/cm³ Inlet[c]	Particle Concentration p/cm³ Outlet[c]	Efficiency[c]	Remarks[d]
0	0.0280	-	-	-	On filter mat 9
30	-	20	15*	0.25*	-
66	0.0285	-	-	-	Stop - start
104	0.0295	-	-	-	-
109	-	37*	29*	0.216*	-
114	-	39*	29*	0.255*	-
116	0.0305	-	-	-	-
133	-	39.5*	29*	0.265*	-
144	0.0310	-	-	-	-
150	-	951	654	0.312	3m(0.103)(0.110)
156	0.031	-	-	-	Off f.m. 9
(0)	-	-	-	-	On single fiber 6
(120)	-	-	-	-	Off s.f. 6
156	0.0300	-	-	-	Filter mat 9 continued
228	0.0310	37*	26*	0.30*	-
240	-	1003	661	0.342	3m(0.092)(0.124)
243	0.0320	-	-	-	Off f.m. 9
120	-	-	-	-	Single fiber 6 continued
220	-	-	-	-	Stop s.f. 6

TABLE A3-1-11 (Cont'd)

Test Data for Filter No. 9 and Single Fiber No. 6

Cum. Time[a] min.	Resist[b] in oil	Particle Concentration p/cm³ Inlet[c]	Particle Concentration p/cm³ Outlet[c]	Efficiency[c]	Remarks[d]
243	0.0315	-	-	-	Filter mat 9 cont'd Note decr. res.
313	0.0345	-	-	-	-
318	-	40*	26*	0.35*	-
331	0.0360	-	-	-	-
337	0.0380	40*	25*	0.375*	-
965	0.1360	35*	11.5*	0.671*	-
978	0.1260	44*	10*	0.772*	Note decr. res.
991	0.1295	-	-	-	-
994	-	1294	552	0.574	3m(0.108)(0.115)
998	0.1245	-	-	-	Note decr. res.
1030	0.1345	-	-	-	-
1078	0.1525	-	-	-	-
1137	0.1875	-	-	-	-
1138	-	40*	7*	0.815*	-
1155	0.1725	-	-	-	Note decr. res.
1170	0.1850	47*	5*	0.0893*	Stop f.m. 9
-	0.1570	-	-	-	Note final res. much lower.

TABLE A3-1-11 (Cont'd)

Test Data for Filter No. 9 and Single Fiber No. 6

Cum. Time[a] min.	Resist.[b] in oil	Particle Concentration p/cm^3 Inlet[c]	Particle Concentration p/cm^3 Outlet[c]	Efficiency[c]	Remarks[d]

a. Cumulative times shown in ( ) are for single fiber 6 test; cumulative times shown without ( ) are for filter mat 9 test.

b. Resistance, inches of petroleum gage oil (sp. g. 0.826).

c. Numbers marked with asterisks are light scattering photometer readings, and the filter efficiency calculated from these readings: efficiency = 1- (Out/In).

d. Numbers in ( ) are fractions of particle count composed of more than one particle (Inlet)(Outlet); operating velocity 29 cm/sec; Probe III; numbers beside m are sampling times, min; Generator model II at 60 psig; Ionizer on at 30 psig and 2.5 k.v. a.c.; collecting electrostatic precipitator on at 170 v d.c. center tube negative.

TABLE A3-1-12

Test Data for Filter No. 10 and Single Fiber No. 7

Cum. Time[a] min.	Resist.[b] in oil	Particle Concentration p/cm³ Inlet[c]	Particle Concentration p/cm³ Outlet[c]	Efficiency[c]	Remarks[d]
0	0.0460	-	-	-	On filter mat 10
22	-	23.5*	17.0*	0.25*	-
30	-	817	611	0.252	3m(0.117)(0.151)
34	0.0475	-	-	-	-
36	-	-	-	-	Off f.m. 10
(0)	-	-	-	-	On single fiber 7
(60)	-	-	-	-	Off s.f. 7
36	0.0495	-	-	-	Filter mat 10 continued
69	0.0520	-	-	-	-
86	0.0535	-	-	-	Stop - start
91	0.0545	-	-	-	-
93	-	14.5*	9*	0.38*	-
103	0.0565	-	-	-	-
127	-	19.5*	10.5*	0.46*	-
136	-	1052	661	0.372	3m(0.105)(0.156)
141	0.0620	-	-	-	-
(60)	-	-	-	-	Single fiber 7 continued
(121)	-	-	-	-	Stop s.f. 7
141	0.0585	-	-	-	Filter mat 10 continued

TABLE A3-1-12 (Cont'd)

Test Data for Filter No. 10 and Single Fiber No. 7

Cum. Time[a] min.	Resist.[b] in oil	Particle Concentration p/cm³ Inlet[c]	Particle Concentration p/cm³ Outlet[c]	Efficiency[c]	Remarks[d]
144	0.060	-	-	-	-
189	0.0655	-	-	-	-
234	0.0730	-	-	-	-
305	0.0840	-	-	-	-
340	0.0925	-	-	-	-
342	-	-	-	-	90 cm/sec - on
391	-	27*	12*	0.55*	90 cm/sec - off
399	0.122	-	-	-	-
425	0.1295	-	-	-	-
426	-	23.5*	6.5*	0.725*	-
429	-	23*	6*	0.75*	-
477	0.1545	-	-	-	Stop f.m. 10.

a. Cumulative times shown in ( ) are for single fiber 7 tests, cumulative times shown without ( ) are for filter mat 10 test.

b. Resistance, inches of petroleum gage oil (sp.g. 0.826).

c. Numbers marked with asterisks are light scattering photometer readings and the filter efficiency calculated from these readings: efficiency = 1- (Out/In).

d. Numbers in ( ) are fractions of particle count composed of more than one particle,(Inlet)(Outlet); operating velocity 58 cm/sec; Probe II; numbers beside m are sampling times, min; Generator model II at 60 psig; Ionizer on at 30 psig and 2.5 k.v. a.c.; collecting electrostatic precipitator on at 170 v. d.c. center tube negative.

APPENDIX 3-2

PARTICLE ACCUMULATION AND FILTER PERFORMANCE

TABLE A3-2-1

Particle Accumulation and Filter Performance for Test Filter No. 1

Test Time, t min.	Δ t min.	$\overline{\Delta N}$ p/cm^3	Cum. A[a] 10^6p/cm^2	Pen. P(t)	Resist.[b] $\delta\Delta p(t)$
0-250	250	6.7	14.0	0.081	0.010
250-500	250	12.7	40.6	0.061	0.030
500-818	318	21.6	98.1	0.039	0.080
818-1000	182	27.1	139.3	0.031	0.120
1000-1250	250	25.1	191.6	0.024	0.145
1250-1500	250	18.7	230.7	0.024	0.190
1500-1780	280	10.6	255.5	0.020	0.227
1780-2150	370	23.6	328.3	0.017	0.309
2150-2400	250	20.2	370.5	0.015	0.346
2400-2678	278	15.4	406.1	0.014	0.382

a. Cumulative accumulation, $A = 60U_o \Delta t \overline{\Delta N}$, particles/cm^2 of filter face area, U_o= 139cm/sec.

b. Resistance increase resulting from particle accumulation, inches of petroleum gage oil(sp.g. 0.826).

TABLE A3-2-2

Particle Accumulation and Filter Performance for Test Filter No. 2

Test Time, t min.	Δt min.	$\overline{\Delta N}$ p/cm^3	Cum. A[a] 10^6p/cm^2	Pen. P(t)	Resist.[b] $\delta \Delta p(t)$ in. oil
0-200	200	27.1	4.48	0.552	0.001
200-400	200	37.4	10.67	0.541	0.0025
400-600	200	41.4	17.48	0.530	0.002
600-800	200	33.6	23.04	0.520	0.003
800-1000	200	24.6	27.11	0.509	0.004
1000-1346	346	12.1	30.57	0.490	0.0045
1346-1546	200	36.5	36.62	0.480	0.0045
1546-1726	180	34.8	41.80	0.470	0.0045
1726-1876	180	39.7	46.73	0.461	0.004

a. $A = 60U_o \Delta t \overline{\Delta N}$, $U_o = 13.78$ cm/sec.

b. Resistance increase resulting from particle accumulation, inches of petroleum gage oil(sp. g. 0.826)

TABLE A3-2-3

Particle Accumulation and Filter Performance for Test Filter No. 3

Test Time, t min.	Δ t min.	$\overline{\Delta N}$ p/cm^3	Cum. A[a] 10^6p/cm^2	Pen. P(t)	Resist.[b] $\delta\Delta p(t)$ in. oil
0-100	100	193	15.94	0.740	0.0010
100-200	100	202	32.62	0.706	0.0035
200-280	80	275	50.82	0.67	0.0050
280-400	120	308	81.32	0.66	0.0080
400-460	60	268	94.62	0.64	0.0105
460-572	112	287	121.22	0.62	0.0115

a. $A = 60U_o \Delta t \overline{\Delta N}$, U_o= 13.78 cm/sec.

b. Resistance increase resulting from particle accumulation, inches of petroleum gage oil(sp.g. 0.826).

TABLE A3-2-4

Particle Accumulation and Filter Performance for Test Filter No. 4

Test Time, t min.	Δt min.	$\overline{\Delta N}$ p/cm^3	Cum. A[a] $10^6 p/cm^2$	Pen. P(t)	Resist.[b] $\delta \Delta p(t)$ in. oil
0-180	180	23	3.36	0.554	0.00025
180-302	122	140	17.43	0.551	0.0005
302-452	150	333	58.73	0.548	0.00275
452-602	150	375	105.23	0.545	0.0050
602-779	177	420	166.73	0.541	0.0075

a. $A = 60U_o \Delta t \overline{\Delta N}$, $U_o = 13.76$ cm/sec.

b. Resistance increase resulting from particle accumulation, inches of petroleum gage oil(sp.g. 0.826).

TABLE A3-2-5

Particle Accumulation and Filter Performance for Test Filter No. 5

Test Time, t min.	Δt min.	$\overline{\Delta N}$ p/cm^3	Cum. A[a] 10^6p/cm^2	Pen. P(t)	Resist.[b] $\delta \Delta p(t)$ in. oil
0-110	110	39	3.56	0.670	0.000+
110-200	90	169	16.14	0.660	0.0010
200-243	43	342	28.00	0.648	0.0015
243-325	83	345	51.65	0.650	0.0020+
325-400	75	325(est)	71.85	0.640	0.0035
400-500	100	325	98.65	0.628	0.004
500-566	66	317	115.95	0.620	0.005+
566-866	300	267	182.15	0.588	0.0080
866-1100	234	741(est)	325.35	0.507	0.0175
1100-1250	150	769	420.65	0.470	0.024+
1250-1450	200	775(est)	548.75	0.426	0.033+
1450-1634	184	550	632.45	0.400	0.037+
1634-2406	772	492	946.45	0.328	0.061
2406-2728	322	566	1097.15	0.297	0.068

a. $A = 60U_o \Delta t \overline{\Delta N}$, U_o= 13.78 cm/sec.

b. Resistance increase resulting from particle accumulation, inches of petroleum gage oil(sp.g. 0.826).

TABLE A3-2-6

Particle Accumulation and Filter Performance for Test Filter No. 6

Test Time, t min.	Δt min.	$\overline{\Delta N}$ p/cm^3	Cum. A[a] $10^6 p/cm^2$	Pen. P(t)	Resist.[b] $\delta \Delta p(t)$ in. oil
0-186	186	118	18.15	0.61	0.000+
186-451	265	104	40.95	0.56	0.0015
451-804	353	266	118.55	0.49	0.0055+
804-831	27	505	127.36	0.48	0.0060
831-1636	805	397	391.36	0.041	0.015

a. $A = 60U_o \Delta t \quad \overline{\Delta N}$, $U_o = 13.78$ cm/sec.

b. Resistance increase resulting from particle accumulation, inches of petroleum gage oil(sp.g. 0.826).

TABLE A3-2-7

Particle Accumulation and Filter Performance for Test Filter No. 7a

Test Time, t min.	Δt min.	$\overline{\Delta N}$ p/cm^3	Cum. A[a] 10^6p/cm^2	Pen. P(t)	Resist.[b] $\delta \Delta p(t)$ in. oil
0-109	109	8	0.69	0.792	0
109-300	191	150	24.39	0.779	0.0010
300-513	213	242	66.89	0.744	0.0020
513-900	387	170	121.29	0.716	0.0040+
900-1299	399	340	233.39	0.661	0.0060
1299-1421	122	220	255.59	0.638	0.0075
1421-1441	20	76	256.84	-	-
1441-1461	20	15	257.09	-	-
1461-1478	17	13	257.29	-	-
1478-1527	49	514	278.09	-	-
1527-1545	18	394	283.95	-	-
1545-1560	15	339	288.15	0.634	0.0080
1560-1773	213	650	402.25	0.620	0.0105

a. $A = 60U_o \Delta t \overline{\Delta N}$, $U_o = 13.78$ cm/sec.

b. Resistance increase resulting from particle accumulation, inches of petroleum gage oil(sp.g. 0.826).

TABLE A3-2-8

Particle Accumulation and Filter Performance for Test Filter No. 7b

Test Time, t min.	Δt min.	$\overline{\Delta N}$ p/cm^3	Cum. A[a] $10^6 p/cm^2$	Pen. P(t)	Resist.[b] $\delta \Delta p(t)$ in. oil
0-21	21	244	4.24	0.680	0
21-123	101	264	26.24	0.630	0.0010-
123-317	194	446	97.74	0.560	0.0035-
317-500	167	628	184.44	0.490	0.0095-
500-942	442	662	424.44	0.369	0.0255-

a. $A = 60U_o \Delta t \overline{\Delta N}$, $U_o = 13.78$ cm/sec.

b. Resistance increase resulting from particle accumulation, inches of petroleum gage oil(sp.g. 0.826).

TABLE A3-2-9

Particle Accumulation and Filter Performance for Test Filter No. 7c

Test Time, t min.	Δ t min.	$\overline{\Delta N}$ p/cm^3	Cum. A[a] 10^6p/cm^2	Pen. P(t)	Resist.[b] $\delta \Delta p(t)$ in. oil
0-200	200	251	41.50	0.478	0.0030
200-400	200	354	100.00	0.418	0.0080
400-624	224	545	200.80	0.348	0.0150
624-655	31	522	214.20	0.340	0.0160+
655-1000	345	330	308.20	0.310	0.0250
1000-1440	440	749	597.20	0.275	0.0410

a. $A = 60U_o \Delta t \overline{\Delta N}$, $U_o = 13.78$ cm/sec.

b. Resistance increase resulting from particle accumulation, inches of petroleum gage oil(sp.g. 0.826).

TABLE A3-2-10

Particle Accumulation and Filter Performance for Test Filter No. 8

Test Time, t min.	Δt min.	$\overline{\Delta N}$ p/cm^3	Cum. A[a] $10^6 p/cm^2$	Pen. P(t)	Resist.[b] $\delta \Delta p(t)$ in. oil
0-51	51	4	0.20	0.91	-
51-198	147	22	2.90	0.92	-
198-321	123	40	7.01	0.85	-
321-358	37	202	13.20	0.84	-
358-397	39	137	17.61	0.87	-
397-500	103	156	30.87	0.85	-
500-544	44	194	37.92	0.82	-
544-637	93	253	57.36	0.77	-
637-711	74	355	79.01	0.69	-
711-730	19	400	85.29	0.71	-
730-750	20	420	92.25	0.67	-
750-782	32	478	104.75	0.66	0.0025 (est)
782-1100	318	275	177.05	0.70	0.0060 (est)

a. $A = 60 U_o \Delta t \overline{\Delta N}$, $U_o = 13.78$ cm/sec.

b. Resistance increase resulting from particle accumulation, inches of petroleum gage oil(sp.g. 0.826).

TABLE A3-2-11

Particle Accumulation and Filter Performance for Test Filter No.9

Test Time, t min.	Δt min.	$\overline{\Delta N}$ p/cm^3	Cum. A[a] 10^6p/cm^2	Pen. P(t)	Resist.[b,c] $\delta \Delta p(t)$ in. oil
0-66	66	253	29.0	0.71	0.0005
66-156	90	279	72.6	0.69	0.002
156-243	87	327	122.3	0.66	0.004
243-300	57	368	158.9	0.64	0.006
300-400	100	404	229.1	0.61	0.011
400-500	100	451	307.5	0.58	0.0175
500-600	100	500	394.5	0.55	0.0265
600-700	100	550	490.0	0.52	0.038
700-800	100	602	594.8	0.49	0.0535
800-900	100	656	708.8	0.46	0.072
900-996	96	712	827.8	0.35 (est)	0.096
996-1170	174	795	1068.8	0.20 (est)	0.1290

a. $A = 60U_o \Delta t \overline{\Delta N}$, U_o= 29 cm/sec.

b. Resistance increase resulting from particle accumulation, inches of petroleum gage oil(sp.g. 0.826).

c. Resistance increment estimated between 400 and 1000 minutes.

TABLE A3-2-12

Particle Accumulation and Filter Performance for Test Filter No. 10

Test Time, t min.	Δt min.	$\overline{\Delta N}$ p/cm^3	Cum. A[a] 10^6p/cm^2	Pen. P(t)	Resist.[b] $\delta \Delta p(t)$ in. oil
0-36	36	251	31.5	0.71	0.0013
36-86	50	273	79.0	0.68	0.0075
86-141	55	332	142.5	0.65	0.0130
141-200	59	376	219.7	0.61	0.0200
200-300	100	431	369.7	0.56	0.0375
300-342	42	485	440.5	0.53	0.0480
342-391	49	565	608.5 (est)	0.45 (est)	0.0770
391-477	86	660	803.5 (est)	0.41 (est)	0.1085

a. $A = 60U_o \Delta t \overline{\Delta N}$, $U_o = 58$ cm/sec.

b. Resistance increase resulting from particle accumulation, inches of petroleum gage oil(sp.g. 0.826).

APPENDIX 3-3

GLASS FIBER SIZE DATA

TABLE A3-3-1

Filter Fiber Size Data

Class Interval[a]	Number Observed	Cum. Frequency o/o ≤ Indicated Size
32.25-33.25	1	1
33.25-34.25	0	1
34.25-35.25	0	1
35.25-36.25	1	2
36.25-37.25	0	2
37.25-38.25	1	3
38.25-39.25	5	8
39.25-40.25	5	13
40.25-41.25	10	23
41.25-42.25	10	33
42.25-43.25	15	48
43.25-44.25	13	61
44.25-45.25	15	76
45.25-46.25	5	81
46.25-47.25	5	86
47.25-48.25	6	92
48.25-49.25	5	97
49.25-50.25	2	99
50.25-51.25	1	100

a. Divisions on filar micrometer eyepiece drum, 4.55 divisions/micron.

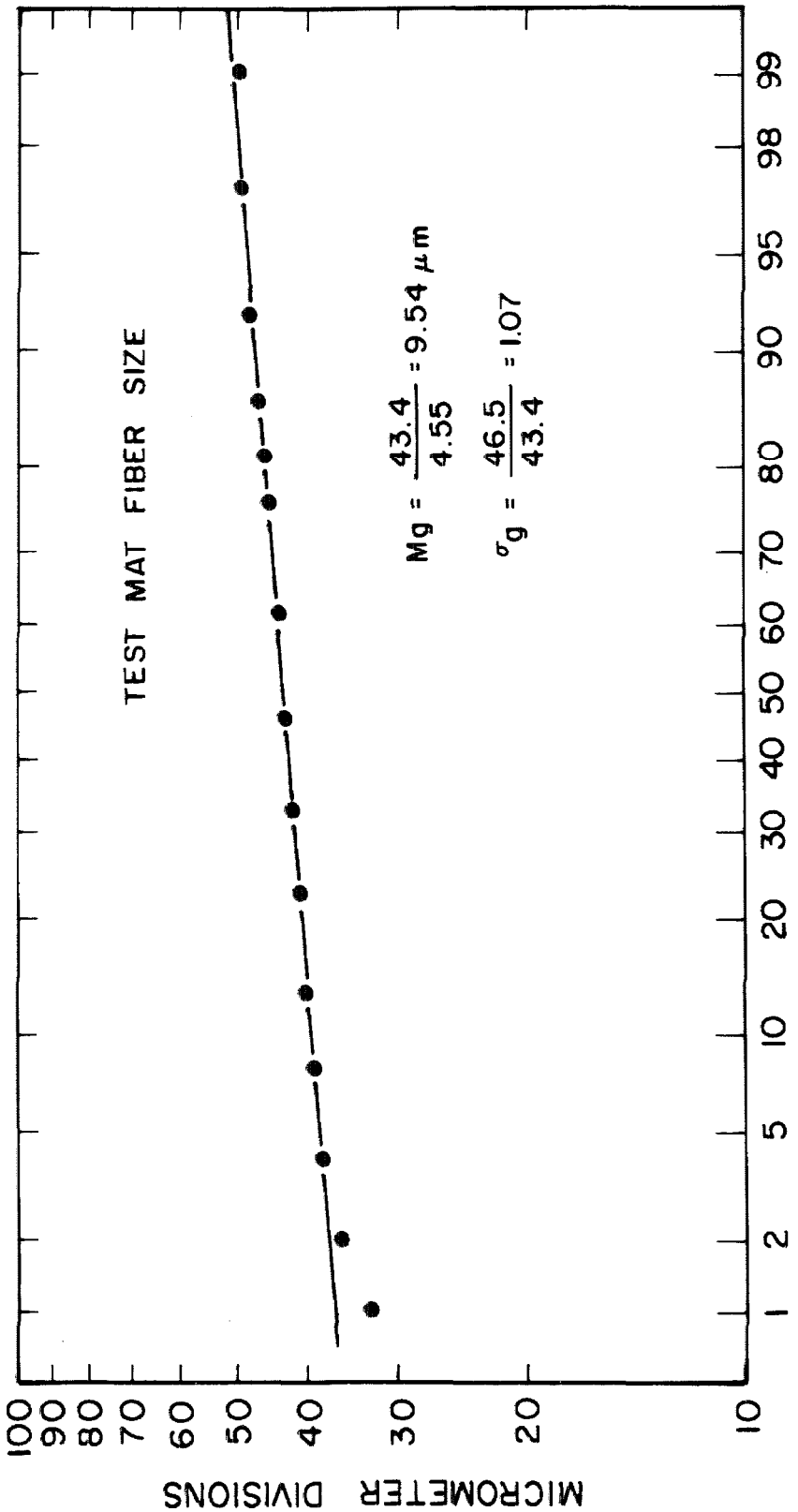

Figure A3-31. Test Filter Fiber Diameter Distribution

APPENDIX 3-4

APPROXIMATE FIBER EFFICIENCY FOR A THIN FILTER

APPENDIX 3-4

APPROXIMATE FIBER EFFICIENCY FOR A THIN FILTER

Consider a cylindrical fiber of length ℓ and diameter d_f over which a fluid flows at velocity U_o containing monodisperse particles at concentration $N_o(p/cm^3)$. The transport of particles to the fiber can be written as:

$$T_f = \eta^*(0) d_f \ell U_o N_o \text{ particles/sec,} \qquad (A3\text{-}4\text{-}1)$$

where $\eta^*(0)$ is the fiber collection efficiency.

Consider a thin filter of area A_F composed of fibers of diameter d_f filtering a volume of aerosol $Q(cm^3/sec)$. The transport of particles to the filter is:

$$T_F = QN_oE \text{ (particles/sec),} \qquad (A3\text{-}4\text{-}2)$$

where E is the filter efficiency and $Q = U_o A_F$.

If the filter is thin:

$$T_f = T_F \qquad (A3\text{-}4\text{-}3)$$

and:

$$\eta^*(0) = E \frac{A_F}{\ell d_f} = E \frac{\text{Area of test mat}}{\text{Area of fiber}} \qquad (A3\text{-}4\text{-}4)$$

But:

$$\ell(\pi d_f^2/4)\, \rho_m = \text{weight of fiber} \qquad (A3\text{-}4\text{-}5)$$

and

$$\ell d_f = \text{wt. of fiber}/(\pi/4)(9.54 \times 10^{-4})2.54 = 526\text{wt.} \qquad (A3\text{-}4\text{-}6)$$

The fiber efficiency determined for the thin bed approximation becomes at the start of filtration:

$$\eta^*(0) = (1\text{-}P(0))0.0302/\text{filter weight.} \qquad (A3\text{-}4\text{-}7)$$

APPENDIX 4-1

SUMMARY OF SINGLE FIBER TEST DATA

TABLE A4-1-1

Summary of Single Fiber Test Data

Fiber No.	Cum. Time min.	No. Particles Counted	No. Fields Counted	Deposit. p/100μm	Count Range[a]
4	30	15	2.46	7.5	-
	60	30	2.46	14	-
	80	46	2.46	23	-
	100	61	2.46	28.8	-
	120	60	2	36.9	26-34
	140	68	2	41.9	30-38
	180	215	3	88.6	71-73
	200	246	3	101	78-89
	241	309	3	127	98-111
	300	379	3	156	117-136
	420	362	2	223	179-183
5	60	85	3	34.8	26-30
	135	196	3	80.4	57-72
	221	315	3	128	91-113
	300	417	3	171	130-147
	420	899	4	279	198-241
	540	810	3	338	265-295
6	120	336	3	138	104-121
	220	629	3	258	197-225
7	60	279	3	113	88-98
	121	571	3	234	168-204
8	61	225	9	30.8	21-32
	189	514	5	127	80-113
	420	1280	5	315	199-301
9	30	322	36	11.0	5-16
	180	417	11	46.6	27-48
	480	886	7	156	108-147
10	61	429	15	34.9	17-34
	184	1119	10	137	79-145
	336	1229	5	304	192-304

a. Range per field defined by microscope ocular graticule, 81-1/4 microns long.

APPENDIX 4-2

SINGLE FIBER TEST DATA

(Note: Records for single fibers 1 through 7 are contained in Appendix 3-1, Tables A3-1-10 through A3-1-12.)

TABLE A4-2-1

Test Data for Single Fiber No. 8

Cumulative Time[a] min.	Particle Concentration p/cm^3	Remarks[b]
0		On, open tunnel
24	888 up	3m (0.071)
-	846 dn	3m (0.11)
-	866 av	
60	994	3m (0.085)
66	-	Stop tunnel
(0)	-	On Single Fiber 8
(61)	-	Off s.f. 8
66	-	On, open tunnel
82	1084	3m (0.070)
84	-	Stop tunnel
(61)	-	Single Fiber 8 cont'd
(189)	-	Off s.f. 8
84	-	On, open tunnel
120	1063	3m (0.063)
121	-	Stop tunnel
(189)	-	Single Fiber 8 cont'd
(469)	-	Stop s.f. 8

a. Cumulative times shown in ( ) are for single fiber 8 tests, cumulative times shown without ( ) are for operation of aerosol tunnel with open test section.

b. Numbers in ( ) are fractions of particle count composed of more than one particle (Inlet); operating velocity 13.78 cm/sec; probe III; numbers beside m are sampling times, min; Generator model II at 60 psig; Ionizer on at 30 psig and 2.5 k.v. a.c.; collecting electrostatic precipitator on at 170 v. d.c. outer tube grounded .

TABLE A4-2-2

Test Data for Single Fiber No. 9

Cumulative Time[a] min.	Particle Concentration p/cm^3	Remarks[b]
0	-	On, open tunnel
20	809	3m (0.075)
24	-	Stop tunnel
(0)	-	On Single Fiber 9
(30)	-	Off s.f. 9
24	-	On, open tunnel
86	640	3m (0.043)
89	-	Stop tunnel
(30)	-	Single Fiber 9 cont'd
(180)	-	Off s.f. 9
89	-	On, open tunnel
102	727	3m (0.083)
107	-	Stop tunnel
(180)	-	Single Fiber 9 cont'd
(480)	-	Stop s.f. 9

a. Cumulative times shown in ( ) are for single fiber 9 tests, cumulative times shown without ( ) are for operation of aerosol tunnel with open test section.

b. Numbers in ( ) are fractions of particle count composed of more than one particle (Inlet); operating velocity 13.78 cm/sec; probe III; numbers beside m are sampling times, min; Generator model II at 60 psig; Ionizer on at 30 psig and 2.5 k.v. a.c.; collecting electrostatic precipitator on at 170 v. d.c. outer tube grounded.

TABLE A4-2-3

Test Data for Single Fiber No. 10

Cumulative Time[a] min.	Particle Concentration p/cm^3	Remarks[b]
-	-	Same susp. from s.f. 9
107	-	On, open tunnel
176	887	3m (0.076)
180	-	Stop tunnel
(0)	-	On Single Fiber 10
(61)	-	Off s.f. 10
180	-	On, open tunnel
197	872	3m (0.085)
201	-	Stop tunnel
(61)	-	Single Fiber 10 cont'd
(184)	-	Off s.f. 10
201	-	On, open tunnel
232	947	3m (0.084)
258	-	Stop tunnel
(184)	-	Single Fiber 10 cont'd
(336)	-	Stop s.f. 10

a. Cumulative times shown in ( ) are for single fiber 10 tests, cumulative times shown without ( ) are for operation of aerosol tunnel with open test section.

b. Numbers in ( ) are fractions of particle count composed of more than one particle (Inlet); operating velocity 13.76 cm/sec; probe III; numbers beside m are sampling times, min; Generator model II at 60 psig; Ionizer on at 30 psig and 2.5 k.v. a.c. ; collecting electrostatic precipitator on at 170 v. d.c. outer tube grounded.

APPENDIX 4.3

AGGREGATE SIZE DISTRIBUTION

ON SINGLE FIBERS

AS A FUNCTION OF TIME

APPENDIX 4-3

AGGREGATE SIZE DISTRIBUTION ON SINGLE FIBERS AS A FUNCTION OF TIME

The following seven tables present the number of particles of a given aggregate size (j) observed on single fibers at each analysis. For instance, Table A4-3-1, column two, indicates that single fiber 4 was removed for analysis after 120 minutes of exposure, and that two fields (of 81-1/4-microns length each) were counted in the microscope. Total number of single particles observed was 37, doublets 8, and one each triplet and quadruplet.

The number of particles per cm^2 of fiber (Z) was calculated from field size and fiber diameter for $1 \leq j \leq 4$ for each fiber and plotted as a function of time, as shown in Figures 4-5 and 4-6 for single fiber nos. 9 and 10. The curves for single fiber nos. 4 through 8 were not substantially different from those shown for fiber nos. 9 and 10.

TABLE A4-3-1

Aggregate Size Distribution[a] On Single Fiber No. 4 At Indicated Times

t/f[b]	120/2	140/2	180/3	200/3	240/3	300/3	420/2
j =1	37	42	95	79	100	91	55
2	8	13	35	46	38	47	45
3	1	-	11	13	16	24	19
4	1	-	3	3	9	8	13
5	-	-	1	2	5	6	4
6	-	-	-	1	1	3	4
7	-	-	-	-	-	2	2
8	-	-	-	1	1	2	1
9	-	-	-	-	-	-	-
10	-	-	-	-	1	-	3
11	-	-	-	-	-	-	-
12	-	-	-	-	-	1	1

a. no. of particles of size j counted on indicated no. of fields.

b. t/f: t= cumulative exposure time, minutes; f= no. of fields observed to obtain indicated count, field= 81-1/4 μm long.

TABLE A4-3-2

Aggregate Size Distribution[a] On Single Fiber No. 5 At Indicated Times

t/f[b]	60/3	135/3	221/3	300/3	420/4	540/3
j =1	33	57	60	67	95	68
2	12	16	31	38	36	34
3	4	14	19	16	23	20
4	-	5	7	13	19	8
5	-	2	6	5	16	8
6	-	2	5	8	11	9
7	-	-	2	7	11	6
8	-	-	2	1	9	6
9	-	-	-	1	7	1
10	-	1	-	1	3	7
11	-	-	-	-	2	4
12	-	-	-	-	3	4
13	-	-	-	-	3	1
14	-	-	-	-	-	1
15	-	-	-	-	3	1
16	-	-	-	-	1	-
17	-	-	-	-	-	-
18	-	-	1	-	-	-
19	-	-	-	-	-	-
20	-	-	-	-	-	2
				(1)22	(1)22	(1)21,(1)28
					(1)27	(1)29,(1)30
						(1)31

a, b. See footnotes Table A4-3-1.

TABLE A4-3-3

Aggregate Size Distribution[a] On Single Fiber No. 6 At Indicated Times

t/f[b]	120/3	220/3
j =1	67	61
2	26	29
3	12	14
4	8	7
5	8	7
6	6	7
7	1	4
8	3	3
9	1	5
10	2	4
11	-	1
12	-	5
13	1	1
14	-	-
15	-	2
16	-	4
17	-	2
		(1)23

a, b. See footnotes Table A4-3-1.

TABLE A4-3-4

Aggregate Size Distribution[a] On Single Fiber No. 7 At Indicated Times

t/f[b]	60/3	121/3
j =1	87	65
2	17	37
3	16	22
4	12	13
5	5	7
6	1	5
7	-	5
8	-	6
9	2	4
10	1	3
11	-	1
12	-	2
13	-	2
14	-	1
15	-	-
16	-	1

a, b. See footnotes Table A4-3-1.

TABLE A4-3-5

Aggregate Size Distribution[a] On Single Fiber No. 8 At Indicated Times

t/f[b]	61/9	189/5	469/5
j =1	105	106	123
2	28	45	37
3	14	26	27
4	3	16	18
5	2	11	15
6	-	9	19
7	-	2	10
8	-	2	5
9	-	-	5
10	-	-	8
11	-	-	4
12	-	2	6
13	-	1	4
14	-	-	2
15	-	-	7
16	-	-	2
17	-	-	3
18	-	-	1
19	-	-	-
20	-	-	1
			(1)21,(1)22
			(1)24,(1)26

a, b. See footnotes Table A4-3-1.

TABLE A4-3-6

Aggregate Size Distribution[a] On Single Fiber No. 9 At Indicated Times

t/f[b]	30/36	180/11	480/7
j =1	250	218	228
2	28	52	79
3	4	16	22
4	1	6	15
5	-	1	14
6	-	3	10
7	-	-	4
8	-	-	6
9	-	-	7
10	-	-	3
11	-	-	3
12	-	-	-
13	-	-	1
14	-	-	1
15	-	-	1

a, b. See footnotes Table A4-3-1 .

TABLE A4-3-7

Aggregate Size Distribution[a] On Single Fiber No. 10 At Indicated Times

t/f[b]	61/15	184/10	336/5
j =1	149	156	82
2	61	67	31
3	23	34	15
4	16	24	13
5	3	17	4
6	-	26	7
7	1	11	10
8	-	10	3
9	-	5	7
10	-	5	7
11	-	7	2
12	-	1	7
13	-	1	1
14	-	-	4
15	-	1	3
16	-	-	5
17	-	1	2
18	-	-	1
19	-	-	2
20	-	-	1
			(1)21,(1)22,(2)23 (1)27,(2)29,(1)45 (1)49

a, b. See footnotes Table A4-3-1.

APPENDIX 5-1

INITIAL FILTER FIBER EFFICIENCY, AND IMPACTION NUMBER AND PÉCLET NUMBER

TABLE A5-1-1

Initial Filter Fiber Efficiency, and Impaction Number and Peclet Number

Filter No	Efficiency $\eta_c(0)$	$I^{1/2}$ [a]	Pe^{b} x10-4	$Pe^{1/3}$	$RPe^{1/3}$ [c]	$\eta_c RPe$
1	0.167	0.93	66.5	87	11.9	1.52×10^4
2	0.062	0.30	6.6	40	5.5	5.5×10^2
3	0.057	0.30	6.6	40	5.5	5.2×10^2
4	0.156	0.30	6.6	40	5.5	1.40×10^3
5	0.088	0.30	6.6	40	5.5	8.0×10^2
6	0.110	0.30	6.6	40	5.5	9.9×10^2
7a	0.175	0.30	6.6	40	5.5	1.58×10^3
7b	0.154	0.30	6.6	40	5.5	1.39×10^3
7c	0.153	0.30	6.6	40	5.5	1.38×10^3
8	0.122	0.30	6.6	40	5.5	1.10×10^3
9	0.159	0.43	13.8	52	7.1	3.0×10^3
10	0.238	0.61	27.7	65	8.9	9.0×10^3

a. I= impaction number = $2 \rho_p C_s a_p^2 U_o / 9 \mu a$.

b. Pe= Peclet number = $2aU_o/D$.

c. R= Interception number = $a_p/a = 0.14$.

APPENDIX 5-2

INITIAL SINGLE FIBER EFFICIENCY; AND INTERCEPTION NUMBER, IMPACTION NUMBER, AND PÉCLET NUMBER

TABLE A5-2-1

Initial Single Fiber Efficiency; and Interception Number, Impaction Number, and Peclet Number

Fiber No	Efficiency $\eta(0)$	Fiber Diam. μm	R^a	$I^{1/2b}$	$Pe^c \times 10^{-4}$	$Pe^{1/3}$	$RPe^{1/3}$	ηRPe
4	0.051	9.6	0.14	0.30	6.6	40	5.5	460
5	0.077	8.7	0.15	0.31	6.0	39	5.9	690
6	0.074	9.7	0.13	0.43	14.1	52	7.0	1400
7	0.053	11.0	0.12	0.57	32	68	8.1	2030
8	0.065	10.4	0.12	0.28	7.2	42	5.2	580
9	0.040	8.5	0.15	0.32	5.8	39	6.0	360
10	0.100	9.2	0.14	0.30	6.3	40	5.6	900

a. R= interception number = 1.305/(fiber diam.).

b. I= Impaction number = $2 \rho_p C_s a_p U_o / 9 \mu a$.

c. Pé= Peclet number = $2aU_o/D$.

NOTATION

A	=	accumulation of solid particles in a fiber filter, particles per cm^2 of filter face area
C_c	=	a function of fiber Knudsen number for slip flow
C_D	=	fiber drag coefficient
	=	2 Drag force/Area Exposed ($\rho_f U_o^2$)
C_i, C_i'	=	numerical coefficients (i = 1,2,3,...)
C_S	=	Cunningham-Millikan slip correction factor for spherical particles in a gas,
	=	($(1+0.42Kn)^{-1}$ + 1.67Kn)
D	=	Stokes-Einstein diffusion coefficient for aerosol particles = kT/f, cm^2/sec
$\bar{E}$	=	average filter collection efficiency over an interval of time
F_D	=	$F_D(0)+(S_p \mu U_o a_p)2aZ$, drag force per unit length on a cylindrical fiber containing deposited particles, dynes/cm
$F_D(0)$	=	initial drag force per unit length on a cylindrical fiber, dynes/cm
I	=	inertial impaction group = mU_o/af
K'	=	shape factor
K''	=	orientation factor
K_1	=	empirical coefficient, $\sim$ 6.1
K_2	=	empirical coefficient, $\sim$ 0.41

NOTATION (Cont'd.)

K_3	=	empirical coefficient, = 30 at STP
$K_o(\alpha)$	=	theoretical fiber filter resistivity coefficient
K_o'	=	experimental fiber filter resistivity coefficient
Kn	=	Knudsen number based on fiber radius = λ/a
Kn'	=	Knudsen number based on particle radius = λ/a_p
L	=	total depth of filter mat in direction of flow, cm
N	=	local aerosol particle concentration, particles/cm^3
N_o	=	aerosol particle concentration in undisturbed flow, particles/cm^3
N_L	=	aerosol particle concentration at filter outlet, particles/cm^3
P	=	filter penetration = N_L/N_o
P(A)	=	filter penetration as a result of particle accumulation
P(0)	=	filter penetration at start of filtration
Pe	=	Péclet number = $2aU_o/D$
R	=	interception parameter = a_p/a
R'	=	radial dimension in aerosol tunnel contraction, inches
Re	=	Reynolds number = $2aU_o/\nu$
S	=	a coefficient related to particle capture as a result of local particle deposition and geometry, cm^2/particle

NOTATION (Cont'd.)

S_p	=	a coefficient related to drag on deposited particles, dimensionless
T	=	temperature, ^oK
U_o	=	undisturbed fluid velocity, cm/sec
Z	=	number of particles deposited locally on a fiber per cm^2 of fiber cross-section normal to flow
a	=	radius of cylindrical fiber, cm
a_p	=	radius of spherical aerosol particle, cm
d_f	=	diameter of filter fiber, cm
d_p	=	diameter of aerosol particle, cm
f	=	fluid resistance per unit of velocity = $6\pi\mu a_p/C_s$ dynes/(cm/sec)
j	=	number of elementary particles in aggregate
k'	=	intrinsic permeability of porous medium, cm^2
k	=	Boltzmann constant, 1.38×10^{-16} erg/^oK
ℓ	=	length of filter fiber of radius a per unit volume of filter mat, cm of fiber/cm^3 of filter
m	=	mass of particle, grams
n	=	a number
p	=	local pressure, dynes/cm^2
p_o	=	total pressure at inlet to filter, dynes/cm^2
p_L	=	total pressure at outlet of filter, dynes/cm^2
t	=	time, seconds
x	=	distance from filter entrance, cm
x'	=	distance on center-line of contraction, inches

NOTATION (Cont'd.)

y_o = half-width of region of flow completely cleared of particles by a cylindirical fiber, cm

α = fraction solids, filter volume occupied by fiber
= ρ_b / ρ_m cm^3 of fiber/cm^3 of filter

β = accommodation coefficient for effectiveness of contacts between particles and fiber, 0

γ = an empirical coefficient ($1 < \gamma < 2$) to account for the effect of random fiber orientation in Langmuir theoretical filter permeability

$\overline{\Delta N}$ = average difference in up- and downstream aerosol concentration during time interval Δt, p/cm^3

Δp = filter resistance to gas flow, dynes/cm^2

$\Delta p(0)$ = initial filter resistance, dynes/cm^2

$\Delta p(A)$ = filter resistance as a result of the accumulation of solid particles, dynes/cm^2

$\delta \Delta p(A)$ = change in filter resistance arising from the accumulation of deposited particles, dynes/cm^2, = $\Delta p(A) - \Delta p(0)$

Δt = a time interval, sec

η = cylindrical fiber efficiency = y_o/a

$\eta(0)$ = initial cylindrical fiber efficiency at start of filtration

$\eta(Z)$ = $\eta(0) + SZ$ = local single fiber efficiency as a result of particle accumulation on the fiber

NOTATION (Cont'd.)

η_{AV} = $\frac{1}{L}\int_0^L \eta(z)\,dx$, average particle collection efficiency through the depth of a filter mat

$\eta_c(0)$ = $\eta(0)/(1+4.5\alpha)$ = initial filter fiber efficiency of Chen (23) as corrected for solid fraction effect

$\eta^*(0)$ = filter fiber efficiency from thin filter approximation

λ = molecular mean free path in a gas, cm

μ = fluid viscosity, grams/cm-sec

μm = micron, 10^{-6} meter

ν = kinematic viscosity of fluid, cm^2/sec =

ρ_b = fiber filter packing density, gm/cm^3

ρ_f = fluid density, gm/cm^3

ρ_m = filter fiber material density, gm/cm^3

ρ_p = aerosol particle density, gm/cm^3

τ = variable of integration

REFERENCES CITED

1. White, P. A. F. and Smith, S. E. (Eds.), "High-Efficiency Air Filtration," Butterworths, 314 pp. (1964).

2. Green, H. L. and Lane, W. R., "Particulate Clouds: Dusts, Smokes, and Mists," second edition, D. Van Nostrand Co., Inc., 471 pp. (1964).

3. Davies, C. N., "Fibrous Filters for Dust and Smoke," The Ninth International Congress on Industrial Medicine, London, September 13th-17th, 1948, John Wright and Sons, Ltd., 1 (1949).

4. Silverman, M. D. and Browning, W. E., Jr., "Fibrous Filters as Particle-Size Analyzers," Science, 143, 573 (1964).

5. Shleien, B., Glavin, T. P., and Friend, A. G., "Particle Size Fractionation of Airborne Gamma-Emitting Radionuclides by Graded Filters," Science, 147, 290 (1965).

6. Lockhart, L. B., Jr., Patterson, R. L., Jr., and Saunders, A. W., Jr., "The Size Distribution of Radioactive Aerosols," Journal of Geophysical Research, 70, 6033 (1965).

7. Roesler, J. F., "Application of Polyurethane Foam Filters for Respirable Dust Separation," Journal of the Air Pollution Control Association, 16, 30 (1966).

8. Lockhart, L. B., Jr., "The Sorting of Radioactive Aerosols by Particle Size," paper number D67, presented at 151st American Chemical Society Meeting (March 1966).

9. Langmuir, I., "Report on Smokes and Filters," The Collected Works of Irving Langmuir, Volume 10, Pergamon Press, 394 (1961).

10. Davies, C. N., "The Separation of Airborne Dust and Particles," Proceedings of the Institution of Mechanical Engineers, B, 1B, 185 (1952).

11. Fuchs, N. A. and Stechkina, I. B., "A Note on the Theory of Fibrous Aerosol Filters," Annals of Occupational Hygiene, 6, 27 (1963).

12. Happel, J. and Brenner, H., "Low Reynolds Number Hydrodynamics," Prentice-Hall, Inc., 394 (1965).

13. Kuwabara, S., "The Forces Experienced by Randomly Distributed Parallel Circular Cylinders or Spheres in a Viscous Flow at Small Reynolds Number," Journal of the Physical Society of Japan, 14, 527 (1959).

14. Saffman, P. G., "The Lift on a Small Sphere in a Slow Shear Flow," Journal of Fluid Mechanics, 22, 385 (1965).

15. Gillespie, T., "The Adhesion of Drops and Particles on Impact at Solid Surfaces," Journal of Colloid Science, 10, 266 (1955).

16. Gallily, I., "On the Filtration of Aerosols by Filter Models of Various Porosities," Journal of Colloid Science, 12, 161 (1957).

17. Gallily, I. and LaMer, V. K., "On the Behavior of Liquid Droplets after Impinging on Solid Surfaces," Journal of Physical Chemistry, 62, 1295 (1958).

18. Corn, M. and Silverman, L., "Removal of Solid Particles from a Solid Surface by a Turbulent Air Stream," American Industrial Hygiene Association Journal, 22, 337 (1961).

19. Larsen, R. I., "The Adhesion and Removal of Particles Attached to Air Filter Surfaces," American Industrial Hygiene Association Journal, 19, 265 (1958).

20. Wright, T. E., Stasny, R. J., and Lapple, C. E., "High Velocity Air Filters," Donaldson Co., Inc., WADC Technical Report 55-457, ASTIA Document No. AD-142075 (1957).

21. Zebel, G., "Deposition of Aerosol Flowing Past a Cylindrical Fiber in a Uniform Electric Field," Journal of Colloid Science, 20, 522 (1965).

22. Lundgren, D. A. and Whitby, K. T., "Effect of Particle Electrostatic Charge on Filtration by Fibrous Filters," Industrial and Engineering Chemistry Process Design and Development, 4, 345 (1965).

23. Chen, C. Y., "Filtration of Aerosols by Fibrous Media," Chemical Reviews, 55, 595 (1955).

24. Fuchs, N. A., "The Mechanics of Aerosols," The Macmillan Co., 408 pp. (1964).

25. Friedlander, S. K., "Mass and Heat Transfer to Single Spheres and Cylinders at Low Reynolds Numbers," American Institute of Chemical Engineers Journal, 3, 43 (1957).

26. Natanson, G. L., "Diffusion of Aerosol Particles Flowing Past a Transverse Cylinder," Proceedings of the Academy of Sciences of the USSR, Section: Physical Chemistry (In Russian), 112, 100 (1957).

27. Friedlander, S. K., "Theory of Aerosol Filtration," Industrial and Engineering Chemistry, 50, 1161 (1958).

28. Radushkevich, L. V., "The Theory of the Deposition of Particles From a Gas Stream on an Isolated Cylinder," Russian Journal of Physical Chemistry, (In Russian) 32, 282 (1958).

29. Natanson, G. L. and Ushakova, E. N., "Critique of Some Papers on the Theory of the Filtration of Aerosols," Russian Journal of Physical Chemistry (English Translation), 35, 224 (1961).

30. Radushkevich, L. V., "Present State of the Theory of the Filtration of Aerosols (Reply to the Critical Comments in the Paper by G. L. Natanson and E. N. Ushakova)," Russian Journal of Physical Chemistry (English Translation), 35, 227 (1961).

31. Friedlander, S. K., With the Assistance of Ralph E. Pasceri, "Aerosol Filtration by Fibrous Filters," Biological and Biochemical Engineering, Pergamon Press, Chapter 3 (In Press).

32. Pich, J., "Die Filtrationstheorie hochdisperser Aerosole," Staub, 25, 186 (1965).

33. Friedlander, S. K., "Particle Diffusion in Low Speed Flows," paper to be presented at 59th Annual Meeting, Air Pollution Control Association (June 1966).

34. Fuchs, N. A. and Stechkina, I. B., "Resistance of a Gaseous Medium to the Motion of a Spherical Particle of a Size Comparable to the Mean Free Path of the Gas Molecules," Transactions of the Faraday Society, 58, 1949 (1962).

35. Golovin, M. N. and Putnam, A. A., "Inertial Impaction on Single Elements," Industrial and Engineering Chemistry Fundamentals, 1, 264 (1962).

36. Aiba, S., Humphrey, A. E., and Millis, N. F., "Biochemical Engineering," Academic Press, 333 pp. (1965).

37. Dorman, R. G., "The Role of Diffusion, Interception, and Inertia in the Filtration of Airborne Particles," Aerodynamic Capture of Particles, E. G. Richardson (Ed.), Pergamon Press, 112 (1960).

38. Torgeson. W. L., "The Theoretical Collection Efficiency of Fibrous Filters Due To the Combined Effects of Inertia, Diffusion and Direct Interception," Paper No. J 1057, Applied Science Division, Litton Systems, Inc., (Undated).

39. Whitby, K. T., "Calculation of the Clean Fractional Efficiency of Low Media Density Filters," American Society of Heating, Refrigeration, and Air Conditioning Engineers Journal, 7, 56 (1965).

40. Wong, J. B. and Johnstone, H. F., "Collection of Aerosols by Fiber Mats," University of Illinois Engineering Experiment Station, Technical Report No. 11, U. S. Atomic Energy Commission Report No. COO-1012 (1953).

41. Thomas, D. G. and Lapple, C. E., "Deposition of Aerosol Particles in Fibrous Filters," American Institute of Chemical Engineers Journal, 7, 203 (1961).

42. Thomas J. W. and Yoder, R. E., "Aerosol Size for Maximum Penetration through Fiberglas and Sand Filters," American Medical Association Archives of Industrial Health, 13, 545 (1956).

43. Ramskill, E. A. and Anderson, W. L., "The Inertial Mechanism in the Mechanical Filtration of Aerosols," Journal of Colloid Science, 6, 416 (1951).

44. Humphrey, A. E. and Gaden, E. L., Jr., "Air Sterilization by Fibrous Media," Industrial and Engineering Chemistry, 47, 924 (1955).

45. Stern, S. C., Zeller, H. W., and Schekman, A. I., "The Aerosol Efficiency and Pressure Drop of a Fibrous Filter at Reduced Pressures," Journal of Colloid Science, 15, 546 (1960).

46. Sadoff, H. L. and Almlof, J. W., "Testing of Filters for Phage Removal," Industrial and Engineering Chemistry, 48, 2199 (1956).

47. Aiba, S., Shimasaki, S., and Suzuki, S., "Experimental Determination of the Collection Efficiencies of Fibrous Air Sterilization Filter," Journal of General and Applied Microbiology 7, 192 (1961).

48. Scheidegger, A. E., "The Physics of Flow Through Porous Media," The Macmillan Co., 313 pp.(1960)

49. Pich, T., "Pressure Drop of Fibrous Filters at Small Knudsen Numbers," Annals of Occupational Hygiene, 9, 23 (1966).

50. Sullivan, R. R., "Further Study of the Flow of Air Through Porous Media," Journal of Applied Physics, 12, 503 (1941).

51. Blasewitz, A. G., Carlisle, R. V., Judson, B. F., Katzer, M. F., Kurtz, E. F., Schmidt, W. C., and Wiedenbaum, B., "Filtration of Radioactive Aerosols by Glass Fibers," Hanford Works, U. S. Atomic Energy Commission Report Nos. HW-20847 (Parts I and II) (1951).

52. First, M. W., Silverman, L., Dennis, R., Johnson, G. A., Rossano, A. T., Jr., Moschella, R., Billings, C. E., Berly, E., Friedlander, S. K., and Drinker, P., "Air Cleaning Studies Progress Report," Harvard University, U. S. Atomic Energy Commission Report No. NYO-1581 (1951).

53. Kimura, N. and Iinoya, K., "Experimental Studies on the Pressure Drop Characteristics of Fiber Mats," Kagaku Kōgaku (Chemical Engineering, Japan (In Japanese, English Summary), 23, 792 (1952).

54. Aiba, S. "Some Notes on the Design of Fibrous Air Filter," University of Tokyo, Progress Report No. 14 (1961).

55. Wheat, J. A., "The Air Flow Resistance of Glass Fiber Filter Paper," The Canadian Journal of Chemical Engineering, 41, 67 (1962).

56. Werner, R. M. and Clarenburg, L. A., "Aerosol Filters: Pressure Drop across Single-Component Glass Fiber Filters," Industrial and Engineering Chemistry Process Design and Development, 4, 288 (1965).

57. White, C. M., "The Drag of Cylinders in Fluids at Slow Speeds," Proceedings of the Royal Society (London), A186, 472 (1946).

58. Brooks, W. B. and Reis, G. E., "Drag on a Right Circular Cylinder in Rarified Flow at Low Speed-Ratios," Advances in Applied Mechanics, Supplement 2, Volume 11, Academic Press, 291 (1963).

59. Watson, J. H. L., "Filmless Sample Mounting for the Electron Microscope," Journal of Applied Physics, 17, 121 (1946).

60. Leers, R., "Die Abscheidung von Schwebstoffen in Faserfiltern," Staub, 50, 402 (1957).

61. Cheever, C. L., "Recent Air Cleaning Developments at Argonne National Laboratory," Seventh AEC Air Cleaning Conference Held at Brookhaven National Laboratory, October 10-12, 1961, U. S. Atomic Energy Commission Report No. TID-7627 (Book 1), 318 (1962).

62. Dorman, R. G., "Filter Materials," High Efficiency Air Filtration, P. A. F. White and S. E. Smith (Eds.), Butterworths, 104 (1964).

63. Radushkevich, L. V. and Kolganov, V. A., "Study of Collection of Highly Disperse Aerosols from a Gas Stream on Ultra-Thin Cylinders," Aerosols: Physical Chemistry and Applications, K. Spurny (Ed.), Publishing House of the Czechoslovak Academy of Sciences, 247 (1965).

64. LaMer, V. K., "Studies on Filtration of Monodisperse Aerosols," Columbia University, U. S. Atomic Energy Commission Report No. NYO-512, 72 (1951).

65. Fairs, G. L., "High Efficiency Fiber Filters for the Treatment of Fine Mists," Transactions of the Institution of Chemical Engineers, 36, 476 (1958).

66. Bondarenko, V. S., "Formation of Drops on Thin Filaments Covered with a Cylindrical Layer of Liquid," Russian Journal of Physical Chemistry (English Translation), 35, 1372 (1961).

67. Smith, W. J. and Surprenant, N. F., "Properties of Various Filtering Media For Atmospheric Dust Sampling," American Society for Testing and Materials, 53, 1122 (1953).

68. LaMer, V. K., Drozin, V. G., Kruger, J., and Cotson, S., "Filtration of Monodisperse Solid Aerosols," Columbia University, U. S. Atomic Energy Commission Report No. NYO-4526, (1953).

69. Wisehart, D. E., "Preliminary Report of Accelerated Life Tests on Certain Air-Cleaning Media," Sixth AEC Air Cleaning Conference, July 7-9, 1959, U. S. Atomic Energy Commission Report No. TID-7593, 375 (1960).

70. Adley, F. E. and Wisehart, D. E., "Life-Loading Tests on Certain Filter Media," Seventh AEC Air Cleaning Conference Held at Brookhaven National Laboratory, October 10-12, 1961, U. S. Atomic Energy Commission Report No. TID-7627 (Book 1), 116 (1962).

71. Lindeken, C. L., Morgin, R. L., and Petrock, K. F., "Collection Efficiency of Whatman 41 Filter Paper for Submicron Aerosols," Health Physics, 9, 305 (1963).

72. Pradel, J., Billard, F., Madelaine, G., and Brion, J., "Filter Efficiency and Clogging," Eighth AEC Air Cleaning Conference Held at Oak Ridge National Laboratory, October 22-25, 1963, U. S. Atomic Energy Commission Report No. TID-7677, 419 (1964).

73. Kimura, N. and Iinoya, K., "Collection Efficiency of a Fiber Mat Filter with Low Dust Loading," Kagaku Kōgaku (Chemical Engineering, Japan) (Abridged Edition), 2, 136 (1964).

74. LaMer, V. K. and Drozin, V. G., "Filtration of Monodisperse Solid Aerosols," Proceedings of the Second International Congress of Surface Activity: Electrical Phenomena and Solid/Liquid Interface, Butterworths Scientific Publications, 600 (1957).

75. Tsien, H.-S., "On the Design of the Contraction Cone for a Wind Tunnel," Journal of the Aeronautical Sciences, 10, 68 (1943).

76. Drinker, P. and Hatch, T., "Industrial Dust," second edition, McGraw-Hill Book Co., Inc., 152 (1954).

77. Whitby, K. T., "Generator for Producing High Concentrations of Small Ions," Review of Scientific Instruments, 32, 1351 (1961).

78. Whitby, K. T. and Peterson, C. M., "Electrical Neutralization and Particle Size Measurement of Dye Aerosols," Industrial and Engineering Chemistry Fundamentals 4, 66 (1965).